



**Politecnico
di Torino**

Politecnico di Torino

Master of Science in
MECHANICAL ENGINEERING
A.a. 2022/2023

**New solution for gearing optimization through lubrication and
cooling performance**

Academic supervisor:

Prof. Carlo Rosso

Candidate:

Farzad Kolahdouzan

Company supervisor:

Ing. Emanuele Colacito

Academic year 2022-2023

Contents

Abstract	1
1. Introduction	2
2. MPS theory	7
2.1. Governing equations	7
2.1.1. Navier-Stokes equations	7
2.1.2. Continuity equation	8
2.1.3. Energy equation	8
2.2. Semi-implicit methodology	9
2.2.1. Number of density of particles and weight function	11
2.2.2. Boundary conditions	12
2.2.2.1. Boundary conditions of inlet and outlet	13
2.2.3. Turbulence	14
2.3. Particle action model	15
3. Frictional moment in bearings	15
3.1. Rolling frictional moment	16
3.2. Sliding frictional moment	18
3.3. Frictional moment of seals	19
3.4. Drag losses	19
4. Method	21
4.1. Lubrication system of shaft number 1 with number 2	23
4.1.1. Radial channels	26
4.1.2. Spline modification	31
4.2. Lubrication system of shafts number 3 with number 4	42
4.2.1. Inserting shield	44
4.3. Adding jet lubrication	48
5. Temperature and thermal stress analysis	57
5.1. Internal heat generation of bearing	64
5.2. Temperature and stress analyses	67
6. Conclusion	74
References	75

List of figures

Figure 1 (A) mesh approach and (B) meshless approach	7
Fig 2.1. MPS procedure	11
Fig 2.2 Weight function diagram	12
Fig 2.3 Illustration of fluid, wall and dummy particles	14
Fig 3.1. Stribeck curve	16
Fig. 3.2. Illustration of influence of inlet shear heating reduction factor	17
Fig. 3.3. Diagram of weighting factor	17
Fig. 4.1a. Gearbox, heat exchanger and pump	21
Fig. 4.1b. Gearbox, heat exchanger and pump in CAD software	21
Fig. 4.2. Four gear shafts including input, idle and pinion shafts	22
Fig. 4.3. Secondary railways as jet lubrication	23
Fig. 4.4.a. Input shaft with surrounding housing	25
Fig 4.4.b. Nozzle inserted inside input shaft which has 4 holes	25
Fig. 4.5a. Input shaft with radial channels	26
Fig. 4.5b. Radial channels directed toward ball bearing	27
Fig. 4.6. Oil distribution in input shaft	27
Fig. 4.7. Number density of oil on the ball bearing	28
Fig 4.8. Lubricant flowrate reaching ball bearing	28
Fig. 4.9. Total churning torque for input shaft	29
Fig. 4.10. Lubricant pathline for low temperature	30
Fig. 4.11. number density of oil on the balls	31
Fig. 4.12. Illustration of spline modification	32
Fig. 4.13. Jet lubrication on the meshing area	33
Fig. 4.14. Oil pathline on modified spline	33
Fig. 4. 15. Movement of lubricant inside the input shaft	34

Fig. 4.16. Oil number density for roller bearing _____	35
Fig. 4.17. Oil number density for ball bearing _____	35
Fig. 4.18. Oil number density for meshing area _____	36
Fig. 4.19. Lubricant pressure distribution in input shaft _____	37
Fig. 4. 20. Oil flowrate received by ball bearing _____	37
Fig. 4. 21. Oil flowrate received by roller bearing _____	38
Fig. 4. 22. Power loss in input shaft _____	39
Fig. 4.23. Oil number density of ball bearing in low temperature _____	40
Fig. 4. 24. Oil number density of roller bearing in low temperature _____	40
Fig. 4.25. Oil number density for meshing area for low temperature _____	41
Fig. 4.26. Oil flowrate received by ball bearing _____	41
Fig. 4. 27. Churning loss of input shaft for low temperature _____	42
Fig. 4. 29. Schematic view from shaft number 3 and 4. _____	43
Fig. 4. 30. Radial channels inside the shaft _____	43
Fig. 4. 31. The shield inserted in housing _____	44
Fig. 4. 32. Oil number density of both shafts _____	45
Fig. 4. 33. Oil number density of meshing area _____	45
Fig. 4. 34. Oil flowrate received by meshing area at high temperature _____	46
Fig. 4. 35. Oil number density on the shaft 3 and 4. _____	47
Fig. 4. 36. Oil number density of on meshing area. _____	48
Fig. 4. 37. Oil flowrate received by meshing area at low temperature _____	48
Fig. 4. 38. New shape of shield and jet nut _____	49
Fig. 4. 39. Oil pathline of jet nut _____	50
Fig. 4. 40. Jet nut position in gearbox _____	51
Fig. 4. 41. Oil particles inside the shaft _____	51
Fig. 4. 42. Lubrication system in shaft number 3. _____	52
Fig. 4. 43. Oil number density on the shaft _____	52

Fig. 4. 44. Distribution of oil on meshing area _____	53
Fig. 4. 45. Power loss related to shaft 3 for higher temperature. _____	53
Fig. 4. 46. Pressure distribution in shaft 3 in high temperature. _____	54
Fig. 4. 47. Passage of oil particles through cage _____	55
Fig. 4. 48. Oil number density in low temperature _____	55
Fig. 4. 49. Oil number density in meshing area _____	56
Fig. 4. 50. Pressure distribution in shaft 3 in low temperature. _____	56
Fig. 4. 51. Power loss related to shaft 3 for lower temperature. _____	57
Fig. 5. 1. Two critical bearings in input shaft _____	59
Fig. 5. 2a. Heat transfer coefficient of roller bearing _____	60
Fig. 5. 2b. Heat transfer coefficient of roller bearing _____	60
Fig. 5. 3a. Heat transfer coefficient on ball bearing. _____	61
Fig. 5. 3b. Heat transfer coefficient on ball bearing. _____	62
Fig. 5. 3c. Heat transfer coefficient on shaft. _____	62
Fig. 5. 3d. Heat transfer coefficient on shaft. _____	63
Fig. 5. 4. Axial and radial loads applied on bearings _____	65
Fig. 5. 5. a. Contacts in ball bearing _____	69
Fig. 5. 5. b. Contacts in roller bearing _____	69
Fig. 5. 6. Temperature distribution in roller bearing _____	69
Fig. 5. 7. Total heat flux in roller bearing _____	70
Fig. 5. 8. Temperature distribution in ball bearing _____	70
Fig. 5. 9. Total heat flux in ball bearing _____	71
Fig. 5. 10a. Thermal stress analysis on roller bearing _____	72
Fig. 5. 10b. Stress distribution over rollers _____	72
Fig. 5.11a. Thermal stress analysis on ball bearing _____	73
Fig. 5. 11b. Stress distribution over balls _____	73

List of tables

Table 4.1. different speed scenarios _____	23
Table 4. 2. Material properties of steel and cast iron _____	24
Table 4. 3. Properties of lubricant at high temperature _____	24
Table 4.4. Properties of lubricant at low temperature _____	30
Table 5. 1. Roller bearing properties _____	63
Table 5. 2. Ball bearing properties _____	64
Table 5. 3. Properties of lubricant _____	67
Table 5. 4. Stainless steel material properties _____	67

Abstract

Different types of lubrications are utilized in transmission systems to lubricate tribological contacts in order to minimize churning loss and dissipate frictional heat. This project concerns simulation and optimization of lubrication system in truck transmission system to rise efficiency and lubricant in meshing areas using particle-based computational fluid dynamics (CFD). Because of insufficient oil impingement in meshing gears, besides oil immersion additional railways on top gears, inside input and shifting shafts are provided which in some cases can act as jets. This novelty can meet expectation to deliver acceptable amounts of lubricants to critical places in transmission system. In order to study lubrication system elaborately, shafts are analyzed separately and modifications to existing designs for casing, spline, radial channel and jet angle are carried out to ameliorate cooling process with respect to high efficiency. For increasing numerical simulation accuracy and speed, Moving Particle Semi-Implicit (MPS) method, has been taken into account. The advantage of particle-based approach is the ability to simulate lubrication process by omitting mesh generation leading to higher accuracy and minimizing time required. Using this method, exact oil velocity, number of density and pressure are achieved giving the opportunity to determine wet area with high precision. With respect to the MPS method, heat transfer between oil and different components are achieved and their temperatures can be measured. The bearings are of the most vulnerable parts of transmission systems and their failure accounts for a major part of danger. Therefore, with considering all moments generated in ball bearing, internal heat generation is calculated and thermal stress of the ball bearing in input shaft experiencing high load and temperature is analyzed. The churning losses are calculated and compared for every shafts according to the oil viscosity and rotational speeds. Lubrication, heat dissipation as well as churning loss play vital role in functionality of gearbox and therefore well-designed lubrication would rise longevity avoiding failures, hence investigating optimized lubrication system can be conducted considering this thesis results.

1. Introduction

Lubrication is more critical for the performance and lifetime of an electric vehicle (EV) gearbox due to higher rotational speed. The gearbox is made up of several moving parts, including gears, bearings, and shafts and in order to decrease friction and avoid wear and tear, all these components require sufficient lubrication. The main lubrication system objective is generation of a mixed film lubrication which has lower friction compared to boundary and hydrodynamic lubrication leading to elimination of failures and rising efficiency. Lubricants in the gearbox also aid in the dissipation of heat produced by the electric motor and gear set. If the heat is not dispersed effectively, it can cause damage to the gearbox, which an appropriate lubricant can assist with. Besides electric motor, transmission system is in charge for decrease in noise, vibration and harshness (NVH) where the greatest decrease in high-performance gearing systems is feasible. There are three different kinds of lubrication in gearbox including splash lubrication, circulation lubrication and jet lubrication. In case of splash lubrication, the oil is dispersed because of impingement of oil with parts or centrifugal force of rotating components such as gears and bearings of gearbox. In this case, the lubricant circulated in random paths and may not make wet all components equally. Moreover, to have more effective splash lubrication, it needs more oil volume to feed more parts in gearbox. On the other hand, in jet lubrication the oil is directed to a specific component via high-speed jet and it can benefit high accuracy assuring appropriate lubrication and high efficiency. On top of that, it demands lower amount of oil for direction to a particular zone. Jiang et al. [1] studied presence of guideline for splash lubrication function in a bevel gearbox being used for helicopter and effects of hole radii, capacity on flowrate are analyzed. It is concluded the significance of hole radii as well as fillet radius of tubes on lubrication system. Liu et al. [2] conducted a study about splash dip-lubricated transmission system using finite volume method (FVM). It concentrates on no-load gearing losses consisting of churning loss and windage loss at different speeds and viscosities resulting in efficiency loss. It is described that churning loss plays important role in overall loss of gearbox. Málacová and Sivák [3] presented new modifications in transmission system facing failure, in particular for gears and bearings. They have assessed central circulation lubrication in such components to prevent failures. This invention compensates for bevel gear that is inadequately submerged below the lubricant level. It is shown that presence of sufficient oil can bring about elimination of gearbox failures. Lubrication system does not just belong to automotive industry, it also consists of wind turbine. It should be considered that increase in the oil volume in housing can bring about rising the churning torque because of shearing of lubricant leading to increase in power loss. Therefore, complex simulations are needed to use reasonable oil volume that meets the expectations because experiments are not sufficient due to oil adhesion with walls. Singh et al. [4] have shown the importance preventive maintenance practice as

well as intermittent lubricant purification in order to avoid failure in the whole gearbox. Because, purification can result in reduction of surface roughness, maximum oil film and eliminating penetration of contaminants to the lubricant. Mastrone and Concli [5] investigated behavior and distribution of grease as a non-Newtonian fluid in transmission system besides computation of churning loss. Lu et al. [6] carried out a project regarding power loss of helicopter gearbox with splash lubrication. In this study optimal values for two important variables including rotating speed and immersion depth are calculated. It should be noted for computing the power loss, in addition to churning loss, the windage loss is also considered. A paper regarding calculation of accurate churning power loss in lubricated wind turbine gearbox is conducted by Marques et al. [7]. To validate the results, they have referred the data with back-to-back test rig. For estimating accurate churning loss, two oil flow regimes are considered that are connected to the nature of gearbox housing and fluid circulation. In case of jet lubrications numerous researches have been done so far focusing on increase in efficiency. Dai et al [8] investigated optimal oil jet lubrication for meshing gears in a rotorcraft. They hinted at importance of appropriate angle, location and distance toward pinion for the jet.

The Moving Particle Semi-Implicit (MPS) technique is a numerical approach for simulating fluid and particle dynamics. The MPS technique is according to the assumption that particles move using both implicit and explicit methods, allowing for more realistic simulations of complicated fluid dynamics. In this method, the fluid is split into particles interacting with each other and depend upon the environment. The movement of these particles is regulated by a number of physical laws, including the Navier-Stokes equations and the particles shift in accordance with their velocity and acceleration. The MPS approach is particularly appropriate for modeling free-surface flows such as seas and rivers, where particle mobility is critical. The MPS has several superiorities such as flexibility in order to model more complicated flow domains and geometries. It exploits particle-based method to increase accuracy for producing smooth velocity fields. It takes advantage of using particle interactions instead of discrete cells. More importantly, it is more computationally efficient, because it requires less memory and computing power facilitating for simulations of high level of details. Deng et al. [9] studied the mechanism of lubrication related to a high-speed railway train gearbox using MPS. In this work, the churning losses for different cases according to rotating speeds, viscosity and immersion depth have been achieved showing the main role of speed on overall loss. It depicts that increase in rotating speed can rise churning loss exponentially. In another paper, churning power loss is computed using MPS considering different temperature and velocity by Guo et al. [10]. It is concluded that temperature has impressive effect on churning loss owing to its dependence on viscosity and density. The higher the temperature, the lower the churning loss. Hence, it is vital to select a proper lubricant in accordance with the application. The MPS has been utilized in analysis of

lubrication system in chain drive system [11]. In this work, an oil injection is used to make wet the specific part of the chain and the co-simulation is carried out by MPS and RecurDyn. Similarly, different scenarios for temperatures have considered and the role of viscosity in oil output volume is determined. New improvements in accuracy and stability of MPS method in order to alleviate unphysical oscillation of pressure with high frequencies have been presented [12]. In this innovation, new formulation regarding Poisson equation related to pressure is added resulting in distributions of smoother pressure. In another work [13], a new enhancement for instability of MPS method in case of considering tensile stress instead of compressive stress that can lead to tensile instability. The new inventions are adding modified Poisson pressure equation besides corrective Matrix for pressure gradient model. These enhancements are able to stabilize MPS method. Wu et al. [14] looked into modifications in ball bearing lubrication system and the advantages of MPS method. Flowrate and churning loss with respect to various speeds are assessed and it is found out that increase in speed leads to reduction of number of particles, thus churning loss of component. The key variable is viscosity and can affect churning loss. Furthermore, two-phase flow is studied to analyze the impact of air in lubrication system. In another study, a combined numerical and experimental approach of two moving curved surfaces is carried out by Deng et al. [15]. It is shown the authenticity of MPS method compared to mesh-based CFD methods in reaching accurate results.

Thermal stress analysis in components is vital to guarantee reliable as well as safe operation subjected to tense and extreme conditions. Heat mostly brings about expansion and contraction in materials causing critical mechanical stresses which are able to overshadow performance and integrity of components. Omitting thermal stress in design and operation stages results in deformation, premature degradation and cracks in components causing failure and heavy losses. Therefore, thermal stress analysis gives engineers the opportunity to improve and optimize design, materials and manufacturing processes to assure long-term performance, durability and safety of components. Among thermal stress of different parts of transmission system, analysis of bearings is of the most important components owing to tolerating high speed, temperature and load. During operation, bearing produce heat and if it is not dissipated correctly, it leads to wear, failure and crack. Hence, based on analysis the heat generation can be tackled and is helpful to find problems with the lubrication system. This is why many papers are carried out to analyze thermal characteristics of transmission system with respect to different variables. Patil and Kumar [16] investigated thermo-mechanical stress analysis of gearing according to different rotating speed, load and lubrication. In this study, in addition to explaining the importance of lubrication system, it is concentrated on prevention of overheating the oil which leads to better performance of whole system. Considering different oil characteristics, various heat transfer coefficients are analyzed. Moreover, it is declared that increase in rotating speed,

the torque rises. Liu and Xu [17] carried out a paper focusing on oil lubrication of high-power roller bearing utilizing FVM and slip mesh model. In this work, various rotating speed in roller bearing and consequently its heat generation are considered. This gives the opportunity to analyze based on real conditions in static and transient cases and it is declared higher accuracy of transient case with experimental results. It is depicted higher temperature of bearing outer ring compared to inner ring and increase in speed causes higher temperature distributions and also dependent on number of nozzles. In another project [18], lubrication and temperature analysis of transmission system with splash lubrication is studied. The concentration is on bearings and gears in gearbox, it is demonstrated role of lubricant in gear meshing area due to high heat generation, particularly in driving gear. Likewise, temperature distribution in bearings is largely related to lubrication environment between inner and outer ring. Efficiency assessment of racing engine gearbox considering various speed and load is conducted by Douglas and Thite [19]. It is spelled out that in spite of superior behavior of high-pressure viscosity coefficient efficiency of gear has inverse relation with viscosity. It is demonstrated that for optimized performance, the oil lubricant temperature should be controlled closely. Li et al. [20] investigated thermal analysis of helical gear of gearbox showing different heat flux in spur gear and helical gear. Literally, helical gear temperature distribution is asymmetric along tooth direction. The high temperature zone is near gear meshing entry point at the top and at the root is near gear meshing exit point.

Any change or customization done to the shell of gearbox hints at casing modifications. These changes are made usually to enhance efficiency and performance of gearbox. There exist various kinds of modifications of casing consisting of inserting cooling fins, adding shield for lubrications, improving the materials and increment of size of casing to mount larger components. It should be noted that in some modifications, we must pay attention to alleviation of stress concentration and thrive overall gearbox strength. Magerramova et al. [21] analyzed gearbox housing made up of additive manufacturing. They declared that the usual technologies for constructing housings have limitations while additive manufacturing can solve these problems to a large extent. Using this method weight of gearbox can decrease 15% while guaranteeing strength. Moreover, the thickness of tidal wall decreases by 18%. Nasser et al. [22] assessed structural modifications of gearbox casing and their resulted that inserting ribs on the top cover gearbox casing can enhance cooling and lubrication and vibration. In fact, presence of added ribs can enhance lubrication using increment of gravity through rising internal area on the top cover. Patel and Patil [23] investigated modification on triple reduction gearbox casing.

The assessment of lubricant flow field distributions in transmission system is of great importance to performance prediction and to decline churning loss and dissipate frictional heat. In this project, auxiliary railway on top of the gears, inside input and shifting shafts are supplied to optimize performance of critical components. The MPS method is used to simulate lubricant distributions inside and outside of separate shafts to detail behavior of components and different variables including oil viscosity, temperature and rotating speed are studied. Moreover, modifications are applied in order to have maximum oil dispersion in meshing gear areas and bearings. Likewise, the internal heat generation in critical bearings besides heat transfer coefficients are achieved by which thermal stress in that component is analyzed. Consequently, churning loss in different shafts are computed according to different viscosity. This project can present some approaches for optimizing the lubrication system in gearbox.

2. MPS theory

MPS method is according to Lagrangian approach in order to simulating continuum mechanics proposed by Koshizuka et al. [24]. This method was presented to assess incompressible fluids and its main principle is a weighted difference in absence of mesh. The traditional methods such as FVM are based on mesh whereas particle-based methods (Fig. 1) require no mesh in case of discretization of governing equations. Generation of mesh is literally complex in majority of domains and in order to have more accurate results finer mesh is expected that needs more computation time. In MPS method, particle initial arrangement is vital but is simpler than generation of mesh.

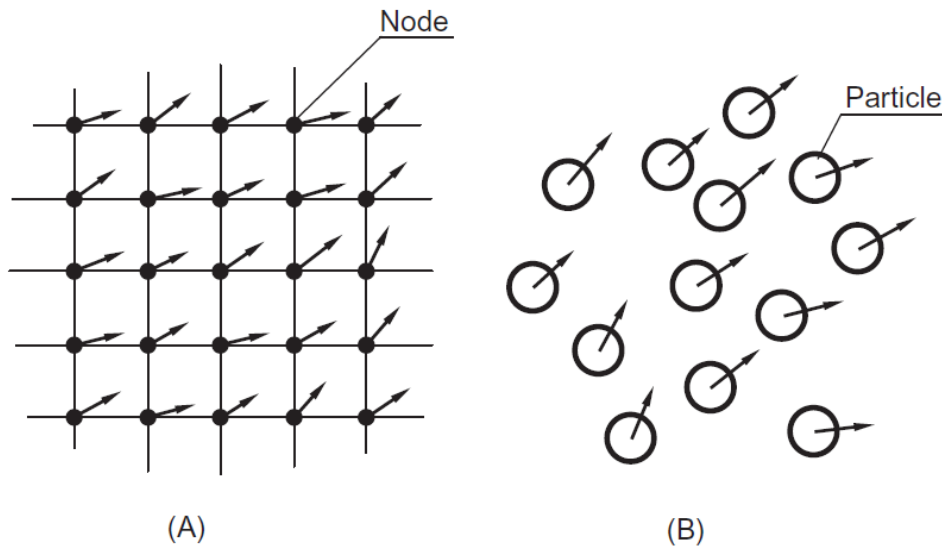


Figure 1 (A) mesh approach and (B) meshless approach

2.1. Governing equations

Similar to other mesh methods, in MPS method the concentration is on the governing equations ascertaining the rules of phenomena. For the MPS method, governing equations include equation of continuity (mass conservation), Navier-Stokes equations (momentum conservation) and energy equation consisting of fluid governing equations. It should be noted that each particle coordinate and velocity vector is updated according to time step and in fact the movement of particle is predicted based on its interaction with adjacent particles.

2.1.1. Navier-Stokes equations

The equation can be written as follow [24]:

$$\frac{D\mathbf{u}}{Dt} = -\frac{1}{\rho}\nabla P + \nu\nabla^2\mathbf{u} + \mathbf{g} \quad (1.2)$$

in which $\frac{D\mathbf{u}}{Dt}$ indicates the material derivative of fluid velocity and defines particle acceleration. The equation shows that fluid acceleration includes three components; the first right-hand side term named pressure gradient term refers to acceleration related to gradient of pressure field. ρ describes fluid density and is essential to determine the effect of fluid mass. The second term, viscous term, refers to acceleration created by viscous force which spread the fluid momentum. To put it simply, the particles interact and collide with each other leading to creation of friction effects and generate fluid velocity similar to adjacent fluid particle velocity.

2.1.2. Continuity equation

The equation can be defined as follow [24]:

$$\frac{D\rho}{Dt} = -\rho\nabla\cdot\mathbf{u} \quad (2.2)$$

This equation shows how density of fluid is altered based on mass flow from a unit volume. The left-hand side term expresses time change of fluid density per unit. The right-hand side term defines the fluid volume that is emitted from a unit volume. It is understood that density is reduced every time the mass is emitted from the unit volume. In the MPS method, continuity equation is fully satisfied, because there are no changes in particle mass and number by passage of time.

2.1.3. Energy equation

The energy equation is expressed as follow [24]:

$$\rho\frac{De}{Dt} = -\nabla\cdot\mathbf{q} - p\nabla\cdot\mathbf{v} - \boldsymbol{\tau}:\nabla\mathbf{v} \quad (3.2)$$

In above equation, e describes specific internal energy per unit of mass and q refers to heat flux vector. The second term on the right-hand side is reversible rate of increase in internal energy per volume and the last term is irreversible rate of increase in internal energy per volume owing to dissipation of viscosity. This equation includes net convective flow rate, net heat flux and rate of work done by pressure, gravity and viscous stresses. It should be noted that for the incompressible fluids, ρ is considered constant.

2.2. Semi-implicit methodology

Assuming incompressible fluid and by applying continuity equation to Navier-Stokes equations, we can remove the terms containing velocity and compute pressure. Implicit method is able to compute pressure with respect to solution of simultaneous linear equations that are defined by unknown pressures of fluid related to the next time step. Explicit method computes unknown values without solution of simultaneous equation and is according to values at the current time step. However, in semi-implicit method, the motion of particles can be predicted based on acceleration terms on Navier-Stokes equations right-hand side. Since the particle pressures are unavailable, at the first step, the pressure gradient term is disregarded. Therefore, as a result the particles take the behavior according to viscous term and gravity. It should be noticed that in this step, owing to omitting pressure gradient term, an area exists in which the particle densities are not constant and the incompressibility condition is not fulfilled. In the next step, the pressure gradient term is calculated, by which the appropriate particle positions and velocities can be updated and achieved. The mentioned series of strategy are repeated until the time of simulation reaches.

In the MPS method, the Navier-Stokes equations are solved using fractional step approach. Generally, the operators such as Lagrangian derivative, Nabla, Gradient and Laplacian can not be analytically computed. For integration of $\frac{D\mathbf{u}}{Dt}$ and gaining the velocity for the next step, it can be discretized:

$$\frac{D\mathbf{u}_i}{Dt} \cong \frac{u_i^{k+1} - u_i^k}{\Delta t} \quad (4.2)$$

where u_i^{k+1} and u_i^k describe respectively the velocity of i th particle at k and $k + 1$ time step. Δt is the difference between the next and current time step. Hence, k refers to known parameters and $k + 1$ refers to unknown parameters. By substituting Eq. (4.2) in Eq. (1.2), new form of Navier stokes equations yield as follow:

$$\frac{\mathbf{u}_i^{k+1} - \mathbf{u}_i^k}{\Delta t} = -\frac{1}{\rho} \langle \nabla P \rangle_i^{k+1} + \nu \langle \nabla^2 \mathbf{u} \rangle_i^{k+1} + \mathbf{g} \quad (5.2)$$

Where P^{k+1} is unknown pressure at the next time step and as mentioned above, the pressure gradient term is omitted and with respect to utilizing Laplacian (expressed in the 2.2.5 section) operator in MPS method, we have [24]:

$$\mathbf{u}_i^* = \mathbf{u}_i^k + \left\{ \nu \frac{2d}{\lambda^0 n^0} \sum_{j \neq i} (\mathbf{u}_j^k - \mathbf{u}_i^k) w(|\mathbf{r}_j^k - \mathbf{r}_i^k|, r_e) + \mathbf{g} \right\} \Delta t \quad (6.2)$$

In which \mathbf{u}_i^* expresses temporal velocity, d represents the number spatial dimensions and for three-dimensional analysis is equal 3. n^0 is used to normalize the whole weight and λ^0 defines the squared distance average within particles. $w()$ refers to weight function that is defined in next section. These parameters are essential for calibrating the absolute value of the Laplacian. At the next step, in order to calculate the temporary positions \mathbf{r}_i^* , we use the following formula

$$\mathbf{r}_i^* = \mathbf{r}_i^k + \mathbf{u}_i^* \Delta t \quad (7.2)$$

Then, by calculating the temporary position, the particle pressure distributions are calculated as follow [24]:

$$\langle \nabla^2 P \rangle_i^{k+1} = -\rho^0 \frac{1}{(\Delta t)^2} \frac{n_i^* - n^0}{n^0} \quad (8.2)$$

In which n_i^* defines density of particle number of i th particle in temporary particle position. Afterwards, in order to compute the correct velocity vector and position of next time step according to derived pressure, the following equations are used respectively:

$$\frac{\mathbf{u}_i^{k+1} - \mathbf{u}_i^*}{\Delta t} = -\frac{1}{\rho^0} \langle \nabla P \rangle_i^{k+1} \quad (9.2)$$

$$\mathbf{r}_i^{k+1} = \mathbf{r}_i^* + (\mathbf{u}_i^{k+1} - \mathbf{u}_i^*) \Delta t \quad (10.2)$$

In overall, benefit of the MPS method in calculation of convection term would be easy ability of computation of particle displacements, because all equations are implemented to particles consisting of free surface and there is no need special approach. Likewise, the MPS method exploits easy computation of temporary velocity. To put it simply, The Navier-Stokes equation is solved considering continuity condition applying to the particle approximation for incompressible flow. Temporary velocity \mathbf{u}_i^* as well as position \mathbf{r}^* are derived utilizing viscous and external force terms explicitly, Eq. (6-2) and Eq. (7.2). The pressure can be calculated implicitly, Eq. (8.2) and finally the corrected velocity and position are derived with Eq. (9-2) and Eq. (10.2). Following figure can outline the procedure considered in this method.

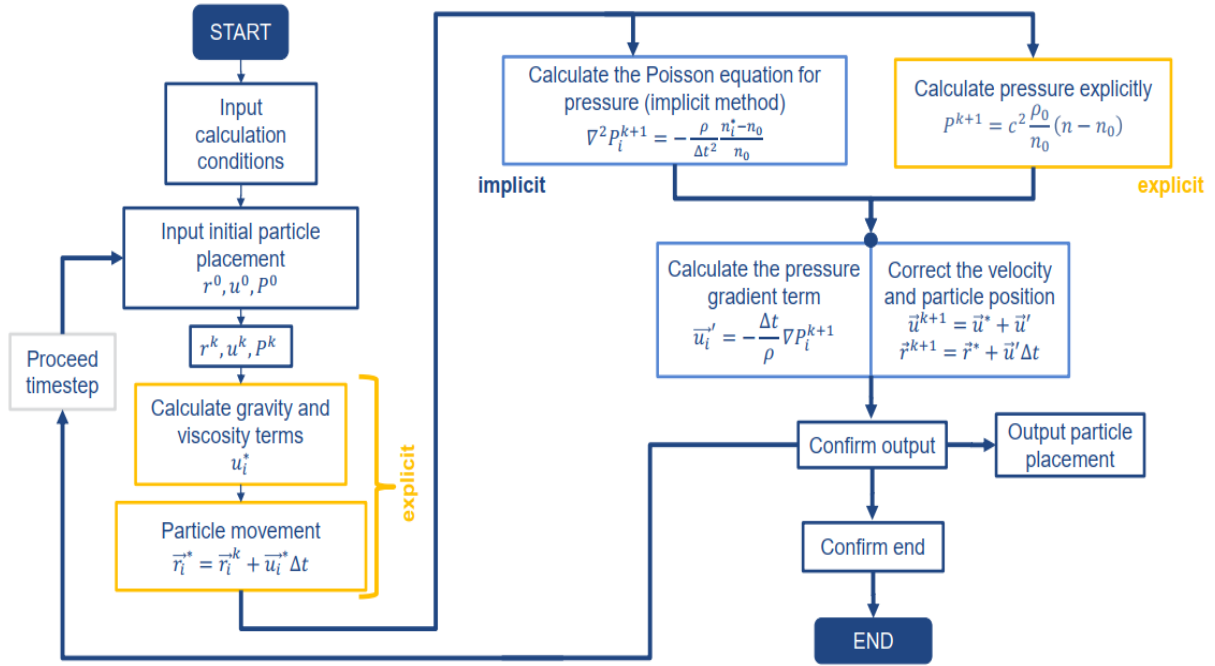


Fig 2.1. MPS procedure

2.2.1. Number of density of particles and weight function

Fluid density plays important role in simulations, because according to (Eq. 2.2) the mass conservation is defined by fluid density and moreover, pressure is achieved with fluid density. In case of analysis of gas that is compressible fluid, pressure can be computed with equation of state. On the other hand, in case of liquid analysis (incompressible fluids), density of fluid is constant and new conditions are applied. For the MPS method, particle number density is utilized in order to gain density of fluid. Literally, density of particle number depicts the particle number around one particle. The particle number density is introduced for aggregation of weight of neighboring particle. That would be a unique variable describing dimensionless amount of arrangement density. Fig. 2.2 illustrates the approach of particle number density computation in position of one specific particle. The color transparency refers to weigh of particles.

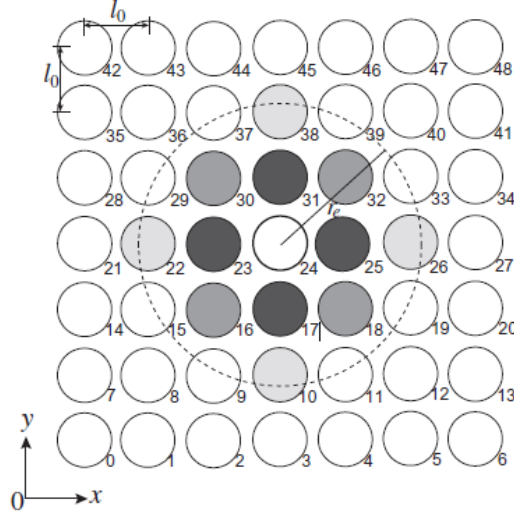


Fig 2.2 Weight function diagram

The darker the color conveys the larger weight and vice versa. Therefore, the following equation is used for calculation of particle number density [24]:

$$n_i = \sum_{j \neq i} w(|\mathbf{r}_j - \mathbf{r}_i|, r_e) \quad (11.2)$$

In which n_i describes particle number related to i th particle, r_i expresses vector of position of i th particle, r_j refers to vector of position of neighboring particles j and $w()$ defines weight function. It is noticed that if the interaction zone area between particles surpasses effective radius r_e , above equation equals zero. In order to achieve real behavior of fluids, one program should be written by which only neighboring particles are considered. With respect to that, the weight function can be written as follow:

$$w(r, r_e) = \begin{cases} \left(\frac{r_e}{r}\right) - 1 & (r < r_e) \\ 0 & (r \geq r_e) \end{cases} \quad (12.2)$$

In which r is the interaction zone between particles and r_e expresses effective radius related to collision zone. Fig 2.2 illustrates the weight function in accordance with Eq. 11.2. It is clear that increment of distance between particles can cause function reduction.

2.2.2. Boundary conditions

Similar to other numerical methods, the MPS method needs to consider boundary conditions for solution of pressure Poisson equation. The first type is Dirichlet boundary condition that is able to assign related parameters to specific values. This kind of boundary conditions is considered standard

value of distribution of pressure in the MPS method. Likewise, the pressure of particles can be regarded relative values that their standard value is zero on free surfaces. Literally, designating zero value to free-surface particles is regarded as Dirichlet boundary condition. It should be noticed that every time the particle number density fulfills Eq. 13.2, the particle is considered as free surface and consequently zero.

$$n_i < \beta n^0 \quad (13.2)$$

In which β describes an empirically-determined scalar parameter and most of the times, it is 0.97. The second kind of boundary condition in the MPS method is Neumann boundary condition. This type of boundary conditions can be utilized in case of wall boundaries in pressure computation. To put it simply, in the MPS method, the Neumann boundary condition is designated to wall boundaries and is zero pressure gradient. Moreover, dummy particles (two layers), that do not have pressure values, are placed behind the wall particles. By applying this boundary condition, penetrating the fluid particles within the walls can be prevented.

In case of velocity boundary condition, no-slip boundary condition related to stationary wall is defined. Slip boundary condition can be described with disregarding neighboring wall particles in computation of viscosity. Likewise, if adjacent particle l is wall particle, hence the interaction between fluid j and wall particle i is not calculated. In this case, the viscosity force does not affect wall and fluid.

2.2.2.1. Boundary conditions of inlet and outlet

The fundamental scheme of inlet and outlet boundaries in the MPS method is presented in [24]. For the inlet case, particles with the assigned velocity or flowrate should be created and positioned into the domain with constant frequency as shown in Fig. 2.3. At the first step, dummy particles in addition to wall particles are positioned regularly with a known distance between particles (l_0) outside the inlet boundary. It should be utilized as well moving particles for representing inflow condition. Therefore, as can be seen after applying the velocity to the particles, the wall particles are converting to fluid particles while entering the domain. This procedure is implemented to dummy particle to be converted to wall particles. It should be noted that the wall particle pressure is unknown and is determined by solution of Poisson equation. The outlet boundary conditions would be simpler than in inlet one. Outflow is regarded as eliminating particles leaving the domain. Dirichlet boundary conditions are considered for outlet boundary. Hence, pressure is inserted on any particle locating close to the boundary.

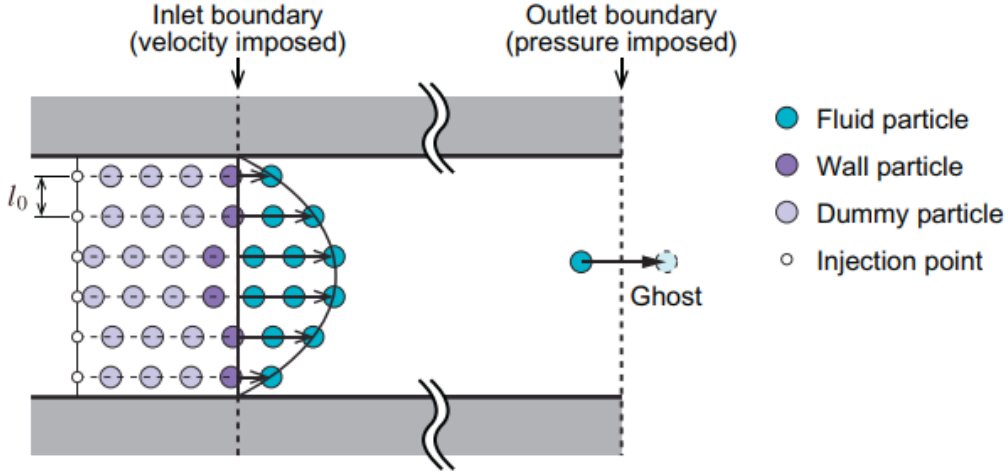


Fig 2.3 Illustration of fluid, wall and dummy particles

2.2.3. Turbulence

In the MPS method, a subparticle-scale turbulence model is used [25]. In this approach, the velocity vector is split to spatially averaged value \bar{u}_α and fluctuating value u'_α as following:

$$u_\alpha = \bar{u}_\alpha + u'_\alpha \quad (14.2)$$

Likewise, all variables in Navier-Stokes equations are substituted with spatially averaged values as well as fluctuating values. Therefore, it yields:

$$\frac{D\bar{u}_\alpha}{Dt} = -\frac{1}{\rho} \frac{\partial \bar{P}}{\partial x_\alpha} + \nu \frac{\partial}{\partial x_\beta} \left(\frac{\partial \bar{u}_\alpha}{\partial x_\beta} + \frac{\partial \bar{u}_\beta}{\partial x_\alpha} \right) - \frac{\partial (\overline{u'_\alpha u'_\beta})}{\partial x_\beta}. \quad (15.2)$$

The last term on the right-hand side of above equation is Reynolds stress deriving from the convection aspect that is a nonlinear term and Lagrangian derivative. It can be written as follow:

$$-\overline{u'_\alpha u'_\beta} = \nu_t \left(\frac{\partial \bar{u}_\alpha}{\partial x_\beta} + \frac{\partial \bar{u}_\beta}{\partial x_\alpha} \right) - \frac{2}{3} k \delta_{\alpha\beta} \quad (16.2)$$

where k expresses turbulence kinetic energy and δ defines delta function. Moreover, ν_t defines eddy viscosity that can be achieved as follow:

$$\nu_t = (C_s \Delta)^2 \left\{ \left(\frac{\partial \bar{u}_\alpha}{\partial x_\beta} + \frac{\partial \bar{u}_\beta}{\partial x_\alpha} \right) \frac{\partial \bar{u}_\alpha}{\partial x_\beta} \right\}^{1/2}. \quad (17.2)$$

In which Δ and C_s are respectively particle size and Smagorinsky constant. By substitution of Eq. 16.2 in 12.2 the following equation can be achieved [25]:

$$\frac{D\bar{u}_\alpha}{Dt} = -\frac{1}{\rho} \frac{\partial \bar{P}_t}{\partial x_\alpha} + (v + v_t) \frac{\partial}{\partial x_\beta} \left(\frac{\partial \bar{u}_\alpha}{\partial x_\beta} + \frac{\partial \bar{u}_\beta}{\partial x_\alpha} \right), \quad (18.2)$$

It should be noticed that in above equation, viscosity and pressure rise in case of turbulent flow.

2.3. Particle action model

In the MPS method several operators including Gradient and Laplacian are utilized in order to solve Eqs. (1-2) - (1-3). For solving the model analytically, the partial derivative operators should be converted to basic operators. Hereby, the gradient operator can be written as:

$$\langle \nabla \phi \rangle_i = \frac{d}{n^0} \sum_{i \neq j} \left[\frac{(P_j - P_i)}{|\mathbf{r}_j - \mathbf{r}_i|} \frac{(\mathbf{r}_j - \mathbf{r}_i)}{|\mathbf{r}_j - \mathbf{r}_i|} w(|\mathbf{r}_j - \mathbf{r}_i|, r_e) \right] \quad (19.2)$$

in which ϕ is an arbitrary physical quantity, d describes the number of spatial dimension and $\frac{(P_j - P_i)}{|\mathbf{r}_j - \mathbf{r}_i|}$ hints at steepness of pressure in the $\mathbf{r}_j - \mathbf{r}_i$ direction at the i th particle location. Similarly, $\frac{(\mathbf{r}_j - \mathbf{r}_i)}{|\mathbf{r}_j - \mathbf{r}_i|}$ expresses, the unit direction vector leaded from the i th particle to the j th particle. Moreover, $w()$ is a weight function. Furthermore, Laplacian operator is used in pressure Poisson equation, viscosity term and for thermal equation. For discretization of Laplacian operator, we have [24]:

$$\langle \nabla^2 \phi \rangle_i = \frac{2d}{\lambda^0 n^0} \sum_{i \neq j} (\phi_j - \phi_i) w(|\mathbf{r}_j - \mathbf{r}_i|, r_e) \quad (20.2)$$

3. Frictional moment in bearings

The frictions in the bearings are dependent upon specific occurrences taking place in lubricant film among inner ring, outer ring and cages. In lubrication fields, Stribeck curve, Fig. 3.1, can be considered as one of the fundamental concepts expressing the friction phenomena (vertical axis), in two fluid-lubricated surfaces, which is related to speed, lubricant viscosity and load (horizontal axis).

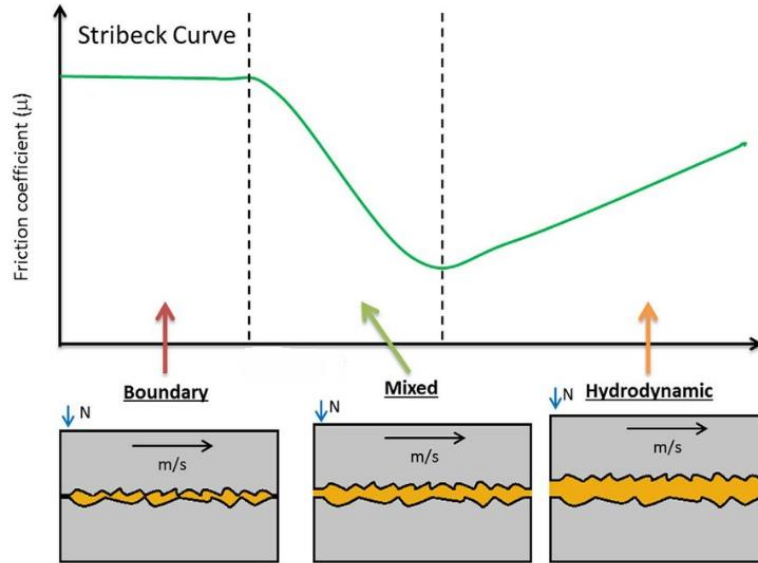


Fig 3.1. Stribeck curve

As can be seen in figure, in boundary regime, a steady contact between the two surfaces (at highest points of surface) takes place at boundary lubrication hence, only the asperities bear the loads. This kind of film lubrication is regarded as most unfavorable due to high friction coefficient leading to energy loss, wear and uneven dispersion of bearing load. It should be noted that most intense bearing failures originate from boundary lubrication and it mainly happens at low-speed friction. In mixed regime, the lubricants between two surfaces are able to bear part of load and friction is reduced thanks to fewer contact between asperities. Hydrodynamic regime occurs at high-speed rotations and low bearing loads. In this case, there is no contact between asperities, because the film can keep the surfaces away from each other due to hydrodynamic force created with the squeezed film. Moreover, increment of temperature in mixed zone leads to growing the friction coefficient and this regime is assumed unstable.

In order to reach the whole frictional moments for bearings, several sources and their influences should be involved including rolling frictional moment, sliding frictional moment and the consequent influence on the lubrication quality, frictional moment due to seal and frictional moment due to drag and churning losses which are defined as follow:

3.1. Rolling frictional moment

The rolling frictional moment is expressed as follow [26]:

$$M_{rr} = \phi_{ish} \phi_{rs} G_{rr} (vn)^{0.6} \tag{3.1}$$

in which ϕ_{ish} defines inlet shear heating reduction factor, ϕ_{rs} describes kinematic replenish reduction factor, n refers to rotating speed, v expresses operating viscosity and G_{rr} is a parameter related to bearing type, mean diameter (d_m), radial and axial loads.

In fact, ϕ_{ish} is a small portion of entire oil quantity in bearing crossing the contact area and only fraction amount is needed for creation of hydrodynamic film. Hence, portion of the lubricant near to contact area is pushed back and creates a reverse flow. This opposite flow can change behavior of lubricant and creates heat resulting in reduction of oil viscosity and thickness of oil film (Fig 3.2).

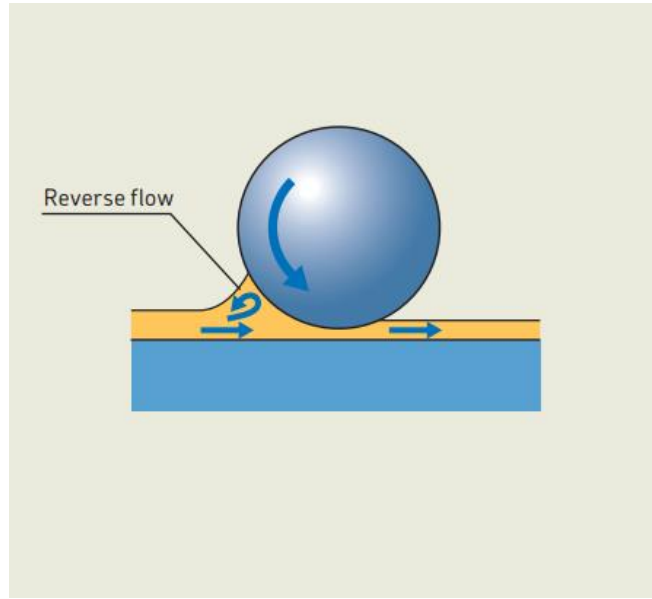


Fig. 3.2. Illustration of influence of inlet shear heating reduction factor

As a result, the inlet shear heating reduction factor is written as follow:

$$\phi_{ish} = \frac{1}{1 + 1.84 \times 10^{-9} (nd_m)^{1.28} v^{0.64}} \quad (3.2)$$

In case of jet lubrication and lubrication at low level in which the lubricant level is below the center of rolling part, steady rolling shows surplus oil from raceways. In conditions that rotating speed or operating viscosity are high, it is possible that the oil won't have enough time to refill the raceways bringing about kinematic starvation influence. This situation can lead to decrease in hydrodynamic film thickness and consequent rolling friction. Therefore, for calculation of kinematic starvation reduction factor, we have [26]:

$$\phi_{rs} = \frac{1}{e^{\left[K_{rs} v n (d+D) \times \sqrt{\frac{K_z}{2(D-d)}} \right]}} \quad (3.3)$$

where K_{rs} describes starvation factor and for our case study is 3×10^{-8} , K_z expresses bearing type geometric constant which is related to characteristics of bearing [26], d and D are respectively bearing bore and outside diameter.

3.2. Sliding frictional moment

The sliding frictional moment is expressed as follow:

$$M_{sl} = G_{sl}\mu_{sl} \quad (3.4)$$

in which G_{sl} is a parameter related to bearing type, mean diameter, radial and axial forces [26]. μ_{sl} describes the sliding friction factor and for mixed and full-film lubrication it can be written as follow [26]:

$$\mu_{sl} = \phi_{bl}\mu_{bl} + (1 - \phi_{bl})\mu_{EHL} \quad (3.5)$$

where ϕ_{bl} is the weighting factor for the sliding friction coefficient according to Fig. 3.3, ϕ_{bl} is a constant related to movement and for this case study is 0.15 and μ_{EHL} describes sliding factor coefficient in full-film situations. As seen in the following figure, in case of full-film lubrication, this value shifts toward zero whereas this value for mixed condition is close to 1 (while the speed is low), since contact increases among asperities.

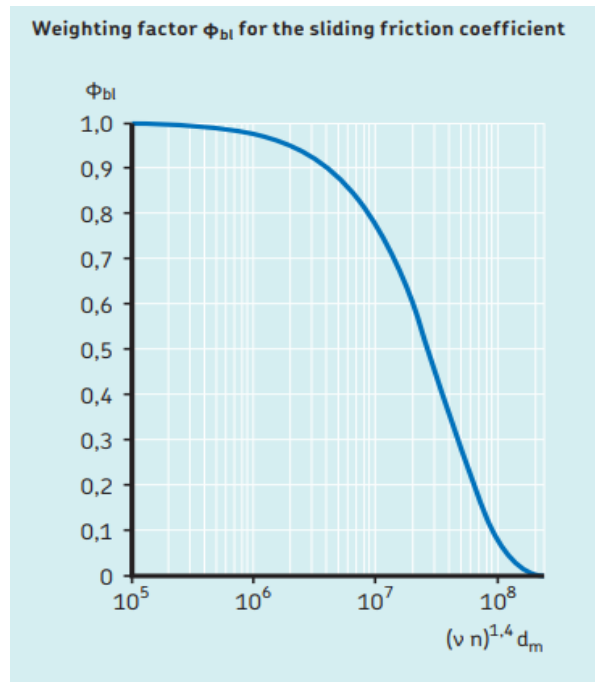


Fig. 3.3 Diagram of weighting factor

3.3. Frictional moment of seals

Seals hint at mechanical parts which hinder from leakage and diffusion of fluid, gas and solid. As a consequent when contact seals are used on bearings, the frictional losses produced with the seal might be greater than those produced with the bearing. The frictional moment related to bearing seals being can be expressed as follow [26]:

$$M_{seal} = K_{S1}d_s^\beta + K_{S2} \quad (3.6)$$

In which K_{S1} is a constant related to size, seal and bearing type, d_s describes seal counterface diameter, β is related to seal and bearing type and K_{S2} is a constant related to size, seal and bearing type. For our case study the values of K_{S1} , β and K_{S2} are respectively 0.0018, 2.25 and 0.

3.4. Drag losses

Lubrication of bearings using oil bath method experiences either fractionally submerged or fully submerged. It should be noticed that the loss related to drag taking place while the bearing is spinning in an oil bath has important role in entire frictional moment and should not be disregarded. In addition, drag losses aren't only dependent upon rotating speed, oil level and viscosity but on oil reservoir geometry and size. External agitation of oil coming from mechanical parts including gears should be considered as well. Eventually, to compute drag losses in oil bath, the resistance of rotating parts crossing through lubricant should also be taken into account. In case of ball bearing, the drag loss can be written as:

$$M_{drag} = 0.4V_m K_{ball} d_m^5 n^2 + 1.093 \times 10^{-7} n^2 d_m^3 \left(\frac{nd_m^2 f_t}{v} \right)^{-1.379} R_s \quad (3.7)$$

in which

$$K_{ball} = \frac{i_{rw} K_z (d + D)}{D - d} \times 10^{-12} \quad (3.8)$$

Where K_{ball} , f_t and R_s are variables depending on size and geometry of ball bearing [26]. V_m describes the drag loss factor, i_{rw} expresses ball rows number, K_z is bearing type related geometry and d and D define bearing bore and outside diameter respectively.

It should be noted that there are other elements affecting frictional moments and one of them can be influence of clearance and misalignment on friction. In bearings, alteration of clearance can affect frictional moment. Generally, a normal internal operating clearance as well as aligned bearing are

considered. Although, in high temperature or speed situations, this clearance could be declined leading to increment of friction. This is valid for misalignment as well.

Finally, for calculation of total frictional moment, we have:

$$M = M_{rr} + M_{sl} + M_{seal} + M_{drag} \quad (3.9)$$

4. Method

In this project gearbox of an electric truck is considered as shown in Fig. 4.1a and Fig. 4.1b.



Fig. 4.1a. Gearbox, heat exchanger and pump

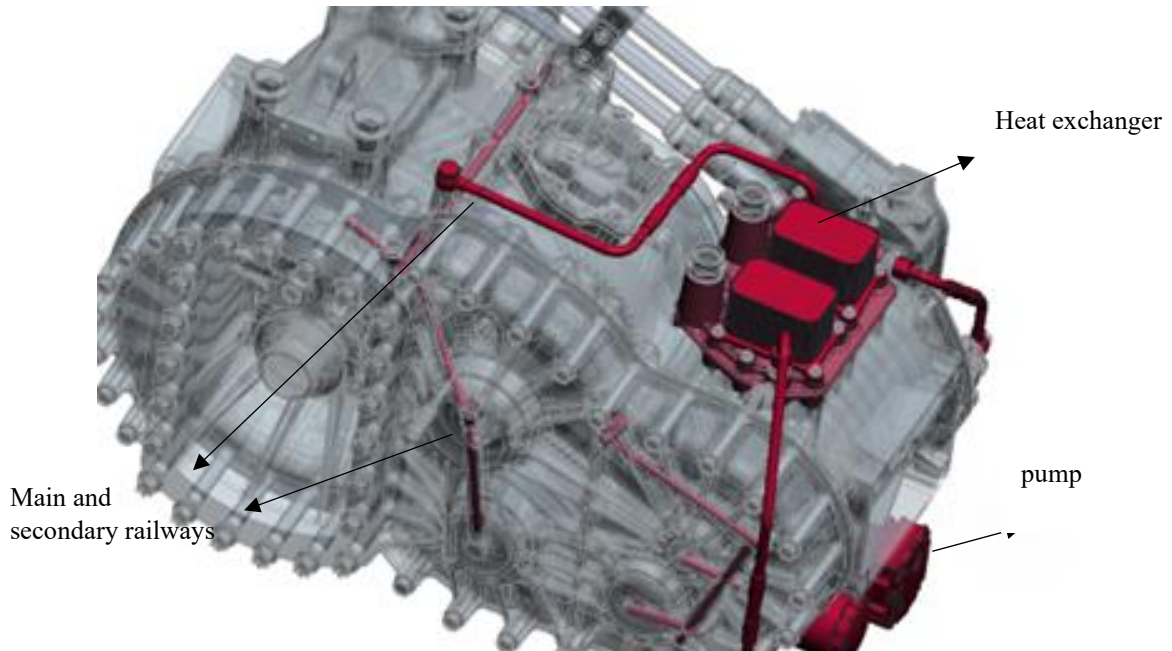


Fig. 4.1b. Gearbox, heat exchanger and pump in CAD software

In general, EV possess higher rotating velocity compared to internal combustion engines. It originates from the fact that electric motors and related gearbox contain higher RPM range and torque output. That leads to maintaining higher velocity easier than internal combustion engine. Therefore, higher

speed can bring about much more friction between various components in gearboxes such as meshing gears, shafts and bearings leading to higher lubricant temperatures. Hence, so as to sustain the efficiency, it is rational to use heat exchanger to cool down lubricant as provided on top of the gearbox housing. Moreover, for creating an effective lubricant distribution system, a pump is inserted that can generate essential pressures. It should be noticed that main and secondary railway lubrication systems have been equipped in order to supply more lubricants to the components experiencing critical situations or is complex and hard to wet with just splash lubrication. Fig 4.1a and 4.1b depict the path of this railway initiated from heat exchanger and distributed inside the shafts. The gearbox includes 4 gear shafts meshing together as shown in Fig. 4.2. It consists of input shaft connected to the motor that has highest speed. The gear in input shaft has contact with idle gear and that has contact with pinion gear on another shaft. Furthermore, Fig. 4.3 illustrates other branches, with details, corresponding to secondary railway that act as jet lubrications in order to reach the oil to the components which are complicated to get wet with splashing.

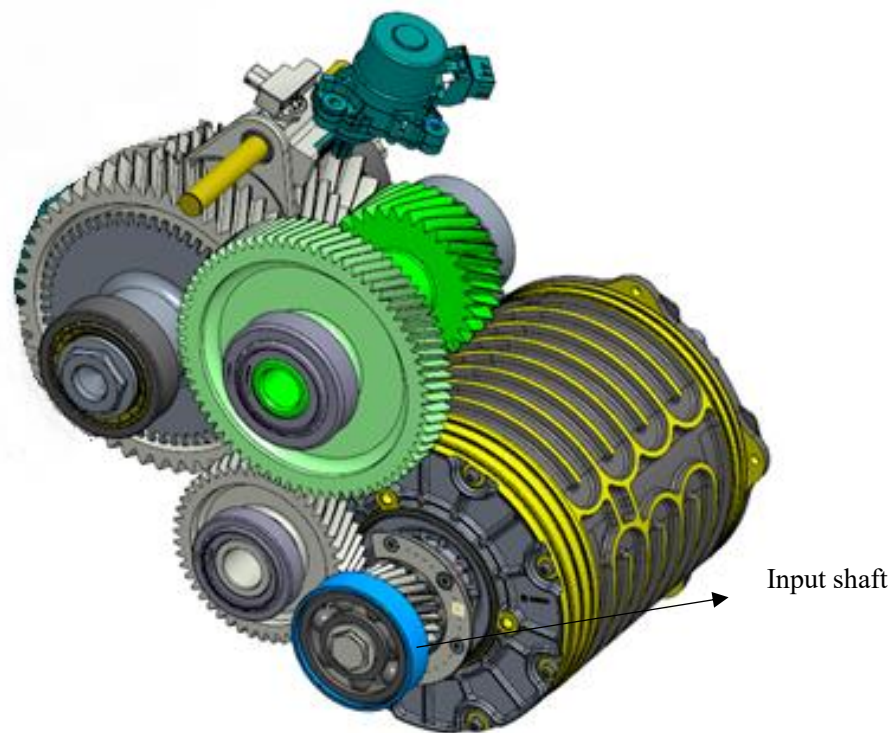


Fig. 4.2. Four gear shafts including input, idle and pinion shafts

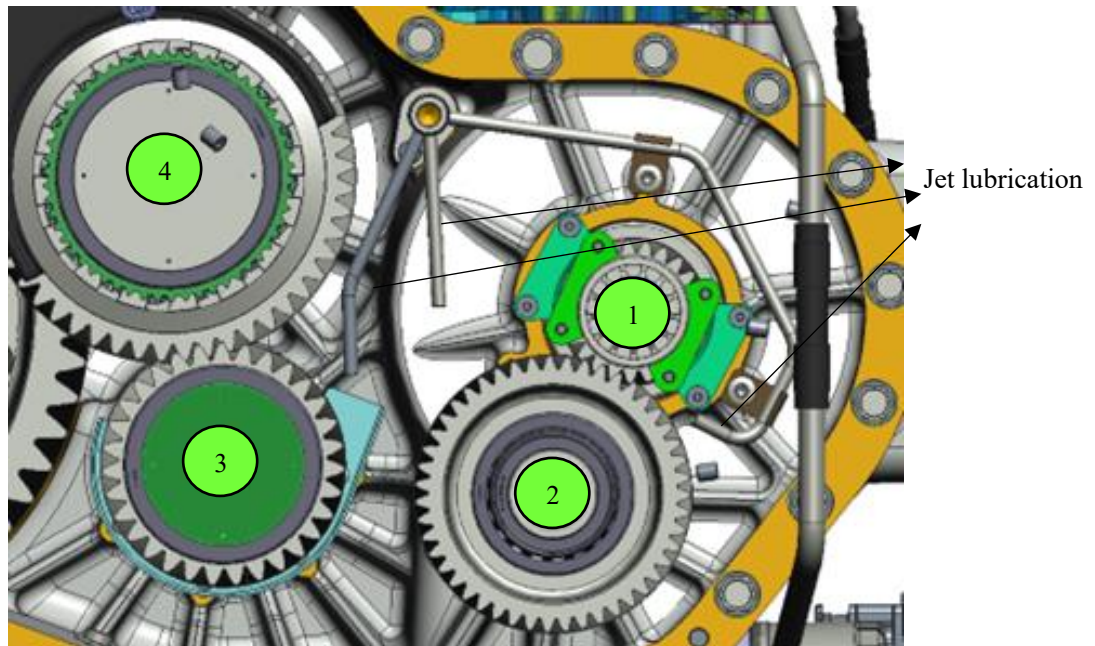


Fig. 4.3. Secondary railways as jet lubrication

In this study, the lubrication system related to main and secondary railways are analyzed to maximize efficiency. To spread our research, we have investigated two different scenarios for temperature. Input shaft has the highest speed and due to transmission ratio, other shafts go through lower speed. The speed for each gear is considered as follow:

	First scenario	Second scenario
1.Input gear (RPM)	9500	10000
2.Idle gear (RPM)	4649	4894
3.Pinion gear (RPM)	3077	3239
4.Shifting gear (RPM)	1947	2048
Vehicle speed (km/h)	120	65

Table 4.1 different speed scenarios

It should be mentioned that, the analyses in this case study are conducted considering 9500 *RPM*. In the next section, lubrication system of every two shafts is investigated in order to reach the accurate results. Hence, at the first step, shaft number 1 with number 2 and at the second step, shaft number 3 with 4 will be analyzed.

4.1. Lubrication system of shaft number 1 with number 2

The input shaft possesses highest speed and temperature among other shafts and therefore requires much cares in case of lubrications. In this shaft there are critical components including ball bearing,

roller bearing and gear. It should be noted that this analysis consists of two different temperatures, in 60°C (low temperature) and in 90°C (high temperature) and two various speeds affecting oil properties and consequent behavior. At the first step, high temperature and lower speed according to Table 4.1 are assigned. The material properties of steel and cast iron can be expressed respectively as follow:

	Steel	Cast Iron
Young's Modulus (<i>GPa</i>)	210	136
Passion Ratio	0.3	0.26
Thermal conductivity (<i>W/mK</i>)	40	50
Hamaker constant	10	10

Table 4.2. Material properties of steel and cast iron

Likewise, the properties of lubricant at high temperature can be written as [23]:

Density (<i>kg/m³</i>)	840
Thermal conductivity (<i>W/mK</i>)	0.136
Specific heat (<i>J/kgK</i>)	2250
Kinematic viscosity (<i>m²/s</i>)	4×10^{-5}
Surface tension coefficient (<i>N/m</i>)	0.072

Table 4.3. Properties of lubricant at high temperature

Fig. 4.4.a illustrates the whole input shaft with surrounding housing by which the lubricant is directed and are important for simulation. As can be seen, it includes roller bearing inside housing, gear and ball bearing.

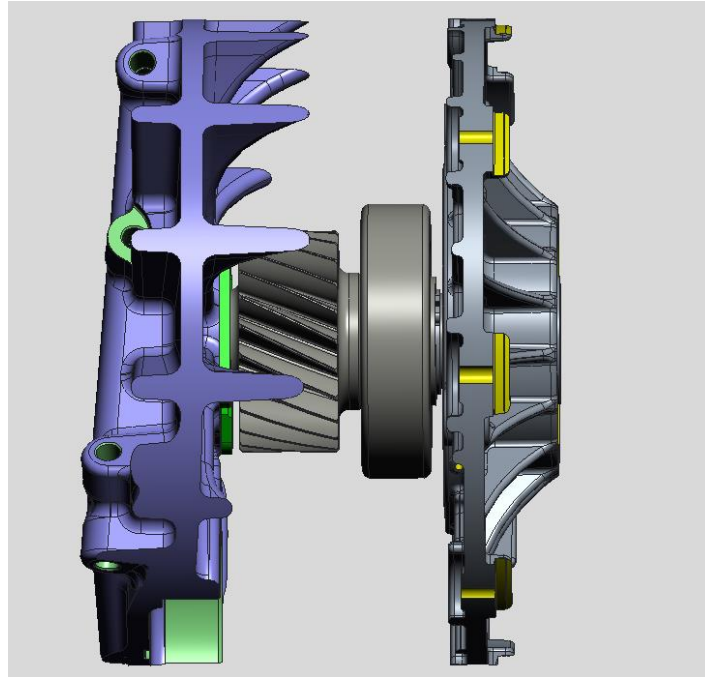


Fig. 4.4.a. Input shaft with surrounding housing

It was thought that splash lubrication is sufficient for making wet meshing area, but it is rational to add jet lubrication near gears. Hence, in order to avert failures in high temperatures, the jet lubrications have been provided to make wet the meshing areas. Furthermore, a nozzle designed and inserted at the entrance of input shaft containing 4 additional holes to direct the lubricant to the roller bearing as well (Fig. 4.4).

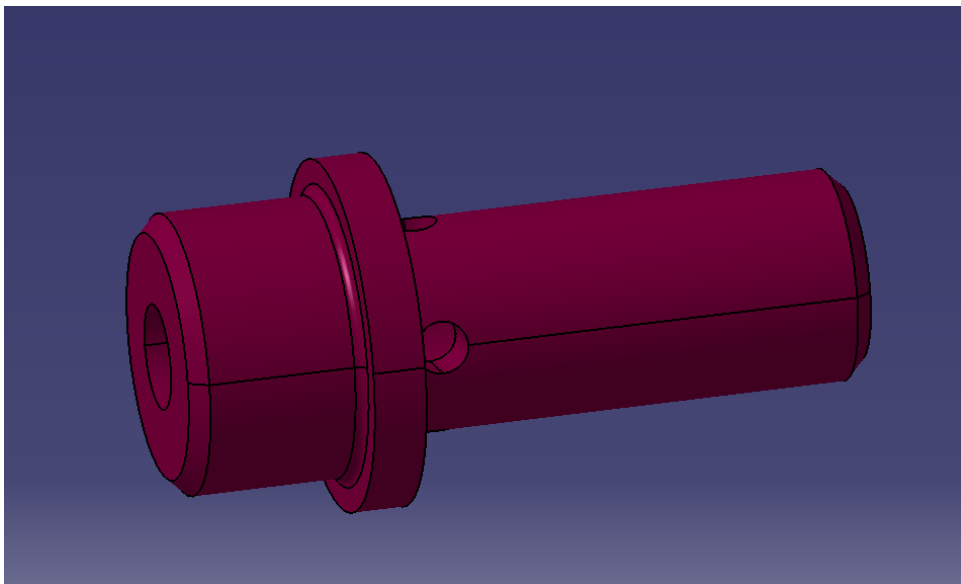


Fig 4.4.b. Nozzle inserted inside input shaft which has 4 holes

Two different methods have been designed and analyzed to make wet the ball bearing and in the next two sections, these are explained. In all simulations, influence of turbulence is discussed. The chaotic

and random motion of fluid particles, which is characterized by irregular oscillations in velocity, pressure, and density, is referred to as turbulence in fluids. It frequently results from the mixing and blending of fluid particles as a result of the interaction between several fluid flows with changing speed, direction, and viscosity.

4.1.1. Radial channels

High temperature

In this scenario, the lubricant reaches inside the input shaft via nozzle and through the radial channel the oil is directed toward ball bearing. It is seen that the efficiency of this scenario is dependent on component rotational speeds and temperature of oil. In this way, owing to high speed the oil is thrown toward ball bearing. The radial channels are depicted in following figures:

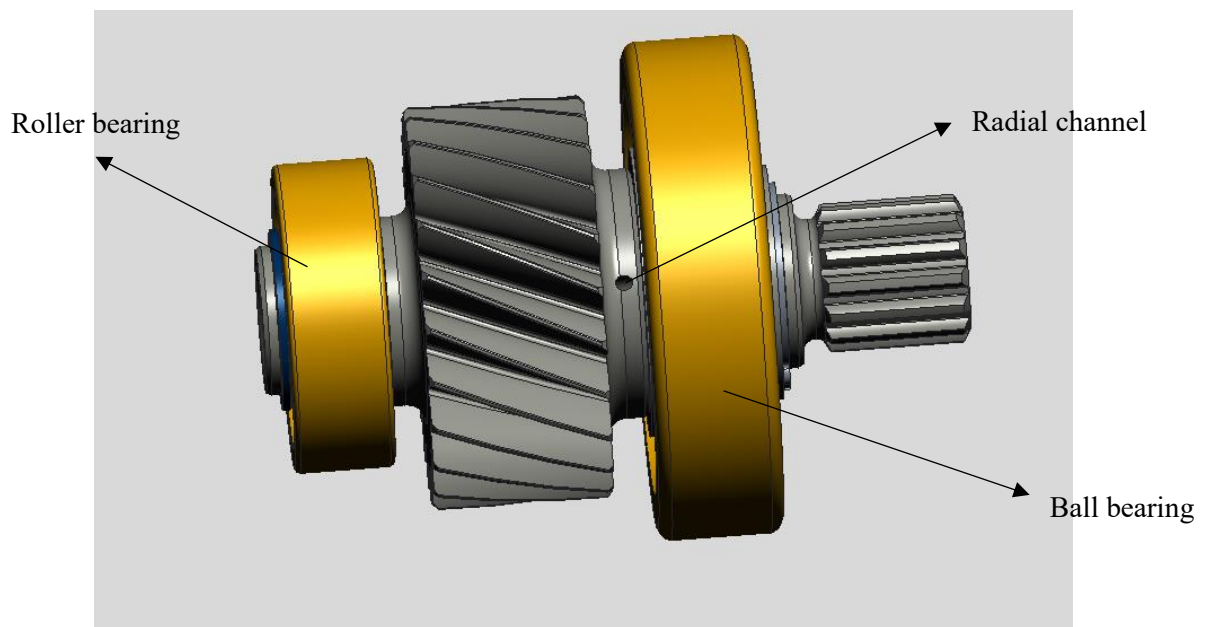


Fig. 4.5a. Input shaft with radial channels

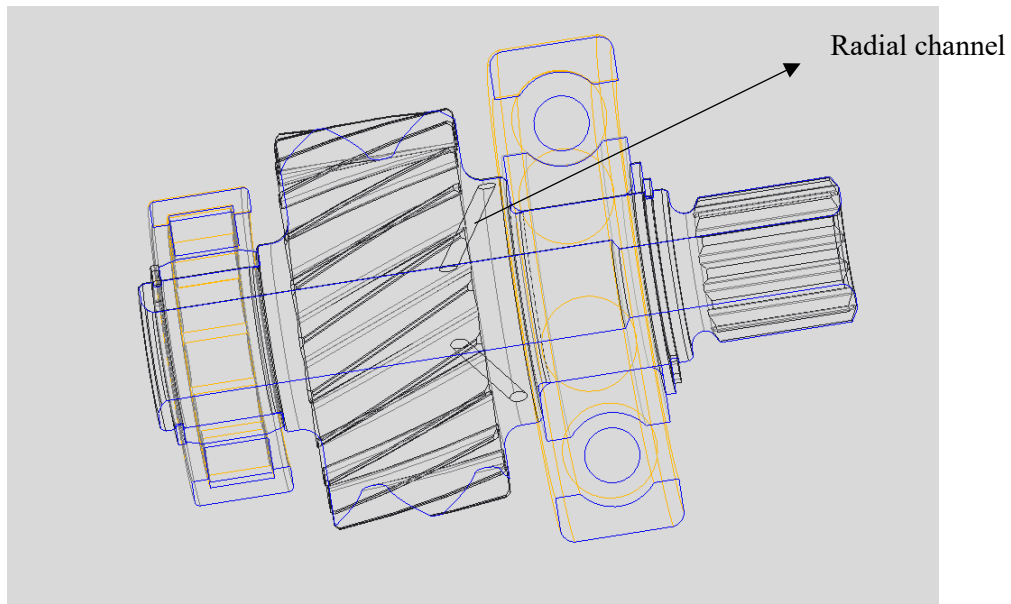


Fig. 4.5b. Radial channels directed toward ball bearing

As mentioned above, we consider high temperature with first scenario for speed in this step and the overall distribution of lubricant inside shaft, roller bearing and ball bearing is illustrated in Fig. 4.6. The dedicated oil flowrate inside the secondary railway to get nozzle is $0.6 \frac{l}{min}$ and the most lubricant speed belongs to droplets coming out of the radial channels which is $31 \frac{m}{s}$. In addition, due to presence of a chamfer in the middle of the shaft, the oil is not able to pass through this step and reach to end of the shaft. In fact, because of high rotational speed, the lubricant turns back to the start point of shaft. It should be noted that the colorbar depicts velocity ranging from $0 \frac{m}{s}$ to $31 \frac{m}{s}$ and particles near balls and rollers have highest speed (red particle) and oil collection inside sealing has the lowest speed (blue particle).

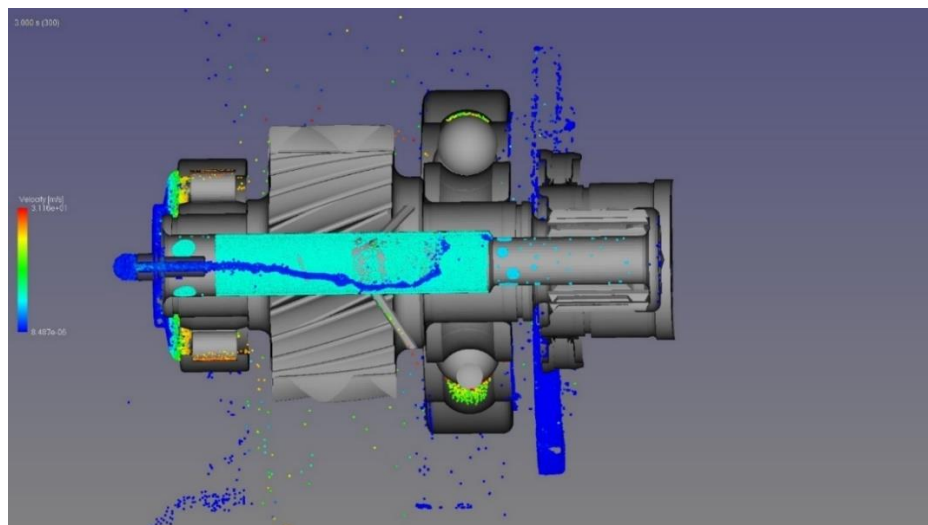


Fig. 4.6. Oil distribution in input shaft

The main purpose of designing secondary railway in this section is to making wet ball bearing going through high speed and temperature that can lead to failures. At high temperature owing to lower viscosity, the lubricant can reach the ball bearing and make it wet. The following figure can illustrate number density of oil surrounded the balls that is satisfying for this step. The colorbar in the following figure illustrates oil number density ranging between 0 and 50 that shows density of oil distributed over ball bearing. On the outer ring and the balls oil distribution is denser which is shown with red.

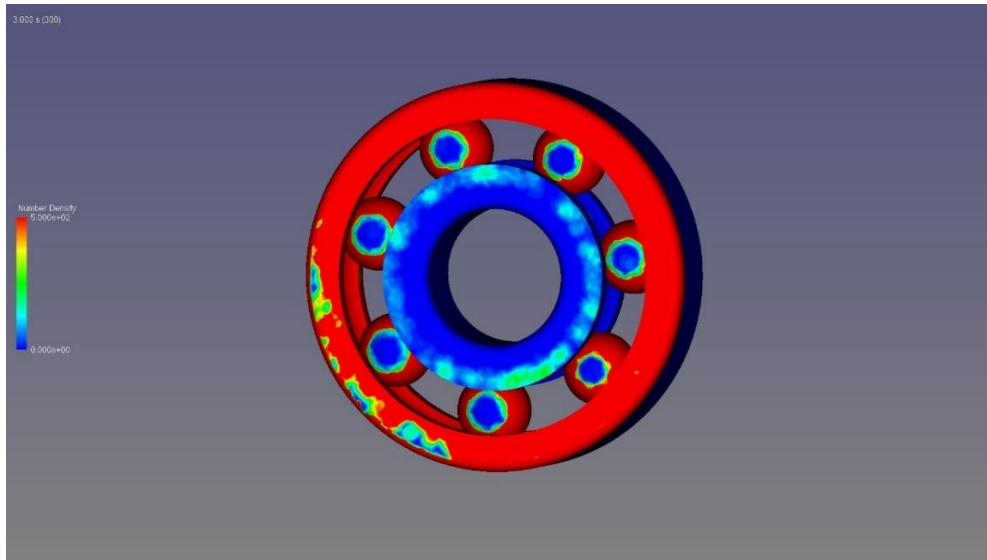


Fig. 4.7. Number density of oil on the ball bearing

One of superiority of particle-based simulation is the ability to calculate number of droplets touching a component and in order to gain the data analytically and realize how much oil reaches the ball bearing in terms of flowrate, we can measure it and it is shown as follow:

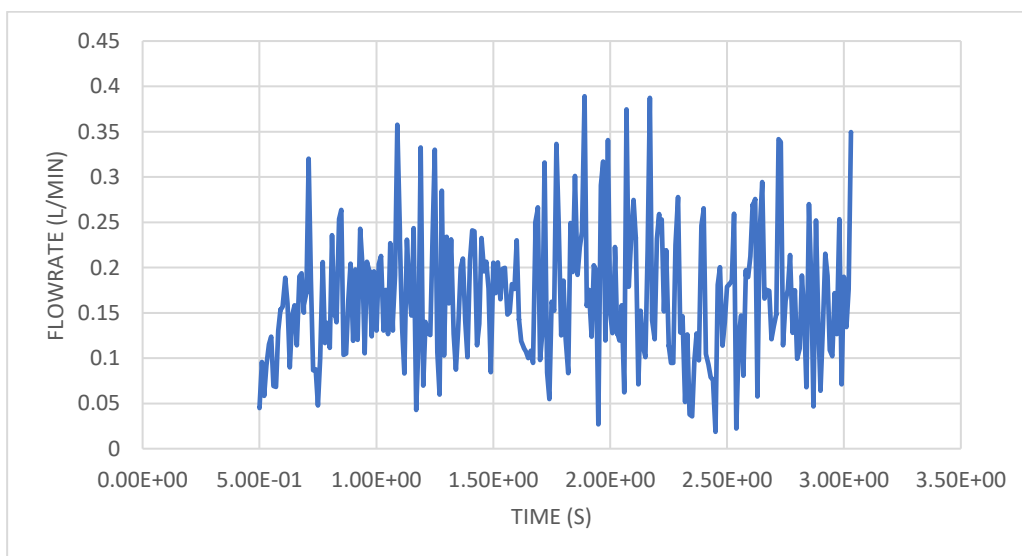


Fig 4.8. Lubricant flowrate reaching ball bearing

With respect to the total flowrate touching inside input shaft, in average $0.2 \frac{l}{min}$ can reach the ball bearing. When oil is moving about inside a gearbox and shaft, there is a power loss known as churning loss. The oil is required to lubricate and cool the shaft's moving elements, but when it is mixed up excessively owing to fast rotational speeds, heat is produced and energy is expended. This energy loss may lower the gearbox's overall efficiency, resulting in diminished performance and increased fuel usage. Designers employ high-performance lubricants that limit shearing losses at high pressures, baffles to reduce oil agitation, and improved gearbox designs that lower the volume of oil being churned to minimize churning loss. Using particle-based software there is the possibility to calculate churning torque which consists of pressure gradient, particle turbulence shear stress and viscous force. Hence, the total churning torque in 3 seconds for this specific shaft (Input shaft) can be shown as follow:

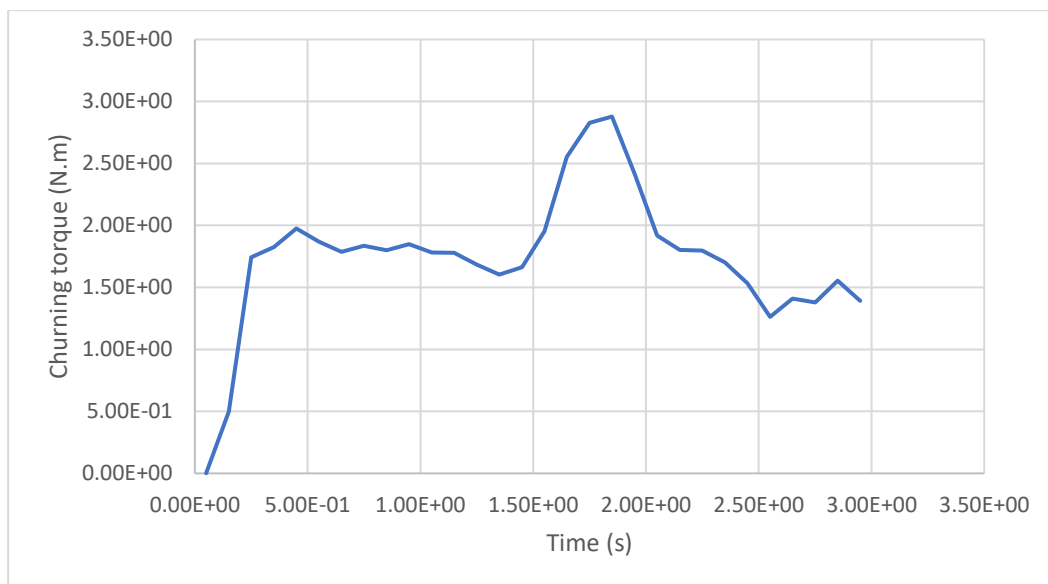


Fig. 4.9. Total churning torque for input shaft

As can be seen, by passage of time and increase in amount of lubricant, the churning torque increases. It should be noticed that this chart is correspondent with rotational speed of 9500 RPM.

Low temperature

Temperature has a notable effect on the lubricant viscosity. As temperature rises up the viscosity is reduced and as temperature declines the viscosity increases. At the lower temperature, lubricant becomes thicker and more viscos, therefore it is harder to flow whereas higher temperatures can lead to thinner lubricant and lower viscosity. In overall, the temperature plays important role in behavior of lubricant and in analysis of oil distribution both high and low temperature should be considered. the properties of lubricant at high temperature can be written as [23]:

Density (kg/m^3)	870
Thermal conductivity (W/mK)	0.145
Specific heat (J/kgK)	2000
Kinematic viscosity (m^2/s)	80×10^{-5}
Surface tension coefficient (N/m)	0.072

Table 4.4. Properties of lubricant at low temperature

As can be observed, the kinematic viscosity is higher in this case and has different behavior that has been shown in following figure:

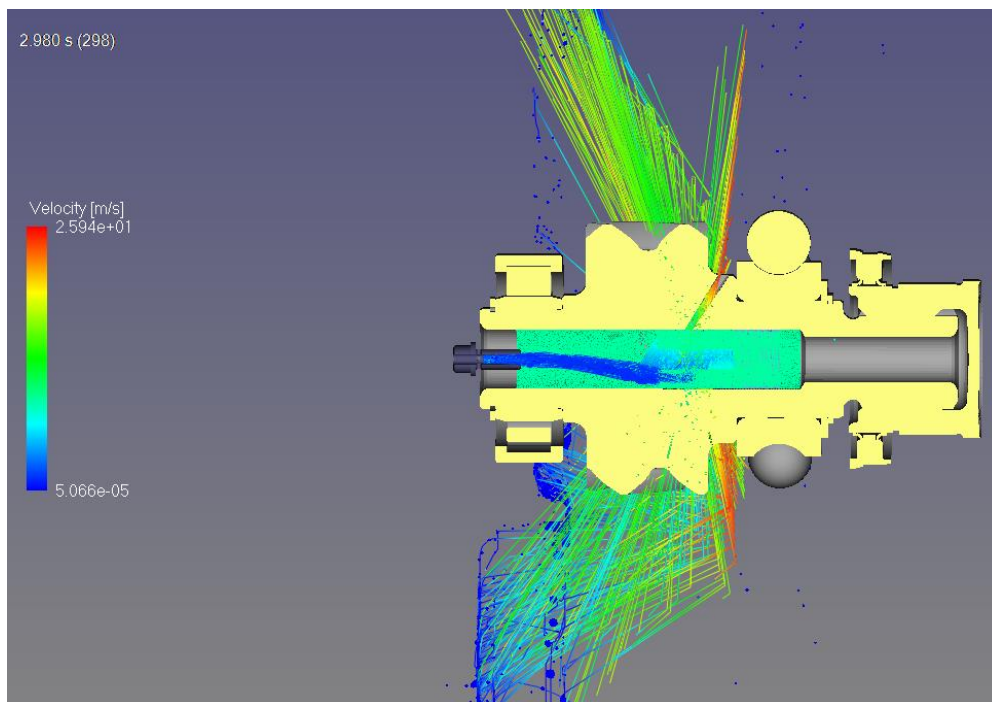


Fig. 4.10. Lubricant pathline for low temperature

As shown in Fig. 4.10, the passed lubricant from channel can't touch ball bearing and make it wet. Moreover, according to the colorbar, the velocity is lower compared to the last analysis and similar to high temperature analysis, the lubricant can't pass the chamfer. For understanding better, Fig. 4.11 is presented that shows number density of oil on the ball bearing. Hence, further analysis and simulation will not carry out.

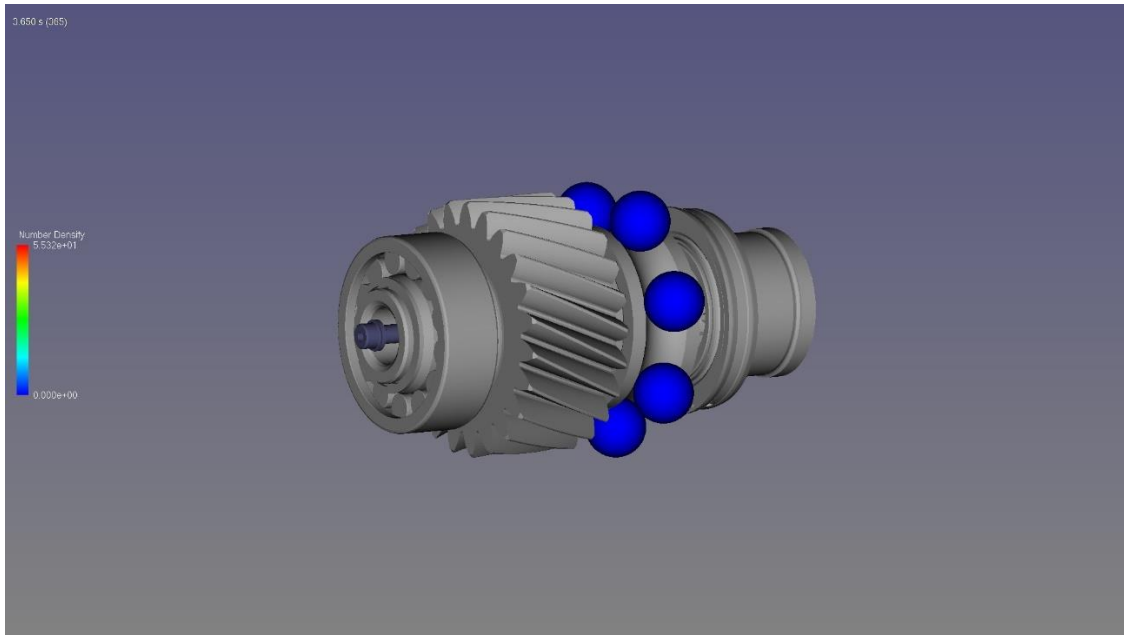


Fig. 4.11. number density of oil on the balls

Inadequate oil in a gearbox can have detrimental effects on the equipment's performance and durability. With insufficient lubrication, the metal balls rub against each other resulting in friction and wear. As a consequence, it can bring about to damaged gears, bearings and ultimately, gearbox failure. Heat generated with bearing can lead to remarkable damages in the absence of sufficient lubrication, resulting in overheating and expansion of the metal sections.

4.1.2. Spline modification

High temperature

In this scenario, the problem of chamfer is solved by inserting a bushing inside the input shaft and therefore, the lubricant reaches inside the input shaft via nozzle and can pass the chamfer. In this moment, due to spline modification, the lubricant cross spline because of centrifugal force and reach the ball bearing. In this analysis, the radial channels have been omitted. It is seen that the efficiency of this scenario is dependent on component rotational speeds and temperature of oil. In this way, owing to high speed the oil is thrown toward ball bearing. Moreover, in this case, the gear number 2 (Fig. 4.3) is added in simulation and we consider the jet lubrication on the meshing area as shown in Fig. 4.13. It should be noted that sealing is added in this new design in order to gather the oil coming from spline and therefore, the gathered lubricant can make wet much more areas (Fig. 4.12).

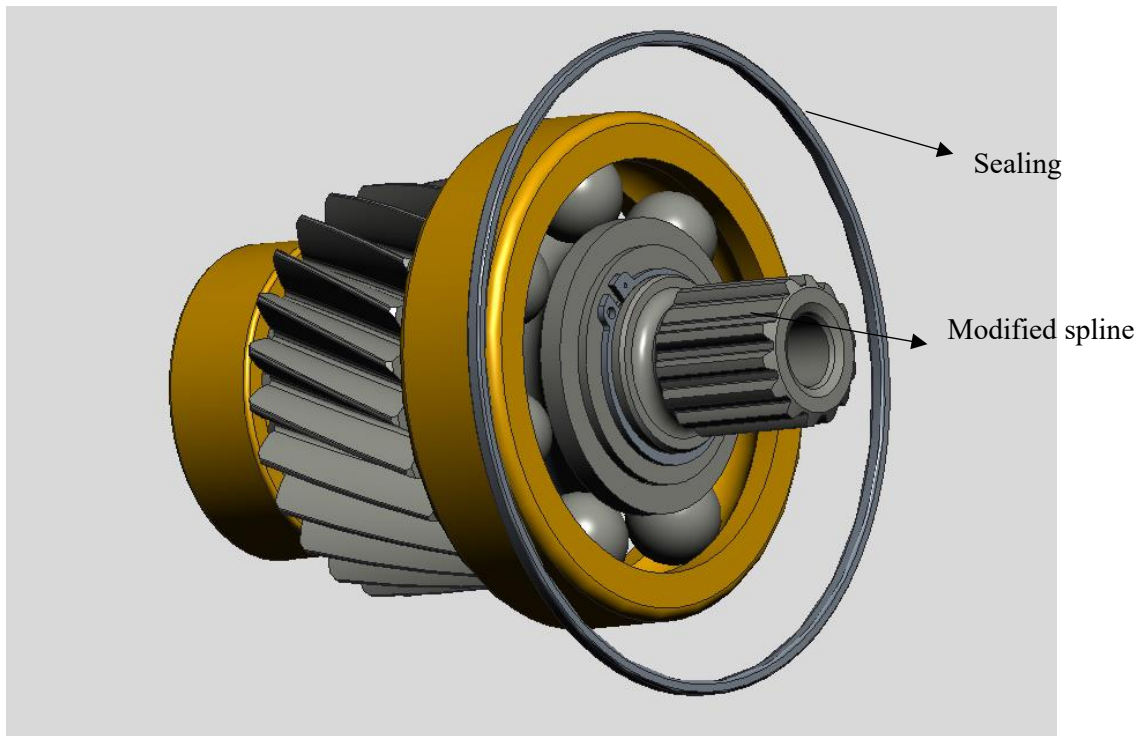


Fig. 4.12. Illustration of spline modification

In cases that splash lubrication can't fulfill sufficient amount of oil on critical components, jet lubrication can guarantee additional oil in meshing area. Meshing gear area are receiving attention because the gears squeeze on each other resulting in friction and heat generation. The distance between jet and gears should be calculated considering the fluid pressure in order to have highest efficiency and it is 40 mm . According to the calculations, the necessary flowrate emitting of nut for jet lubrication is $0.5 \frac{\text{l}}{\text{min}}$. Furthermore, the lubricant properties in this step are according to Table. 4.3.

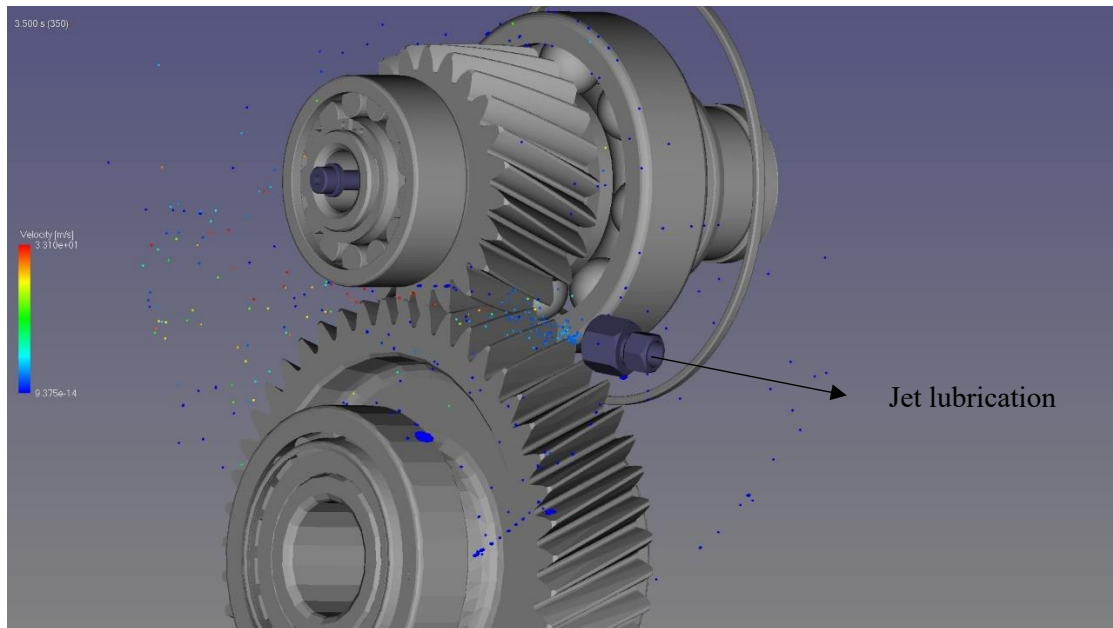


Fig. 4.13. Jet lubrication on the meshing area

As mentioned above, the lubricant passes through bushing and reaches spline and due to centrifugal force, the oil crosses the path on the spline and is thrown toward ball bearing which is critical component owing to high rotational speed. By choosing this method, sufficient amount of oil can make wet bearing that has been shown in the following figure:

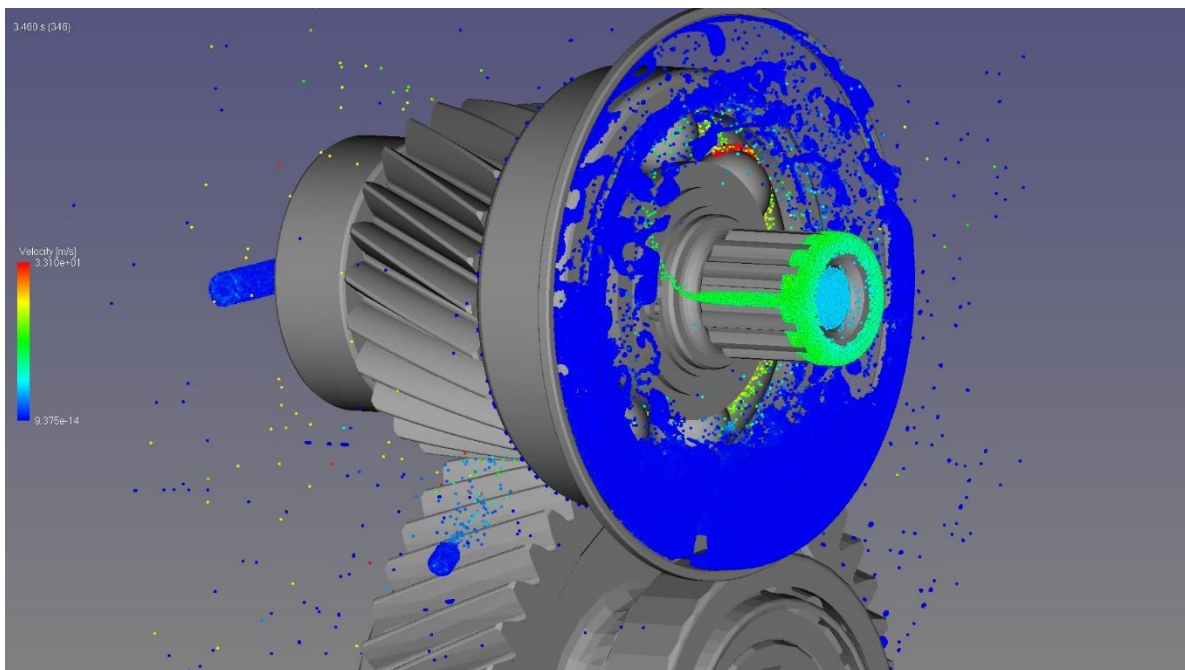


Fig. 4.14. Oil pathline on modified spline

Moreover, this figure depicts the influence of sealing inserted in this design assisting in gathering the lubricant that is helpful in making wet the balls of bearing. The colorbar also refers to particle speeds

in which the oil particles on the spline have speed of $17 \frac{m}{s}$ that is shown by green. It should be noted that the maximum rotational speed in this case is $33 \frac{m}{s}$. By adding bushing inside the shaft, the oil can pass the chamfer as shown in following figure:

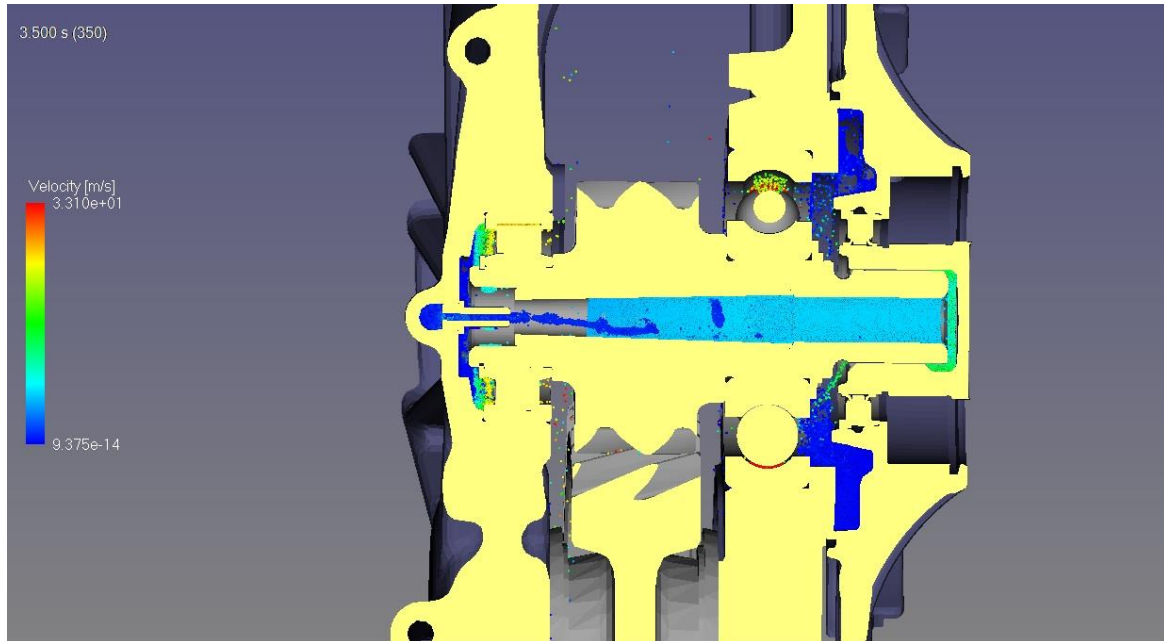


Fig. 4. 15. Movement of lubricant inside the input shaft

Any lubrication system's effectiveness is essential since it influences the functionality and longevity of the machinery. All of the machine's moving elements need to be effectively lubricated in order to decrease wear and friction. By ensuring that the appropriate amount of lubricant is provided to the moving parts at the appropriate time, an effective lubrication system lowers energy consumption and minimizes downtime. Therefore, an efficient lubrication system is a crucial part of any machinery since it guarantees the system's smooth operation while lowering operating expenses and increasing output. In order to recognize efficiency of lubrication system in this analysis, oil number density on the two bearings and meshing area are assessed and according to Figs. 4.16-4.18, the number densities are satisfying As mentioned the colorbars refer to oil number density and red sections show higher oil density.

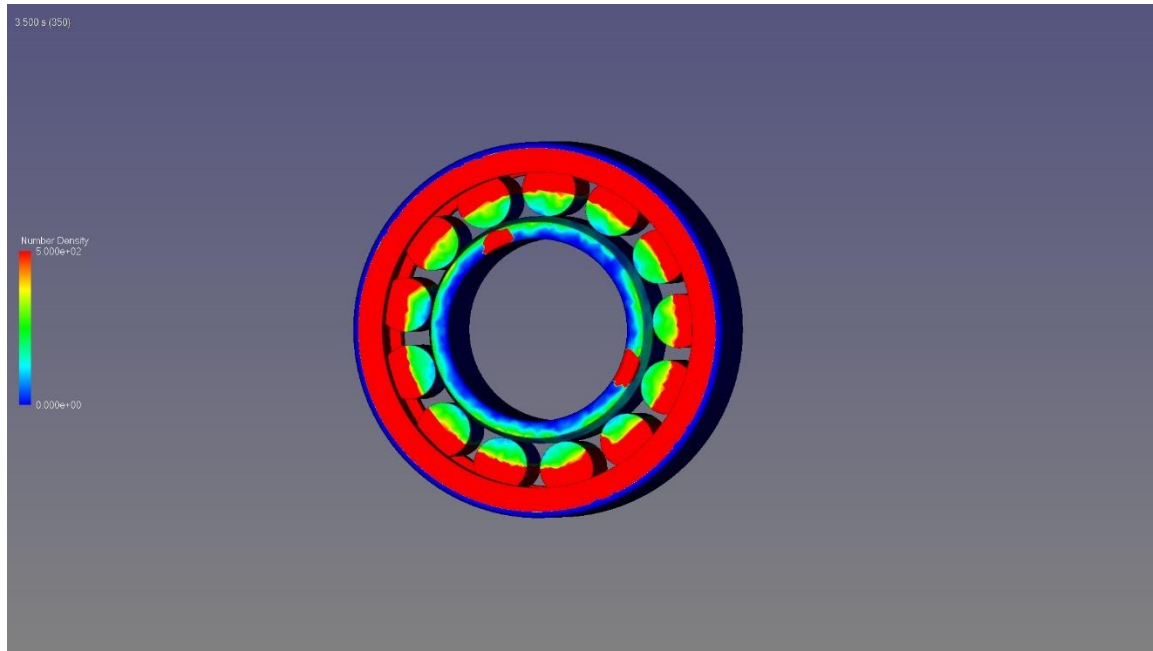


Fig. 4.16. Oil number density for roller bearing

As shown in Fig. 4.15, oil can come out of the holes provided on the nozzle and it distributes lubricant inside roller bearing that with respect to the figure, the oil can reach on the outer ring, inner ring and rollers making it possible to prevent friction and cool down the component.

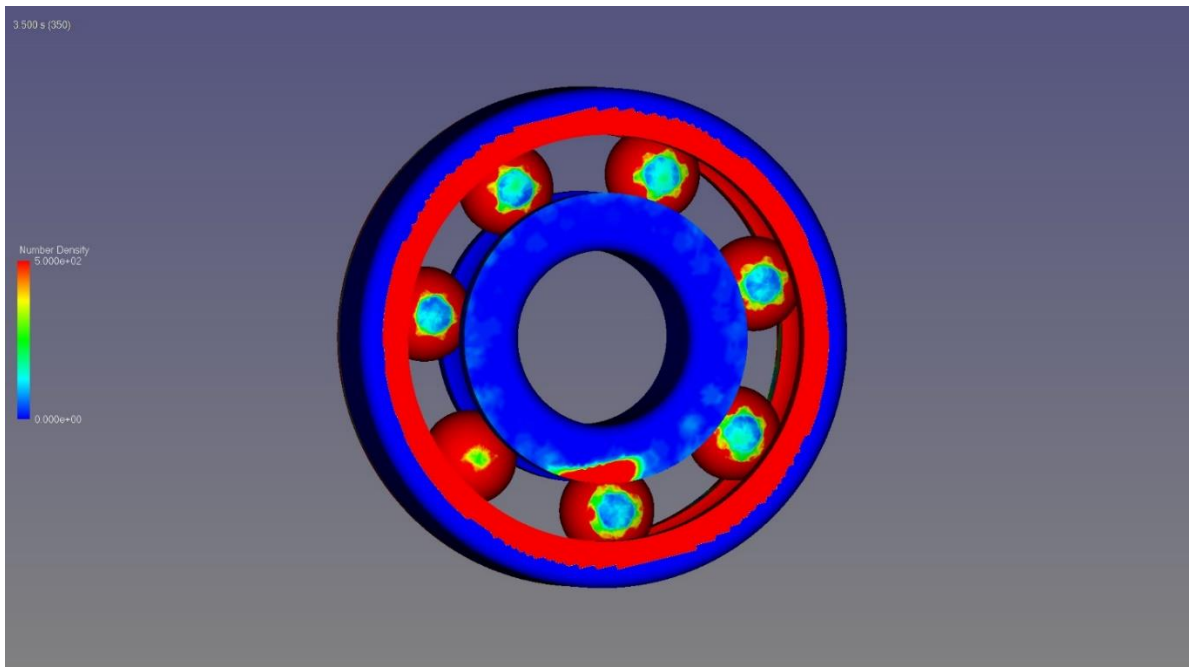


Fig. 4.17. Oil number density for ball bearing

The modified spline has designed in a way to disperse lubricant in all part of ball bearing including inner ring, outer ring and balls and with respect to the Fig. 4.17, all parts of bearing are wet with oil. Lubricant is essential for the meshing of gears. As they come into contact with one another, the gear

teeth generate heat and friction, which can wear out and harm the components. As a result of the oil being provided to these locations, the gears operate more smoothly, are more efficient, and last longer since it helps to minimize friction, dissipate heat, and prevent wear. In addition, the oil film can act as a shield to hamper rust and corrosion. The following figure can show number density of oil on meshing area in which red sections containing higher density.

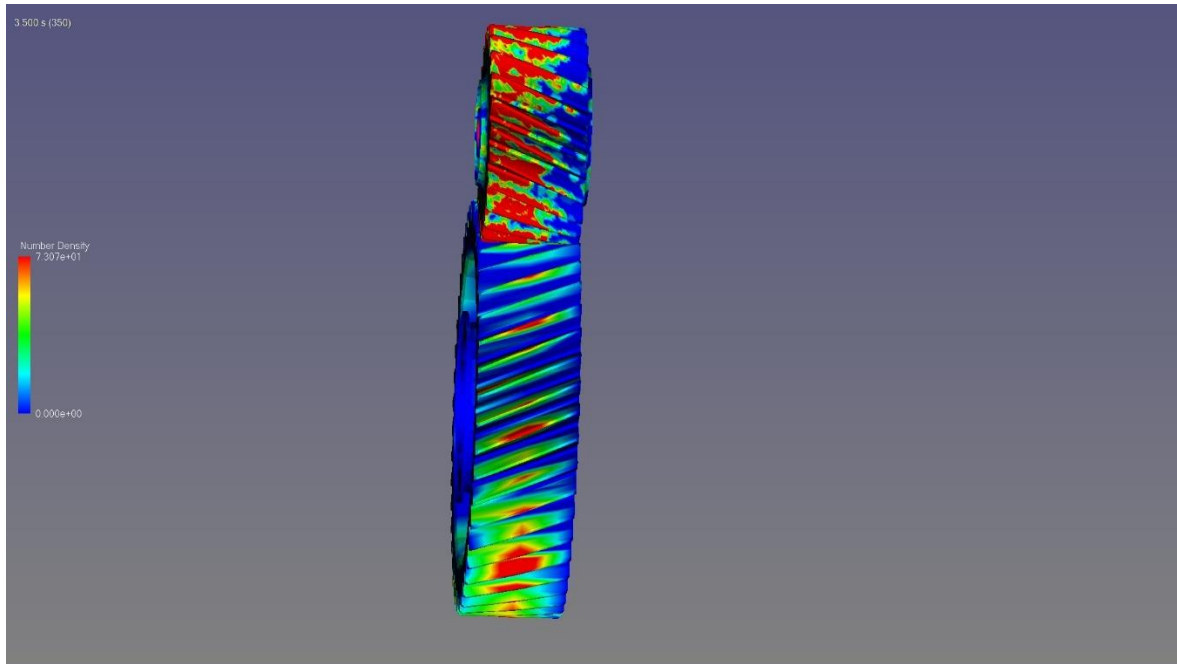


Fig. 4.18. Oil number density for meshing area

Applying particle-based simulations give the opportunity to analyze properties of particles and the consequent behaviors. By flowing the lubricant all over the shaft, the particles may go through different pressure. Fig. 4. 19 illustrates lubricant pressure in different parts of the shaft. The red particles tolerate higher pressure compared to blue ones.

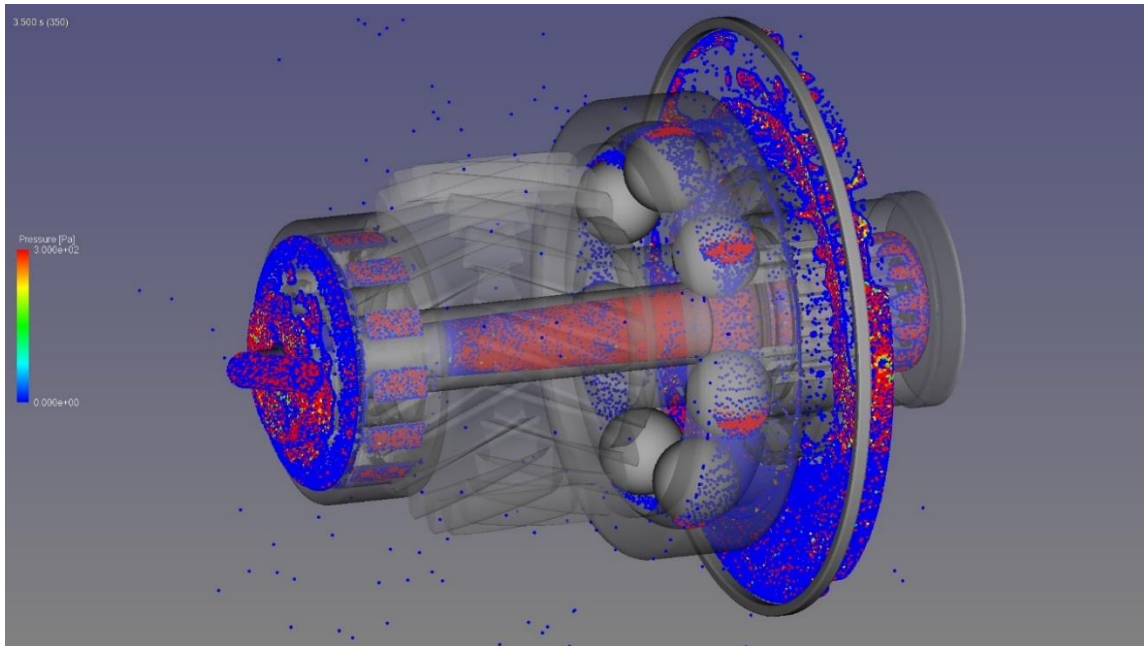


Fig. 4.19. Lubricant pressure distribution in input shaft

The second case has been designed in order to increase oil distribution and oil number density in ball bearing with respect to spline modification. Therefore, in this analysis the whole flowrate can be calculated using particle-based method and compared with the previous method (radial channel). The following figure can show the flowrate touching ball bearing in three seconds:

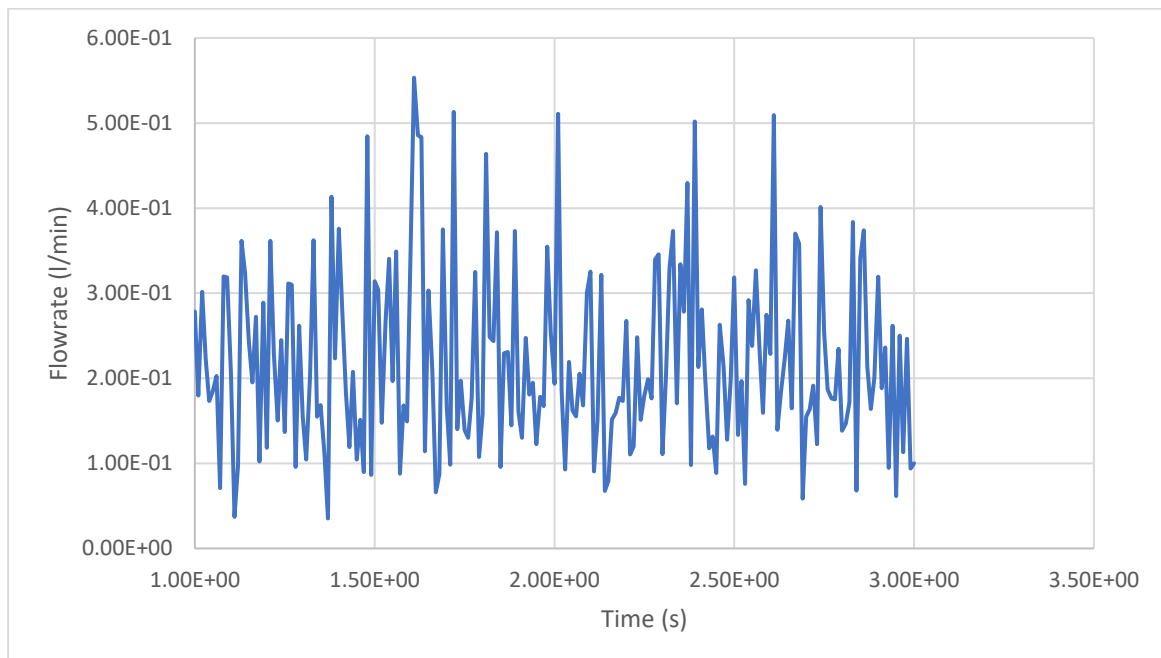


Fig. 4.20. Oil flowrate received by ball bearing

As can be seen, the efficiency of second design for lubricant distribution is better compared to the last design. In fact, higher amount of oil touches the ball bearing and it can guarantee more life and prevent failures. It should be noted that, in the main railway the expected oil flowrate is $1 \frac{l}{min}$ and with respect to the fact that about $0.6 \frac{l}{min}$ enters the input shaft directly, the remained pass through the nozzle holes and can make wet the roller bearing. Therefore, the oil received by roller bearing can be calculated as follow:

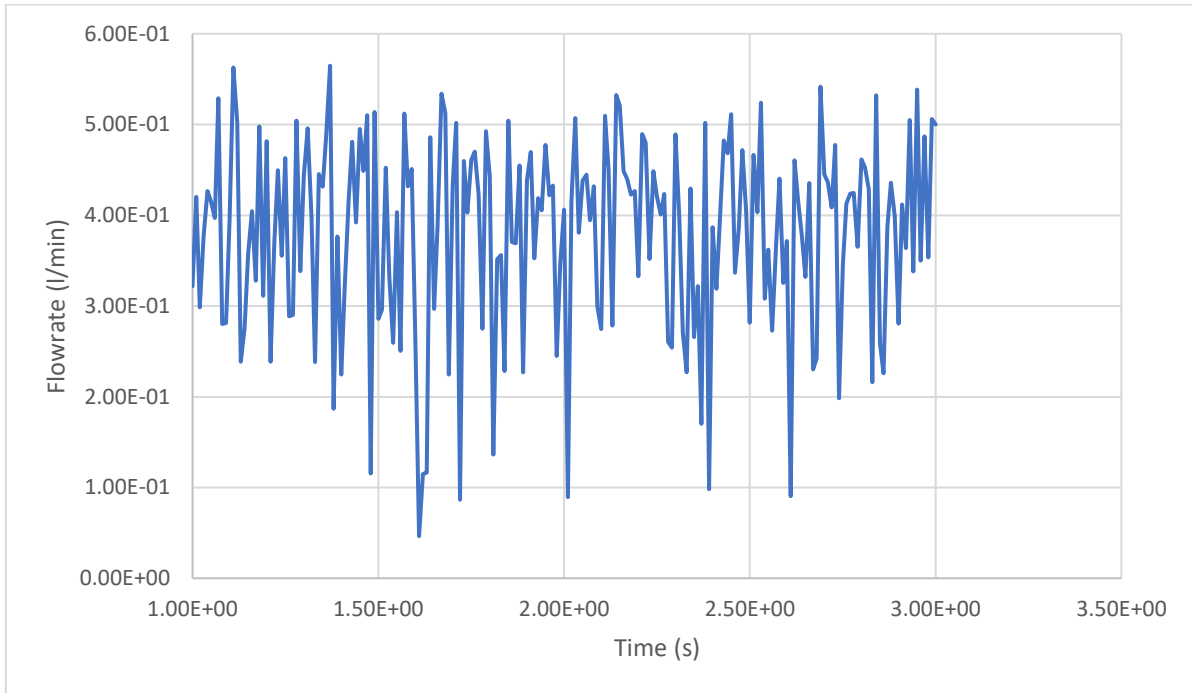


Fig. 4. 21. Oil flowrate received by roller bearing

Using particle-based software there is the possibility to calculate churning torque which consists of pressure gradient, particle turbulence shear stress and viscous force. Hence, the total churning torque in 3 seconds for this specific shaft (Input shaft) can be shown as follow:

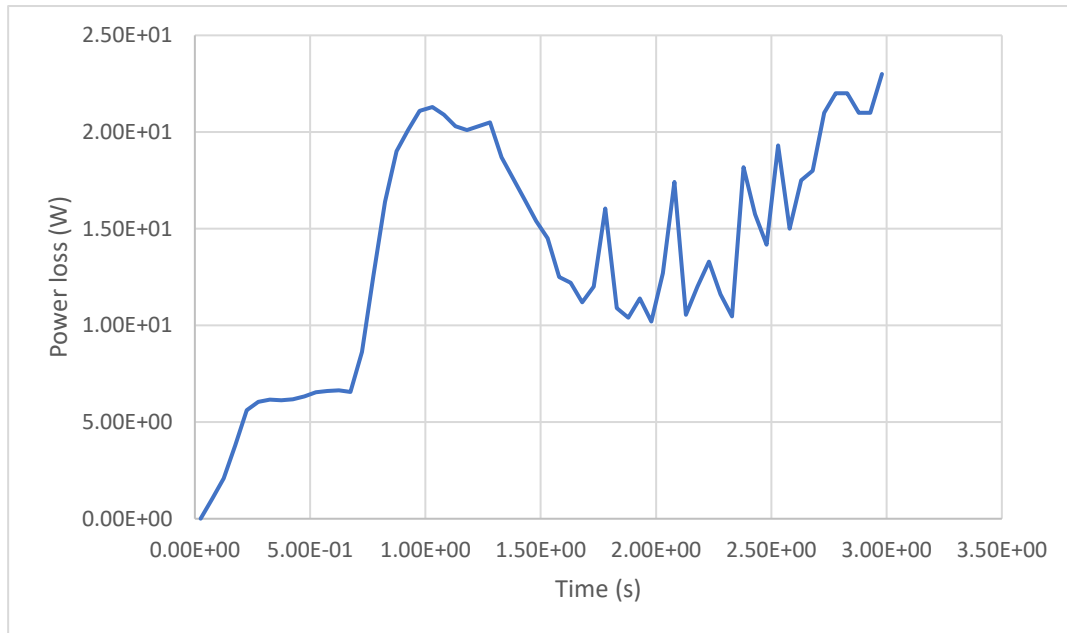


Fig. 4. 22. Power loss in input shaft

As can be seen, by passage of time and increase in amount of lubricant, the churning torque increases. It should be noticed that this chart is correspondent with rotational speed of 9500 RPM and the average power loss is 16.7 W for this specific shaft.

Low temperature

The characteristics of oil are significantly affected by low temperature. Oil becomes thicker and more challenging to flow as a result of its increased viscosity as a result of a reduction in temperature. This makes it more difficult for the oil to lubricate the gearbox parts, which leads to more wear and tear. A complete analysis should involve different temperatures in order to predict oil behavior and consequent damages leading to failures. At low temperature, the concentration is on understanding how lubricant covers rolling and sliding contact surfaces with sufficient layer of oil to avert direct contact among metal parts. If we can make it happen, the friction, heat generation and abrasion are declined and life increases. In this section of our assessment, the lubricant properties are based on Table 4.3 and the oil number density in bearings and gear, flowrate and churning loss are analyzed.

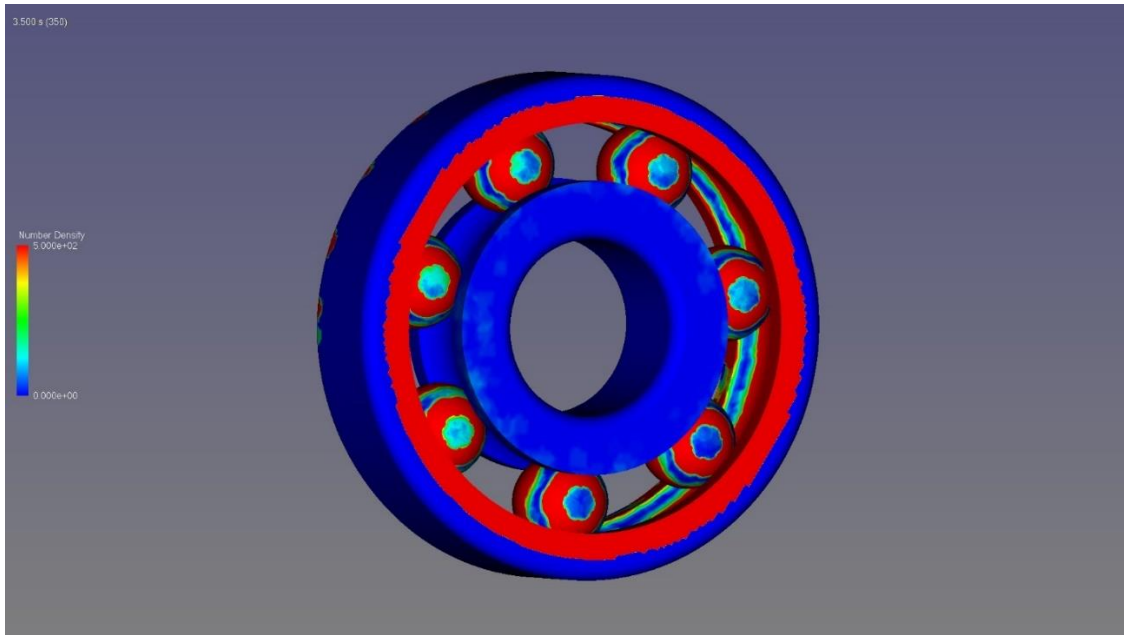


Fig. 4.23. Oil number density of ball bearing in low temperature

Due to higher oil viscosity in this case, it takes more one second for oil to reach the spline and make the bearing wet and according to Fig. 4.23, the oil number density is lower compared to higher temperature, but it is still satisfying because there is layer of oil inside outer ring. Considering oil from splash lubrication, it can avoid friction and excess heat generation. For roller bearing because of presence of holes in nozzle, plenty of oil can touch it and therefore, it can prevent friction and abrasion. The following figure can illustrate oil coverage on the rollers and outer ring:

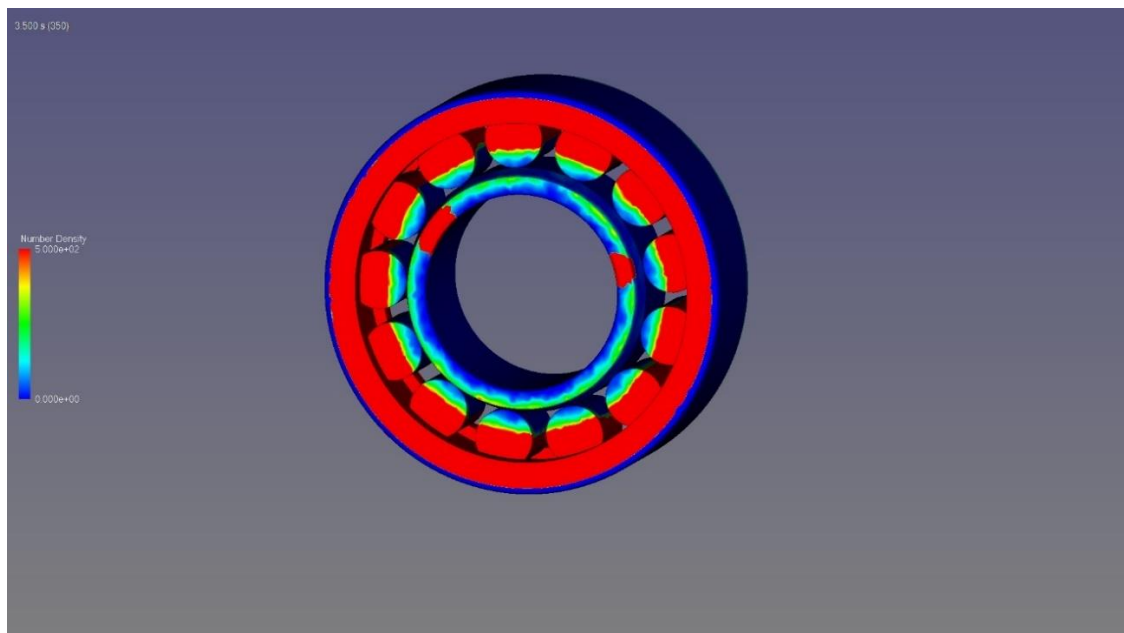


Fig. 4. 24. Oil number density of roller bearing in low temperature

Due to presence of jet lubrication for meshing area, it can guarantee creation of oil layer for either design. As shown in Fig. 4. 25, there is no specific difference between high and low temperature.

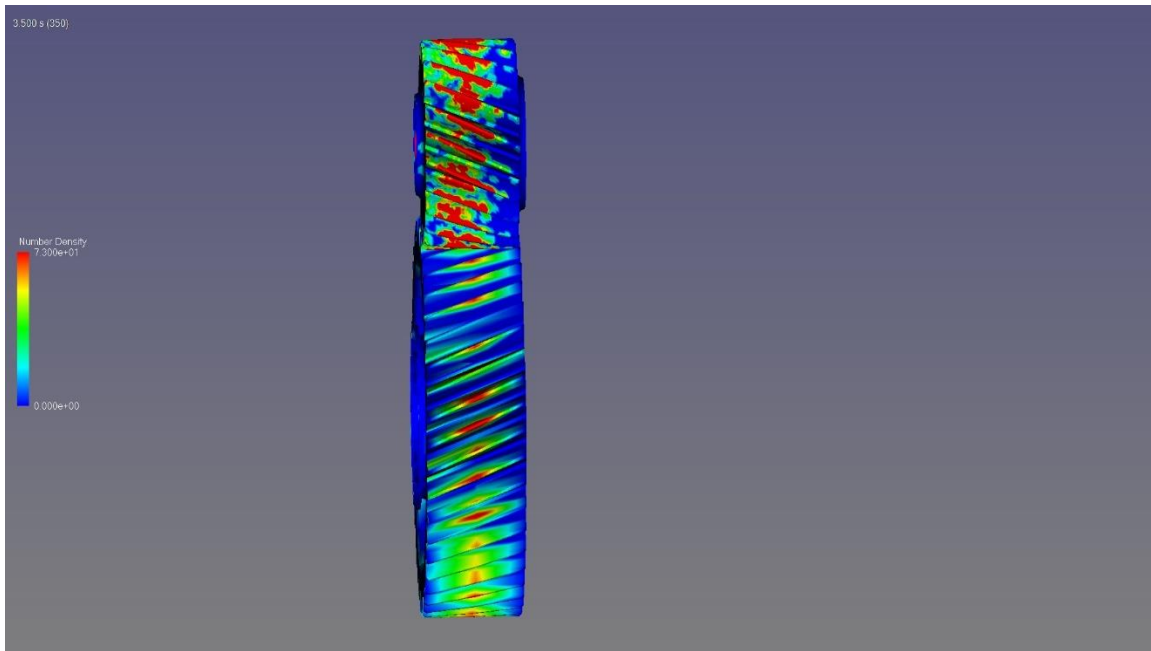


Fig. 4.25. Oil number density for meshing area for low temperature

In low temperature condition, there is a slight difference in maximum rotational speed. In low temperature, owing to higher viscosity, the maximum speed of oil is $34 \frac{m}{s}$. For many sectors, oil flow rate at lower temperatures is a crucial factor. Oil flow rate reduces when temperature drops because oil gets more viscous. Machinery and equipment that depend on a regular flow of oil to prevent wear and tear may be significantly impacted by this. Hence, the exact amount of oil flowrate that is received by ball bearing can be calculated as follow:

90

Fig. 4.26. Oil flowrate received by ball bearing

As expected for high viscous lubricant, it is thicker and harder to move forward and as a result, the average flowrate for this three second is $0.15 \frac{l}{min}$ which is lower compared to low viscous lubricant which is $0.28 \frac{l}{min}$. As mentioned before, churning loss is the term for the power loss that occurs when oil is moving around inside a gearbox and shaft. While the oil is needed to lubricate and cool the moving parts of the shaft, when it is mixed up too much due to fast rotating rates, heat is generated and energy is used. The churning loss for case of low temperature can be depicted as follow:

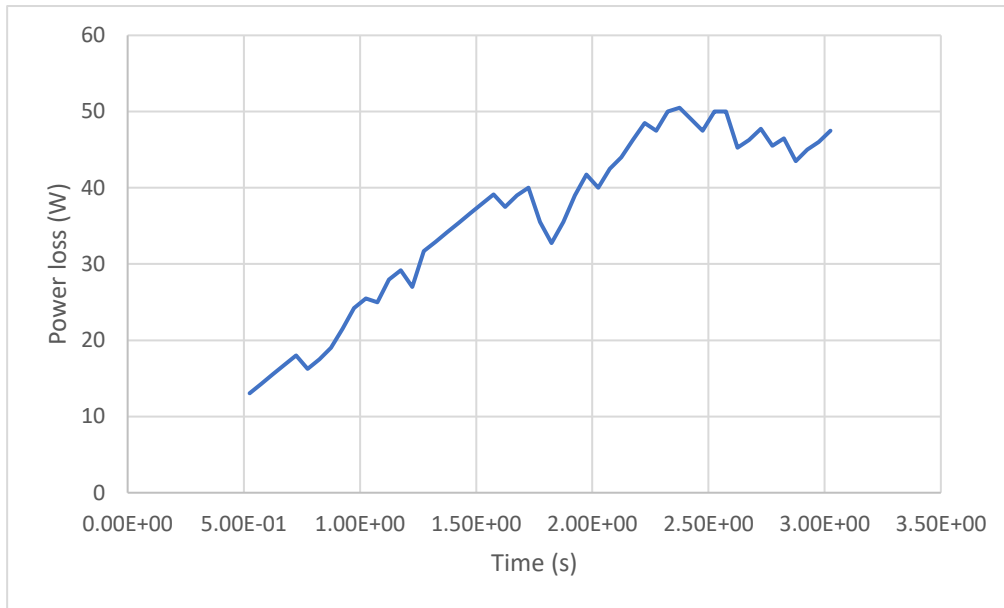


Fig. 4. 27. Churning loss of input shaft for low temperature

The average amount of churning loss is about 40 W which is higher compared to high temperature. As a matter of fact, rotational speed has remarkable influence on the churning loss. Higher speeds cause the fluid inside the gearbox to flow more erratically and chaotically, increasing churning losses. The churning losses increase heat production and shorten the gearbox's overall lifespan and efficiency by causing premature wear on key parts.

4.2. Lubrication system of shafts number 3 with number 4

In this section lubrication system of shafts number 3 and 4 according to Fig. 4.3, and its housing modifications are investigated in order to optimize oil distribution. As can be seen in Fig. 4. 2, due to complexity, insufficient amount of lubricant can reach the gears on the shaft and it needs new design to bring much more oil to critical locations. Fig. 4. 29 can illustrate these two shafts with details. In this part, the essential oil flowrate coming into the shaft 3 is $1 \frac{l}{min}$ to guarantee optimized lubrication in meshing areas.

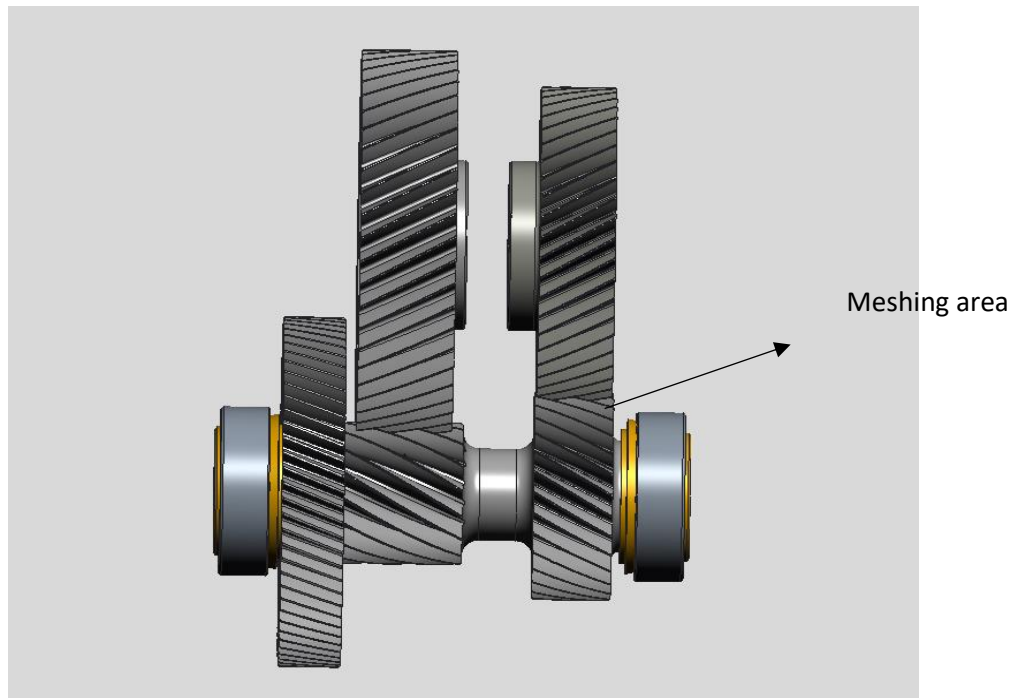


Fig. 4. 29. Schematic view from shaft number 3 and 4.

At the first step, the gear in shaft number 3 has been provided with the radial channel in order to distribute oil in meshing area and this design can satisfy enough wetness for both low and high temperatures as shown in Fig. 4. 30.

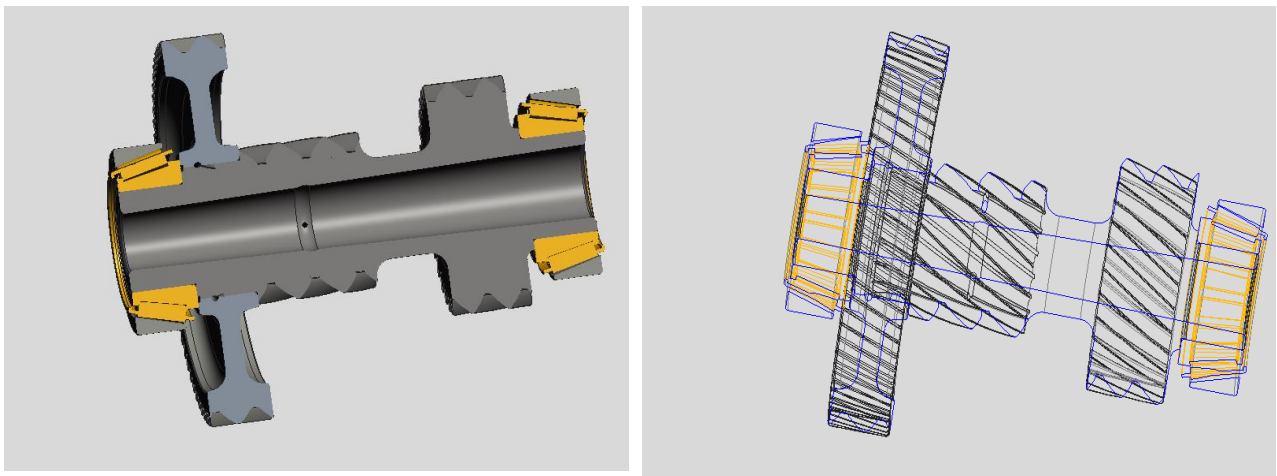


Fig. 4. 30. Radial channels inside the shaft

The challenging problem in this case would be distribution of lubricant at the end of shaft including two meshing gears that in case of insufficient lubrication can lead to wear and failures. In order to solve this problem, we brainstorm to insert a shield at the end of the shaft. Because, due to high rotational speed of shaft, oil moves toward the roller bearing and owing to centrifugal force the oil

will be thrown toward gears and meshing area. This method works for both high and low viscous oil. In this part, two different approaches are analyzed and the best one will be chosen.

4.2.1. Inserting shield

High temperature

In this case, a shield will be installed and stuck to the housing and owing to the edge on it, the oil is directed toward gears to make them wet. As mentioned before, presence of adequate oil in meshing area is vital. Oil acts as a crucial lubricant to lessen wear and friction between the gears. It is essential for keeping the gears from overheating, which could harm the gearbox. Without enough oil, the gears might get overly worn and malfunction, perhaps causing serious harm to the gearbox or other system components. In other words, the effective and secure operation of a gear system depends on the right oil level. To ensure the smooth operation of the gearbox and lengthen its lifespan, it is crucial to maintain the proper oil level and quality. The following figure can depict the shield with detail.

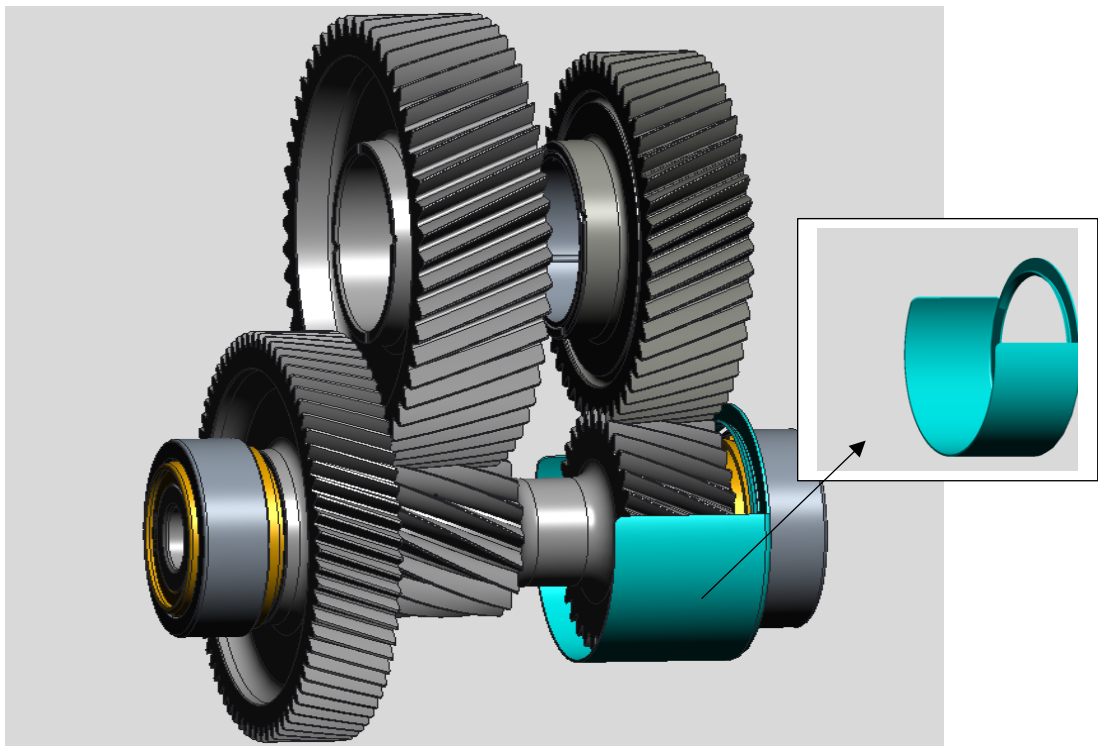


Fig. 4. 31. The shield inserted in housing

The recommended shield isn't complex in design and can be manufactured. It is clear that after passage of time, excess lubricant can be saved and gathered inside the shield making it possible to make wet gear by increase in oil level. Oil distribution in whole shaft and meshing area is shown in Fig. 4. 32 and Fig. 4. 33.

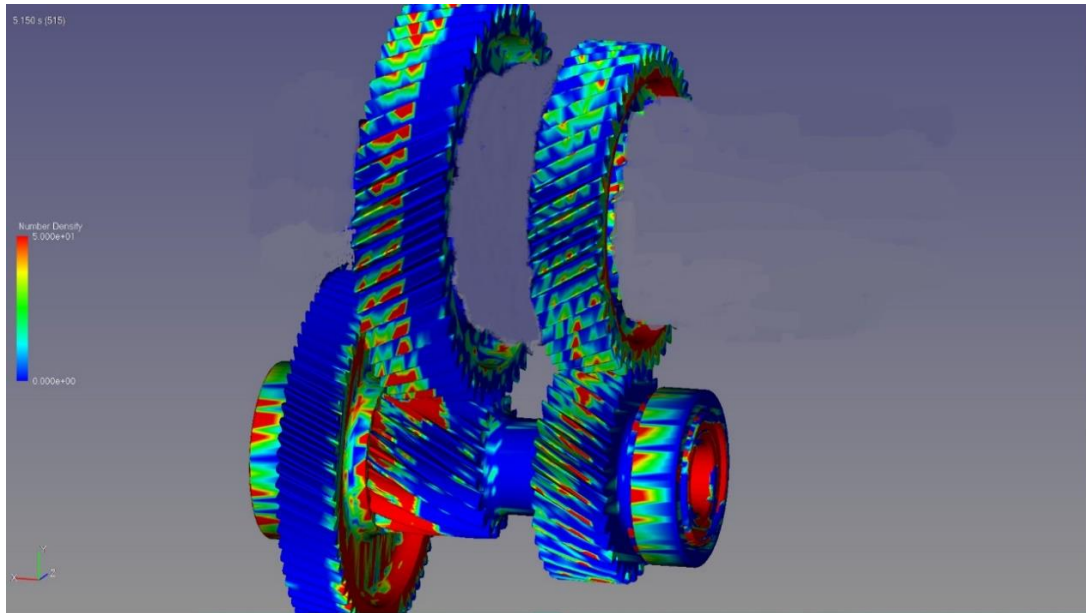


Fig. 4. 32. Oil number density of both shafts

As can be seen, due to presence of radial channel and shield, oil distributions in all meshing areas are satisfying and can guarantee settling sufficient oil layer on the gears.

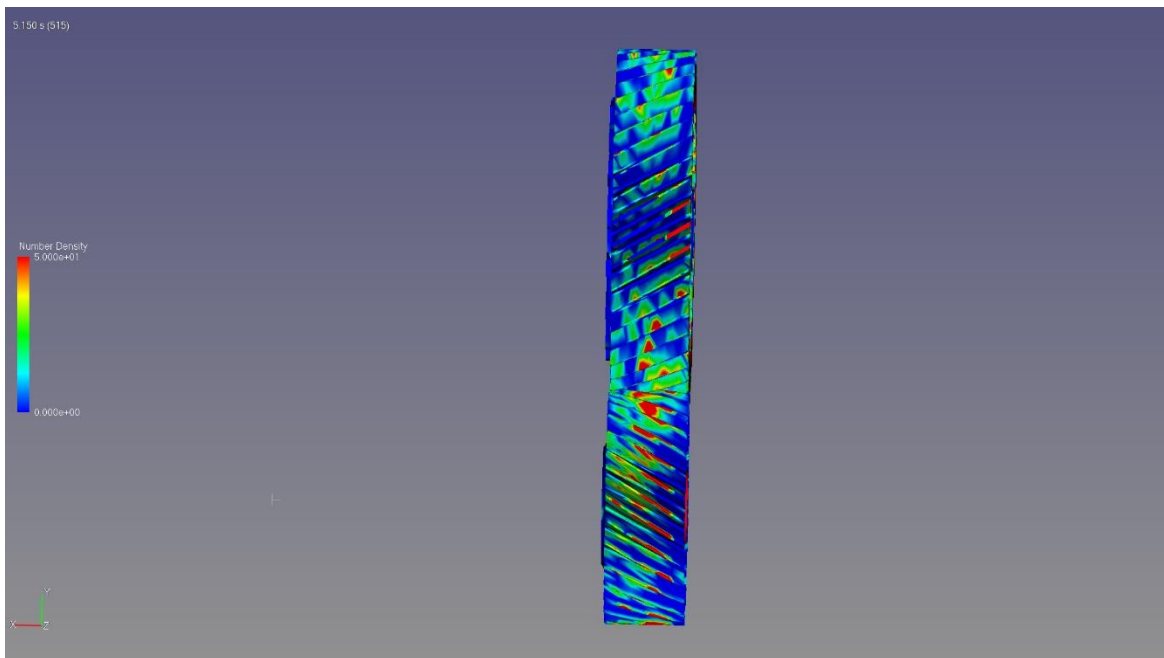


Fig. 4. 33. Oil number density of meshing area

For illustrating exact amount of oil received by the meshing area, we can calculate the flowrate as follow:

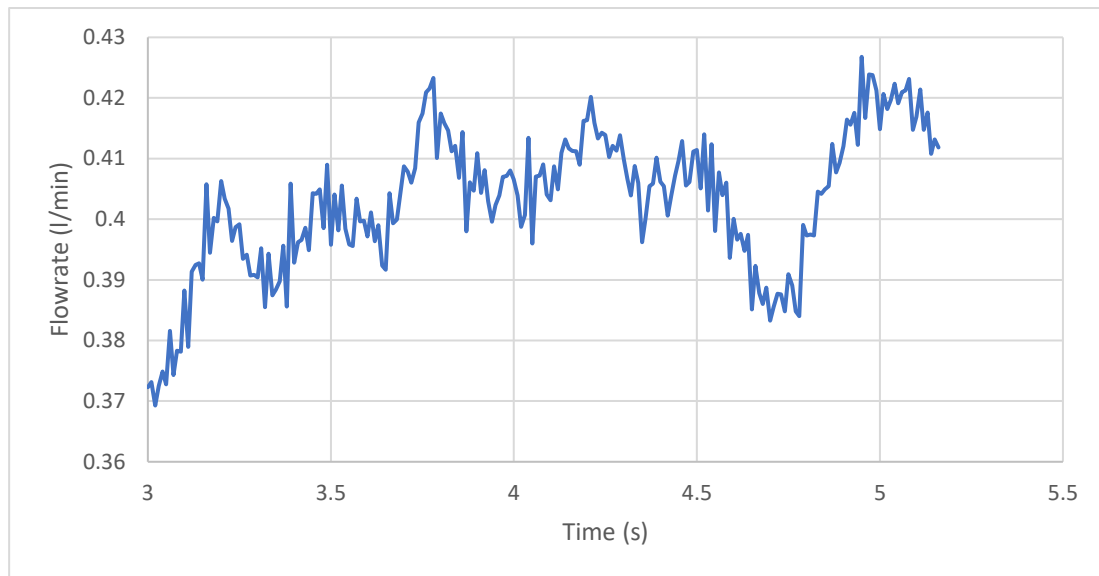


Fig. 4. 34. Oil flowrate received by meshing area at high temperature

Low temperature

For case of low temperature, due to higher viscosity we might have different behavior for lubrication system. The oil is thicker and takes much more time to pass the shaft and reach the roller bearing. Moreover, that is heavier and it makes harder for lubricant to be directed. In this analysis, the same shield is utilized to reach lubricant to meshing area. The following figures can illustrate oil number density for whole and meshing areas after passage of 8 seconds which most sections are blue and the oil number of density is low.

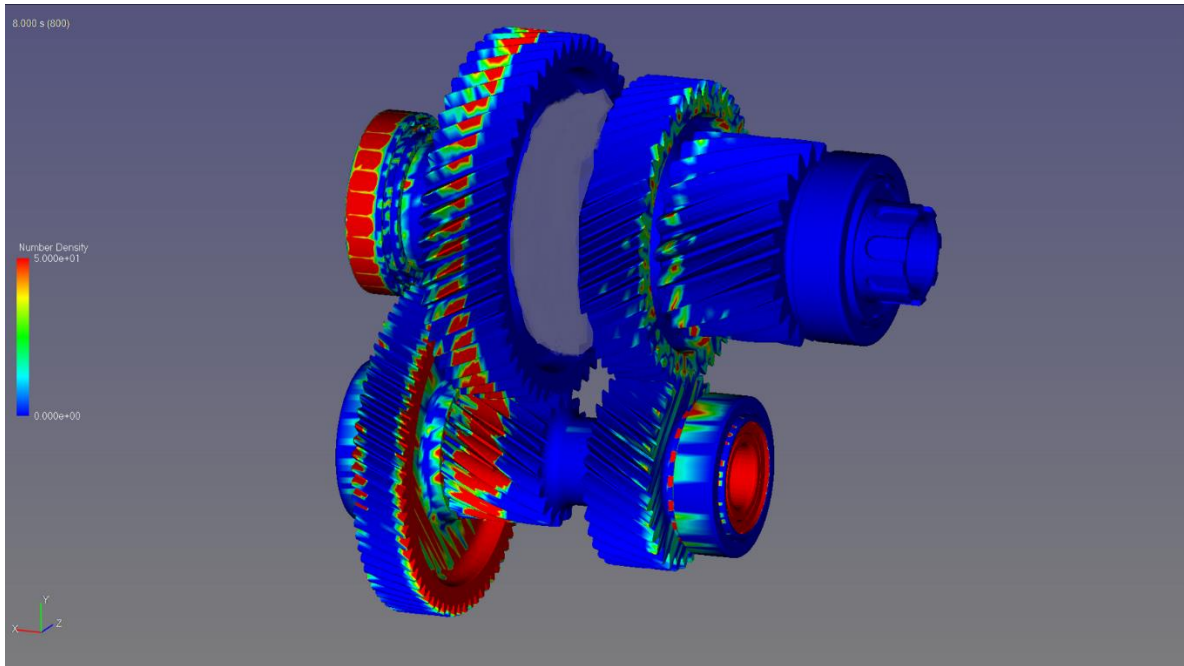


Fig. 4. 35. Oil number density on the shaft 3 and 4.

As can be seen, due to presence of radial channel and shield, oil distributions in only one meshing area is convincing and can guarantee settling sufficient oil layer on the gears. However, the last gears according to following figure, can't receive adequate lubricant and inserting shield can't guarantee optimized lubrication. In this situation, the gears go through overheating leading to damage to transmission system. No need to say that inadequate lubricant brings about worn and malfunctions affecting adversely lifespan.

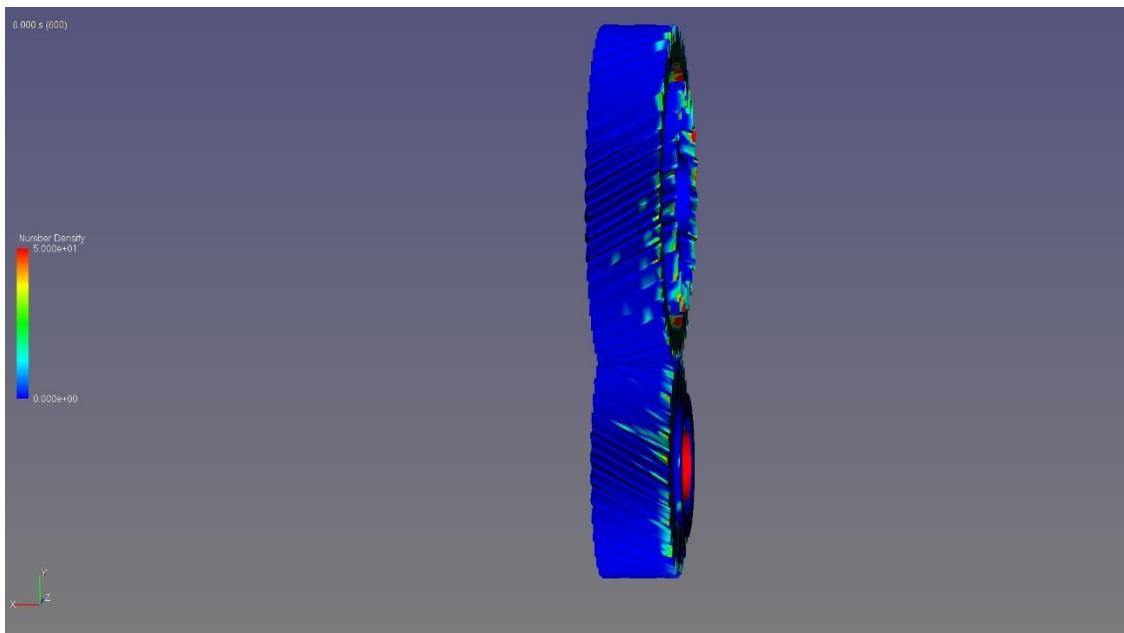


Fig. 4. 36. Oil number density of on meshing area.

With respect to above figure, inserting this shape of shield can't fulfil our expectation in case of lubrication for all range of temperature and considering this design can result in damage and final failure in gearbox. In fact, at low temperature, the lubricants are heavier to be thrown and directed toward meshing area based on our design. Therefore, we disregard this method and in the next section, we brainstorm another approach to fulfil the expectations. In order to find better the mentioned issue, we can investigate oil flowrate received by the gears as follow:

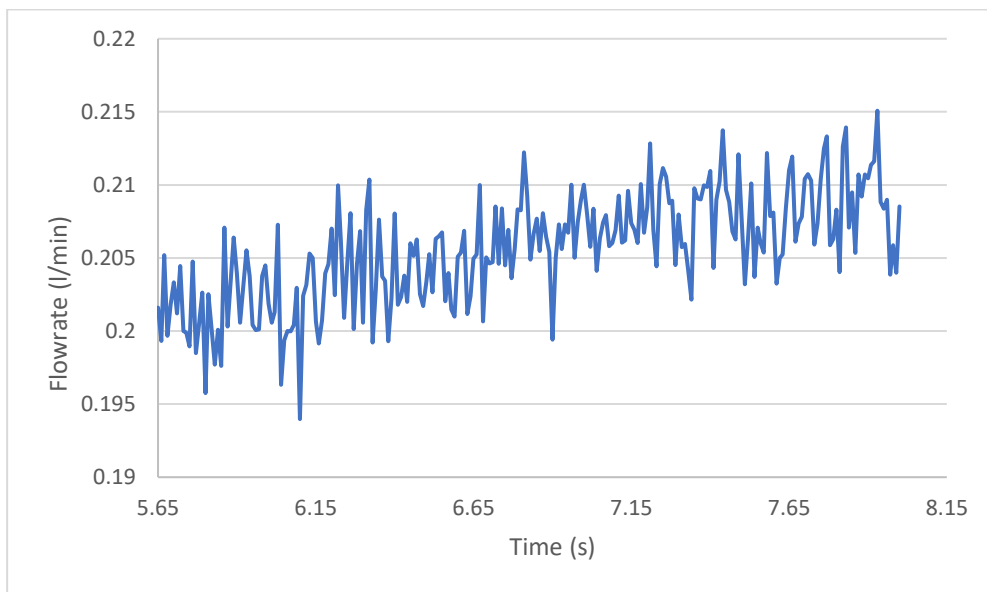


Fig. 4. 37. Oil flowrate received by meshing area at low temperature

4.3. Adding jet lubrication

As investigated in the last part, inserting shield couldn't live up to expectations and using this approach results in failures. New way is considered to make wet meshing areas in both high and low temperatures. Therefore, a new pipe branch connected to the second railway is inserted near to meshing area acting as jet lubrication. In addition, in order to direct the lubricant and gather excess lubricant, new shape of shield is considered according to Fig. 4. 38. A form of lubrication system called jet lubrication sprays lubricant onto the gears' meshing regions using a high-pressure jet. The benefit of employing jet lubrication for these regions is that it accurately and only applies the oil where it is required. As a result, there is less waste and mess because the gear teeth are not covered in oil. Additionally, there is less chance of overheating and wear when the lubricant is applied directly to the meshing areas, which can result in more effective operation and longer gear life. What's more,

compared to conventional lubrication systems, jet lubrication is more simply managed and monitored, making it the perfect solution for gears that are hard to access or that must work in challenging conditions. Moreover, appropriate pressure in the pipe and sufficient flowrate to have adequate oil layer on the gears should be considered.

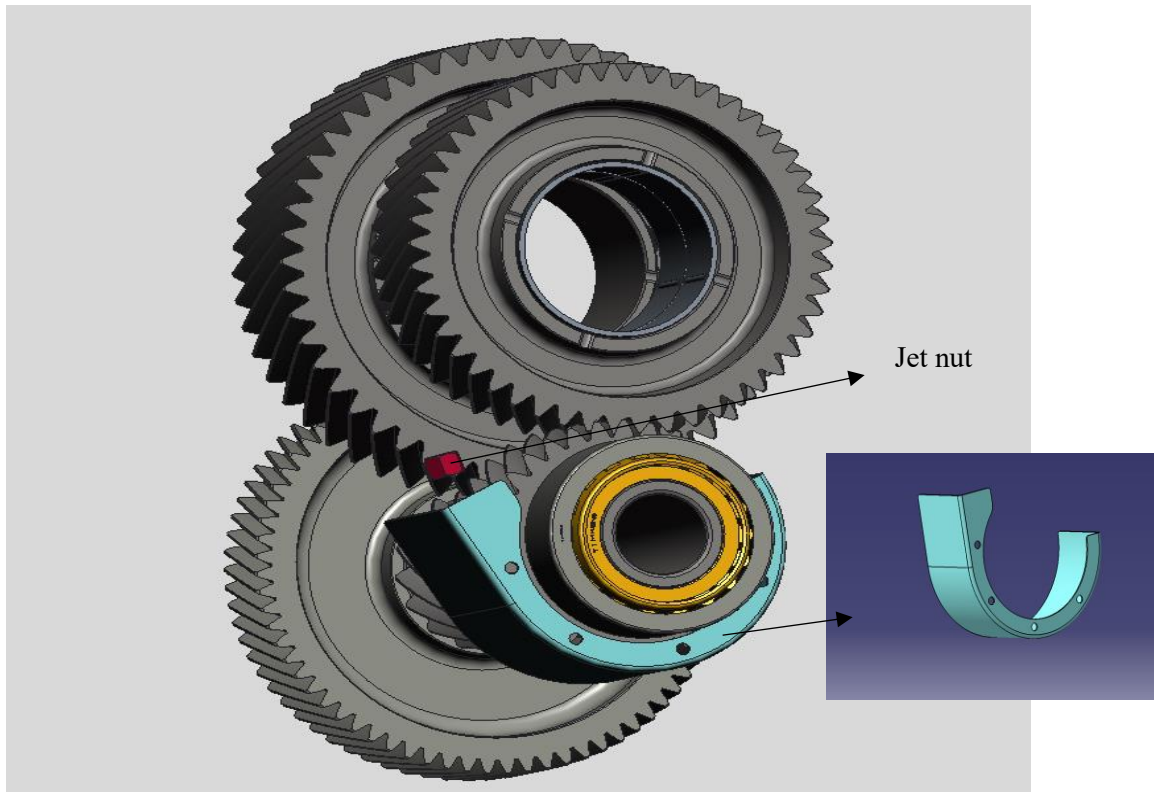


Fig. 4. 38. New shape of shield and jet nut

As matter of fact, jet lubrication can decrease efficiency of high-speed gearboxes if it targets the gears directly. Because, impingement of lubricant with the gear flanks can impose opposite torque on the shaft. In this case, we have higher churning loss overshadowing functionality and effectiveness of system. To solve this issue, the jet is tilted a bit toward shield to eliminate influence of churning loss. Therefore, oil strikes the shield and is dispersed and make wet meshing area. The shield has designed in a way to cover and collect all lubricants emitting the nut. It should be noted that the oil flowrate of jet nut is $0.5 \frac{l}{min}$. Fig. 4. 39 shows how lubricant comes out of nut with details and Fig. 4. 39 illustrates structure of pipe and nut.

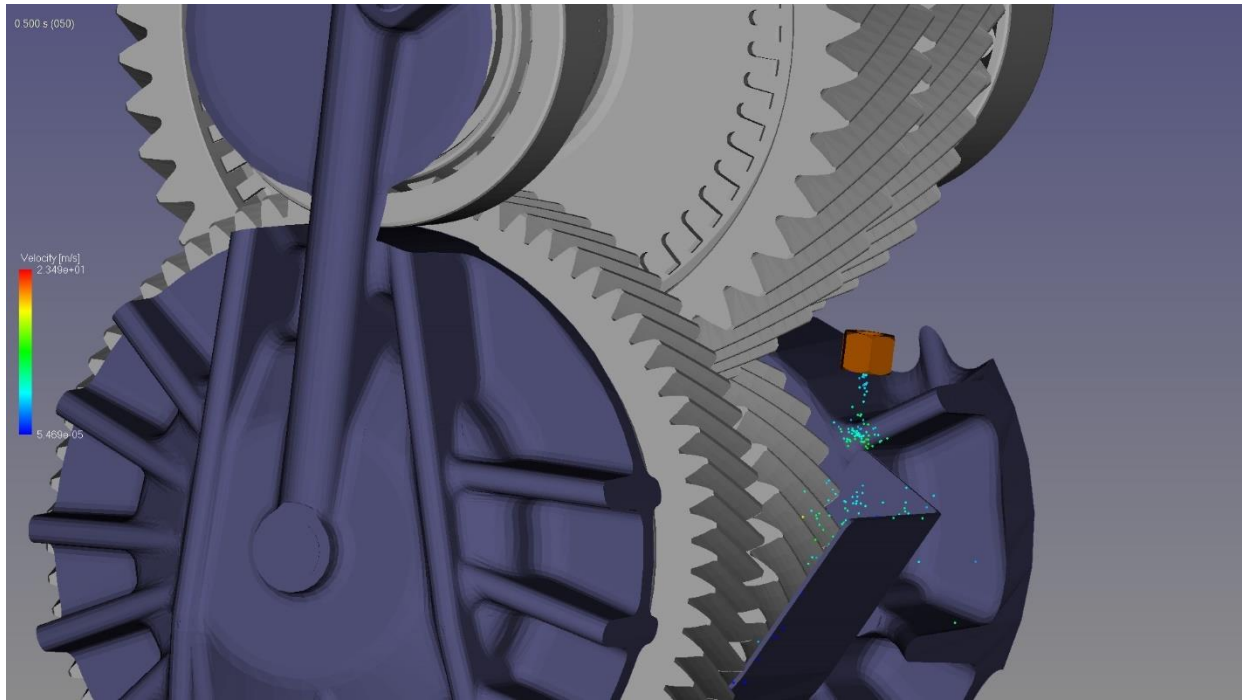


Fig. 4. 39. Oil pathline of jet nut

As can be seen, the inflow is provided inside the nut and the oil particles are hitting the shield and this impingement can put an oil layer on the gear flanks. The remains are gathered inside the shield and after passage of time, oil level increases and can assist in lubrication.

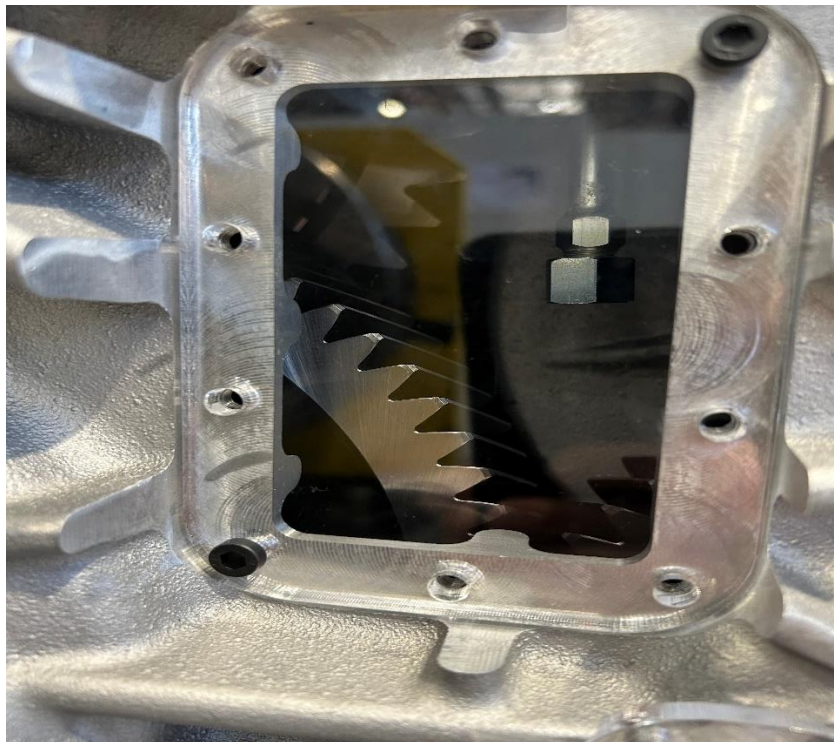


Fig. 4. 40. Jet nut position in gearbox

Similar to previous parts, behavior of the lubricant is investigated according to high temperature and high temperature to spread our study.

High temperature

The material properties and oil properties for this section are based on Table 4.2 and Table 4.3. In case of high temperature, it takes about 2.5 *sec* that oil crosses nozzle and reaches to the last roller bearing. The radial channels are also considered in this analysis which can guarantee adequate lubrication for the first meshing area. The following figures can illustrate all steps of lubrication.

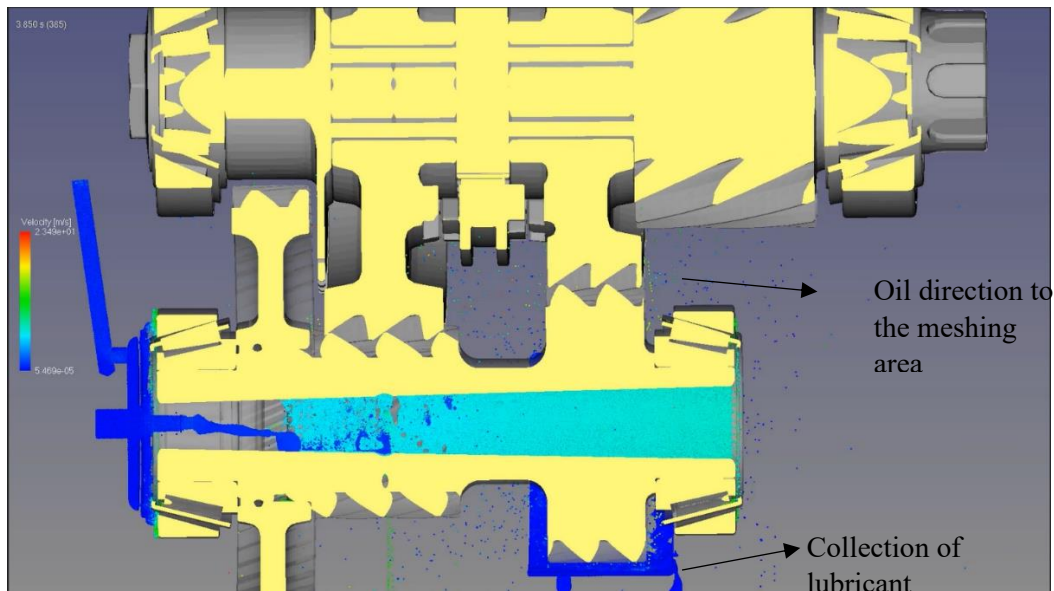


Fig. 4. 41. Oil particles inside the shaft

The above figure depicts particle velocity according to specific locations. It is obvious that the particle velocity inside the railway and shield is the lowest and particles coming out of roller bearings have the highest speed which is $24 \frac{m}{s}$. Moreover, the lubricant emitting the roller bearing are directed toward meshing area and in addition to jet lubrication can satisfy sufficient amount of oil on the gears. It can be noticed that the shield has been designed in a way to collect all lubricant emitting roller bearing that can help lubrication system. In order to detail the lubrication system in the shaft number three Fig. 4. 42 is presented.

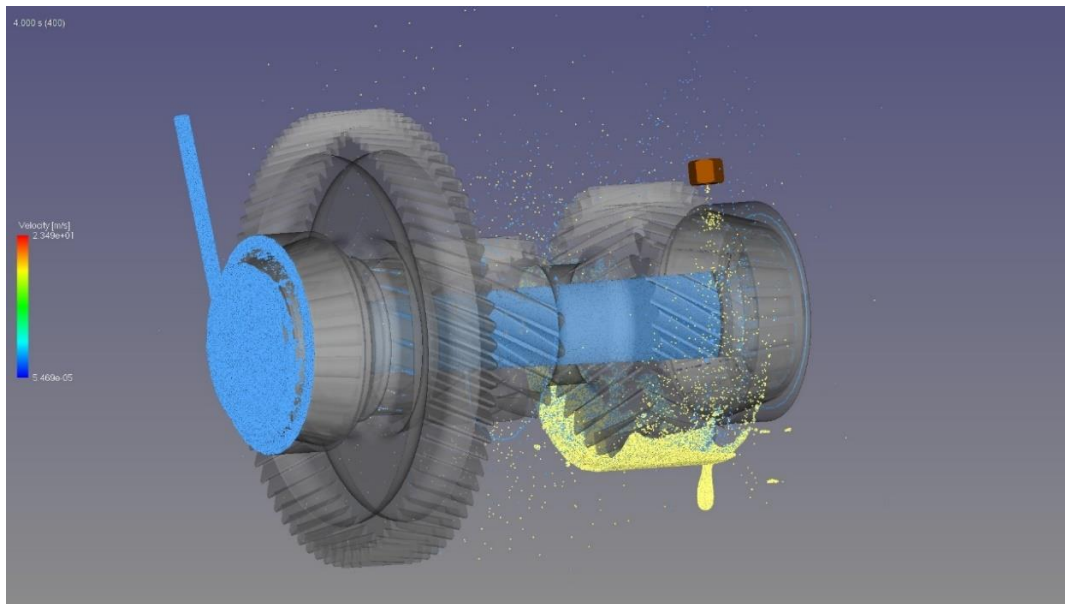


Fig. 4. 42. Lubrication system in shaft number 3.

As seen, the lubricant passed through nozzle in blue and the lubricant passed through jet is yellow. To measure efficiency of lubrication by passage of time, oil number density on the shaft should be analyzed according to flowing figure:

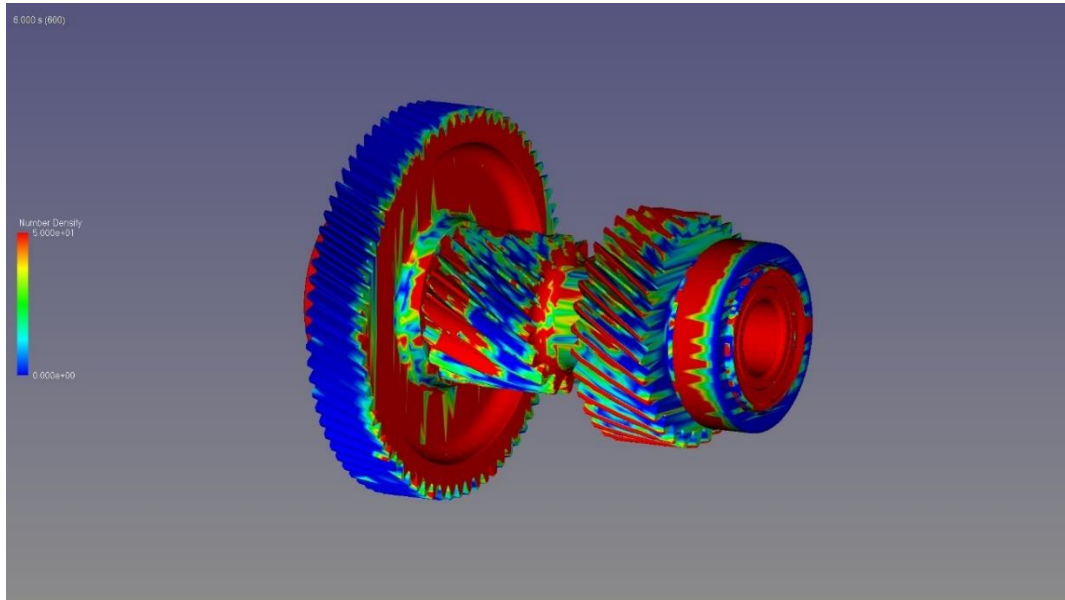


Fig. 4. 43. Oil number density on the shaft

It is clear that presence of channels inside the shaft is beneficial and we can exploit it for the first meshing area. In addition, the gear flanks of second meshing area are covered by lubricant which is, in opposition of last method, satisfying. We can realize that using jet can have far-reaching influence on lubrication system. Likewise, following figure is presented to illustrate oil covering of meshing area.

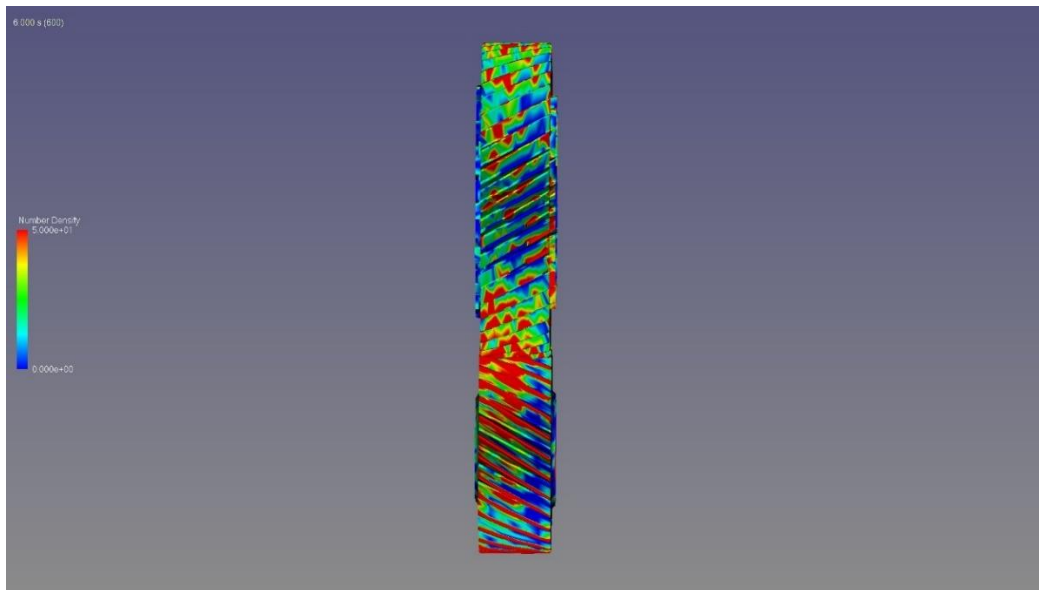


Fig. 4. 44. Distribution of oil on meshing area

Using particle-based software there is the possibility to calculate churning torque which consists of pressure gradient, particle turbulence shear stress and viscous force. As it helps to maintain a thin coating of oil between the gear teeth, efficient jet lubrication is crucial to minimizing the impact of churning loss. The oil acts as a barrier between the teeth and averts direct contact as a result of the correct jet lubrication, which eventually lowers the churning loss. In order to decrease churning loss, increase gearbox efficiency, and lengthen gearbox life, jet lubrication is crucial. The following figure depicts churning loss related to the shaft number 3.

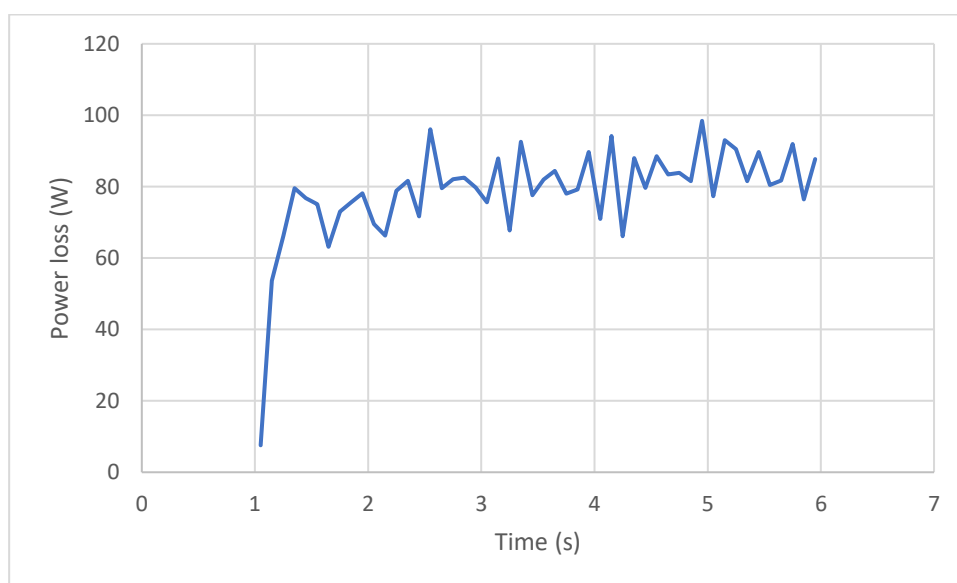


Fig. 4. 45. Power loss related to shaft 3 for higher temperature.

Increase in power loss in above figure hints at jet lubrication and collection of oil inside the shield. Utilizing particle-based simulations pave the road to analyze properties of particles and the consequent behaviors. By flowing the lubricant in all over the shaft, the particles experience different pressures. Fig. 4. 46 illustrates lubricant pressure in different parts of the shaft.

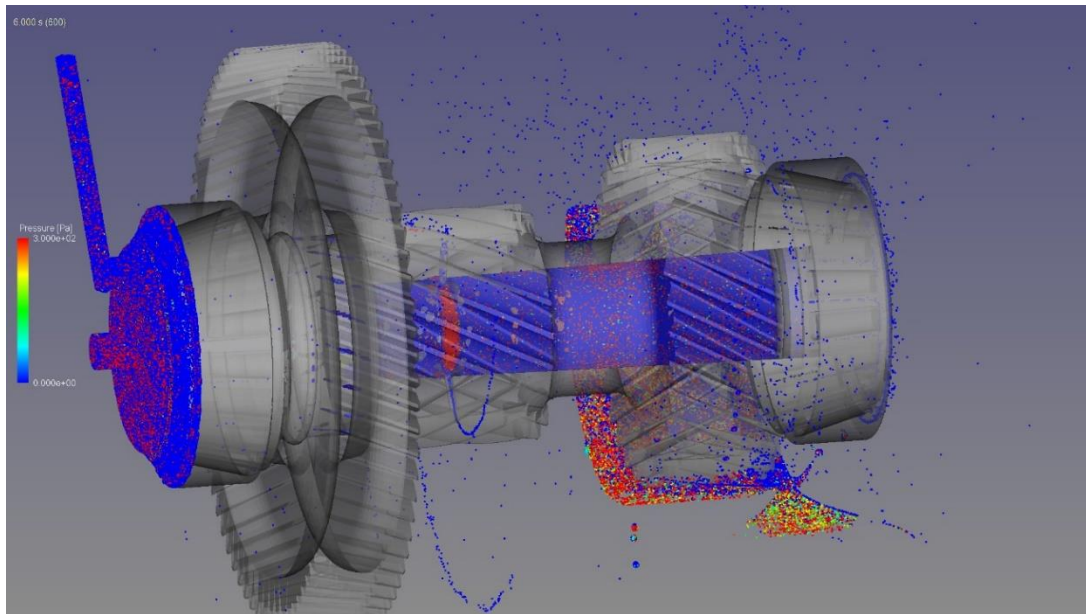


Fig. 4. 46. Pressure distribution in shaft 3 in high temperature.

Low temperature

As mentioned before, lubricant reaches the roller bearing and due to rotational speed, they are directed toward meshing area. The following figure shows how oil particles can pass through the cage and touch gear:

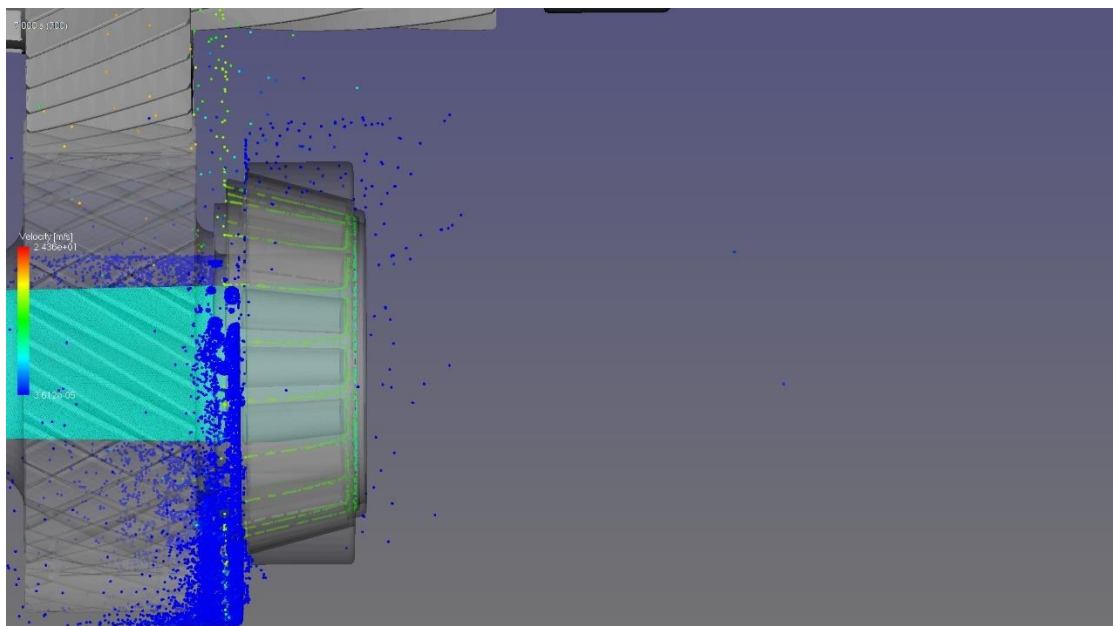


Fig. 4. 47. Passage of oil particles through cage

In order to have complete study, two different temperatures are considered to find out oil behavior. Because, at low temperature, oil flowrate is reduced due to higher viscosity and it can have remarkable effect on equipment relying on oil flow to avoid failures. Similar to previous sections, oil number density on different parts of the shaft is achieved and analyzed. Fig. 4. 48 depicts acceptable deposition of oil in last meshing area in spite of low temperature and can guarantee sufficient lubrication and consequent cooling process. Moreover, high viscose lubricant can make wet first meshing area completely.

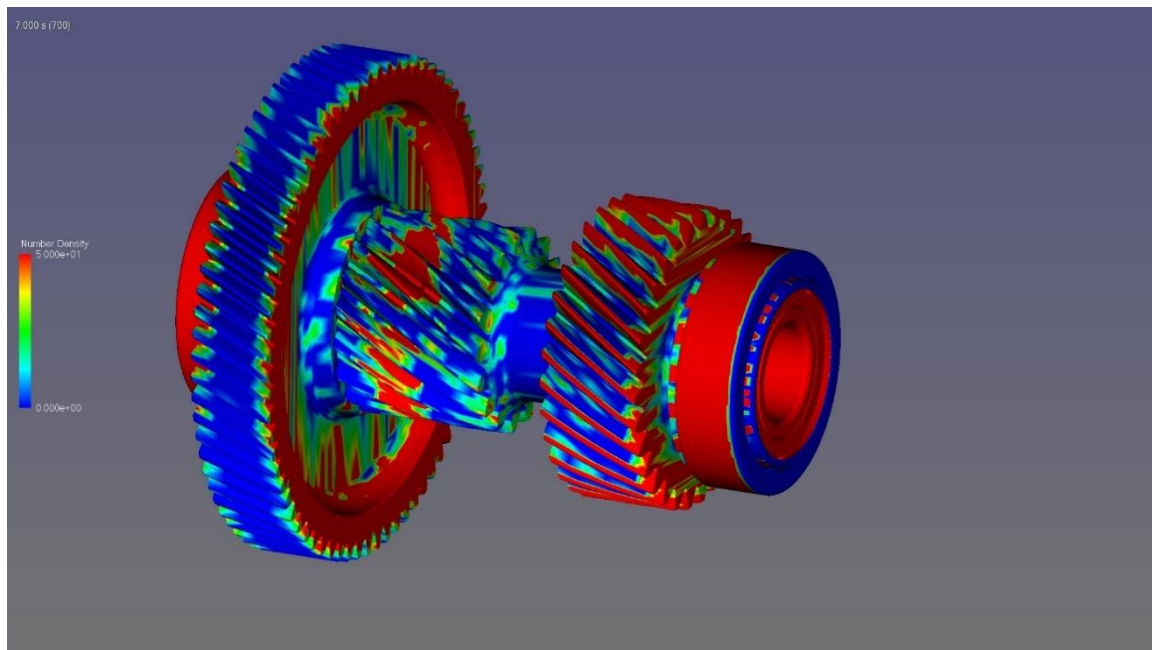


Fig. 4. 48. Oil number density in low temperature

As can be seen, not only on critical places on the shaft, but various places oil are being distributed that can result in cooling of whole shaft. Likewise, following figure is presented to illustrate oil covering of meshing area and as can be seen the meshing area is red showing high oil number density.

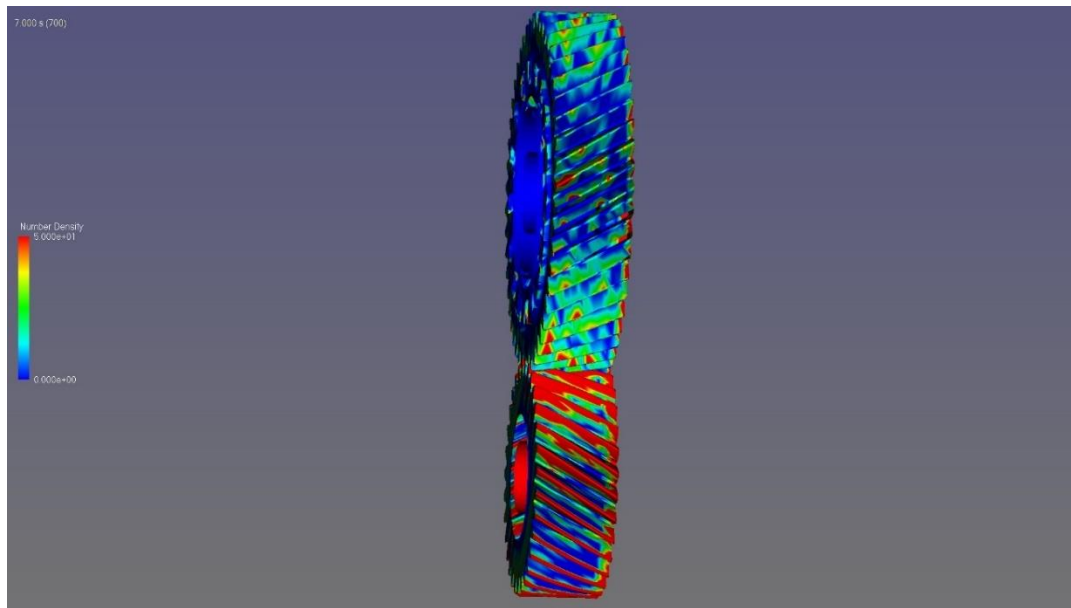


Fig. 4. 49. Oil number density in meshing area

It is clear that both upper and bottom gears are in acceptable conditions due to jet lubrication and oil splashing (for bottom gear). In fact, in low temperatures owing to higher viscosity, the oils emitting jet nut collect inside the shield and by passage of time, oil level rises up and is helpful for oil splashing. We can take advantage of particle-based simulations to analyze properties of particles and the consequent behaviors. By flowing the lubricant in all over the shaft, the particles experience different pressures. It is obvious that oil inside the shaft go through higher pressures compared to higher temperatures. Fig. 4. 50 shows oil pressures inside this shaft.

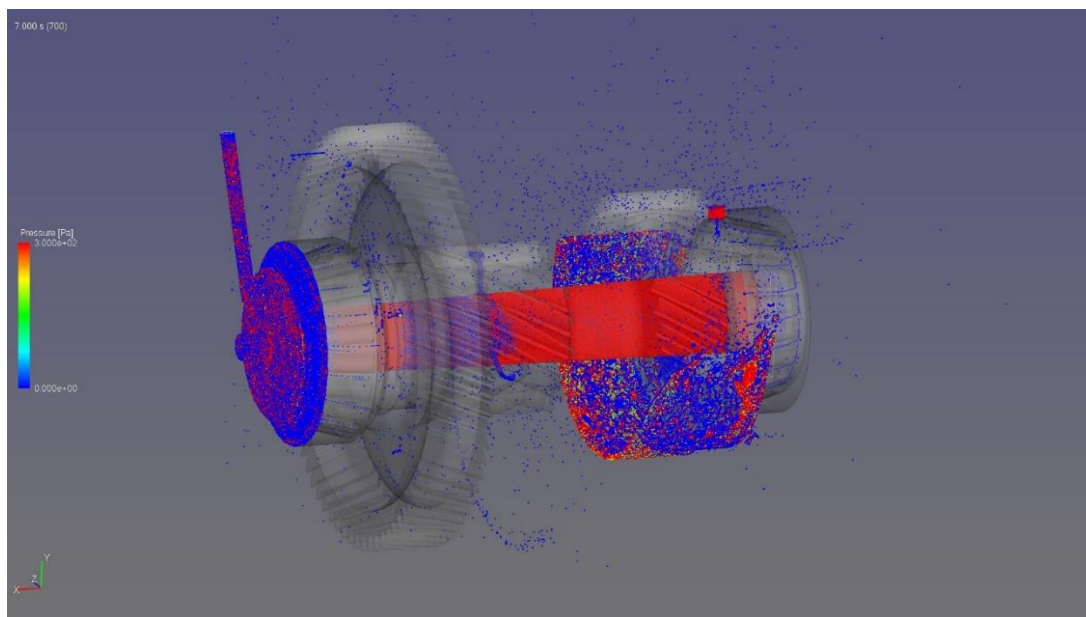


Fig. 4. 50. Pressure distribution in shaft 3 in low temperature.

As last step, the churning loss for this case can be expressed as follow:

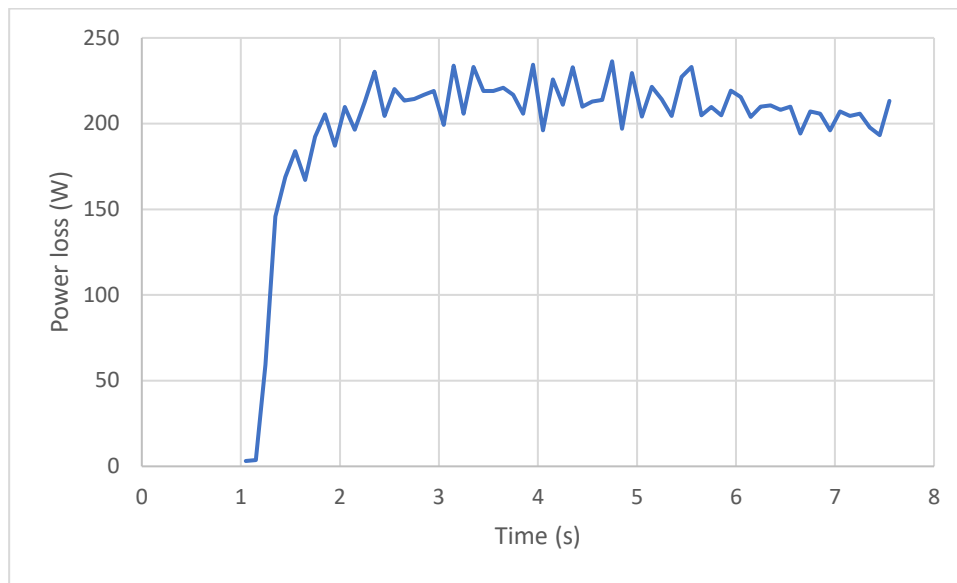


Fig. 4. 51. Power loss related to shaft 3 for lower temperature.

As expected, for higher viscose oil the power loss should be higher compared to last section. All in all, the design of shield besides jet lubrication can fulfill our expectations for these two shafts to prevent failures. It is important to design efficient lubrication system, because the primary function of a gearbox is to efficiently transfer power from the engine to the wheels. This power transfer generates heat and friction, which can result in damage and general wear and tear. The risk of damage from heat and friction is decreased in the gearbox by the use of high-quality oil lubrication. Additionally, it prolongs the life of the gearbox by reducing gear tooth wear. The smooth, silent, and effective operation of the gearbox is another benefit of proper oil lubrication. Additionally, effective oil lubrication in the gearbox lowers noise and vibration, making for a more enjoyable driving experience. In order to ensure safe and comfortable driving, improve vehicle performance, avert expensive repairs, and preserve the gearbox's longevity, it is essential to keep a high grade of oil in the gearbox.

5. Temperature and thermal stress analysis

The two most important factors in guaranteeing best performance and longevity of shafts and bearings are temperature and thermal stress analyses. The temperature analysis assists in determining optimal operating temperature for machinery during the course of its lifetime. Several techniques, including infrared imaging, thermal sensors, and thermocouples, can be used to do it. Monitoring the temperature might help find potential issues with the system's functionality or design. The amount of

heat strain in various components of the machinery, notably in shafts and bearings, can be predicted using thermal stress analysis, a crucial engineering tool. It should be noted that the amount of internal heat generation in bearings are complex to calculate and is function of load, velocity and lubrication. Heat can lead to expansion of bearing materials leading to reduction of lifespan. This study aids in identifying regions that could be vulnerable by thermal stresses and fluctuations. Targeted changes can then be made to these regions to enhance performance, increase durability, and lower the likelihood of premature failure. Intense operating conditions, including high temperatures, hefty loads, shocks, and vibrations, are frequently imposed on shafts and bearings. Therefore, it is essential to do a thermal stress study on these components to ensure their dependability and lifetime. In this analysis, thermal stresses and strains under various operating conditions, such as temperatures and thermal gradients, are examined. The design of these components can be improved to make them more durable and reliable based on the findings of this investigation.

It should be noted that thermal stress and temperature analyses are important components of shaft and bearing engineering. By conducting these evaluations, designers and engineers can pinpoint problem areas and make the required adjustments to guarantee the best performance and longevity of these components. These evaluations are also essential for detecting areas that are vulnerable to damage and wear, lowering the likelihood of early failure and lowering maintenance costs. Omitting thermal stress in design and operation stages results in deformation, premature degradation and cracks in components causing failure and heavy losses. Therefore, thermal stress analysis gives engineers the opportunity to improve and optimize design, materials and manufacturing processes to assure long-term performance, durability and safety of components.

Among thermal stress of different parts of transmission system, analysis of bearings is of the most important components owing to tolerating high speed, temperature and load. During operation, bearing produce heat and if it is not dissipated correctly, it leads to wear, failure and crack. Hence, based on analysis the heat generation can be tackled and is helpful to find problems with the lubrication system. No need to say that the lubrication system can notably affect functionality and performance of mechanical gearbox and in the last sections of this study, novel methods have been suggested and applied in truck transmission system to optimize and increase efficiency of lubrication system. Therefore, additional railways are exerted and the lubricant can move inside the shaft through a nozzle to make wet roller bearing and ball bearing in input shaft. The velocity, axial and radial forces, type of lubrication, lubricant viscosity are able to influence internal heat generation of bearing.

Using MPS method heat transfer can be obtained which consists of thermal energy transformation between particles. The temperature differential between the particles and the fluid's thermal

conductivity both affect how much energy is transported. The ability of the MPS to simulate fluid flow and heat transmission in a variety of situations, including turbulent and complicated geometries, makes it possible to calculate the heat transfer coefficient. MPS solves the Navier-Stokes equations and the energy equations to determine the flow field and temperature distribution, respectively. In MPS, the inter-particle thermal conductivity can be used to compute the heat transfer coefficient, which is crucial for modelling heat transfer issues in particulate medium.

In this section, first we model the temperature of both bearings in input shaft and solve thermal models with utilizing a merging of particle-based oil simulation and steady-state thermal modeling. Using MPS, the heat transfer coefficient for complicated flow is obtained and is imposed to finite element model related to this shaft. Following figure shows the two critical bearings which are analyzed to obtain temperature and thermal stresses.

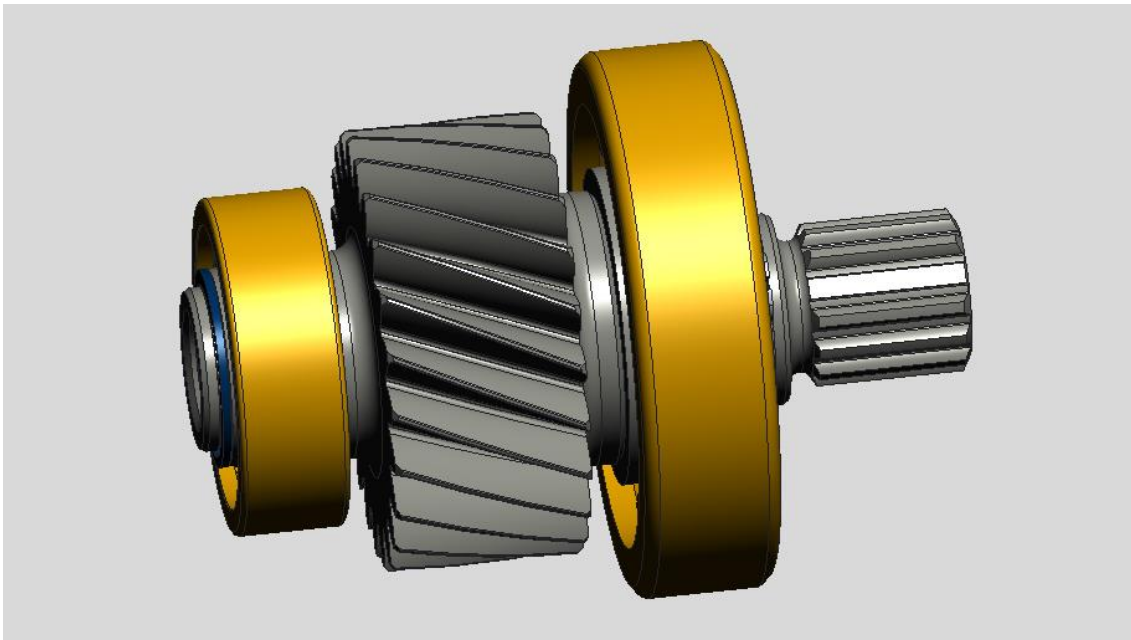


Fig. 5. 1. Two critical bearings in input shaft

As mentioned in last section, the oil enters inside input shaft and using a nozzle, the roller bearing gets wet. At the end, the lubricant can touch ball bearing by modified spline. It should be noted that the rate at which heat is moved between two surfaces typically by convection or conduction is measured by the heat transfer coefficient. A greater heat transfer coefficient indicates faster heat transfer, whereas a lower heat transfer coefficient indicates slower heat transfer. The surface qualities, fluid properties, flow velocity, and temperature difference between the two surfaces are only a few of the variables that affect the heat transfer coefficient. It is a crucial idea in engineering and is used in numerous sectors, including the chemical, automotive, and aerospace industries. In this study, only

heat transfer coefficient related to oil flow (without air) is considered. Fig. 5. 2a and Fig. 5. 2b depict heat transfer coefficient on the roller bearing and gear of input shaft.

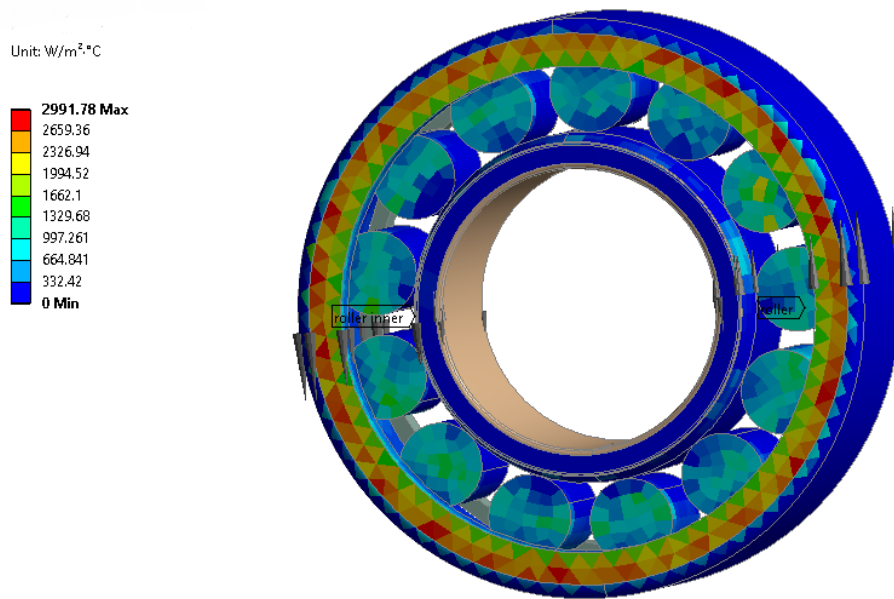


Fig. 5. 2a. Heat transfer coefficient of roller bearing

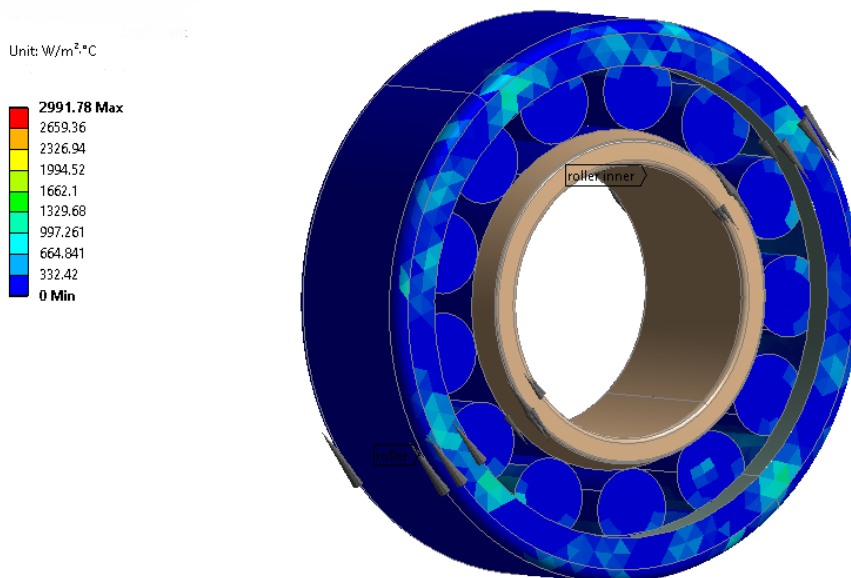


Fig. 5. 2b. Heat transfer coefficient of roller bearing

As can be seen, due to presence of nozzle and nut jet closed to gear, oil distribution and consequent heat transfer coefficient on the roller bearing is acceptable. Similarly, the heat transfer coefficients on the ball bearing are shown in Fig. 5. 3a-b. In this transmission system the heat exchangers are

provided. To keep the temperature of the oil constant in gearboxes, heat exchangers are a crucial component. When the oil in the gearbox heats up too much, it can reduce the oil's capacity to lubricate and harm the gearbox's internal parts. By expanding the surface area of the oil that is in contact with the colder object or fluid, heat exchangers enable the transfer of heat from the oil to the surroundings. By doing so, the oil temperature is lowered and the gearbox's ideal working temperature is maintained.

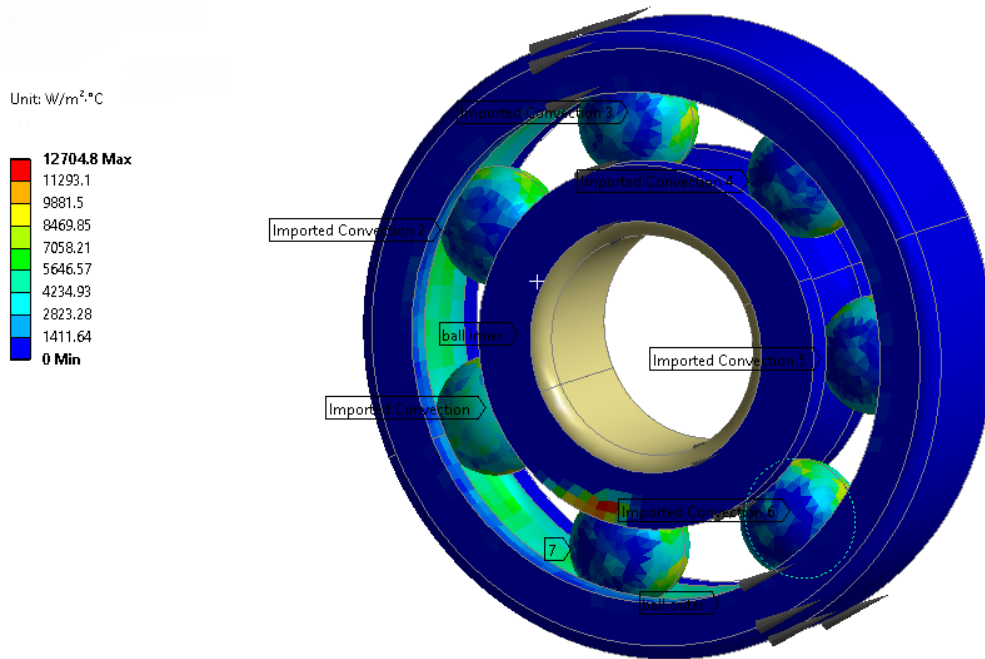


Fig. 5. 3a. Heat transfer coefficient on ball bearing.

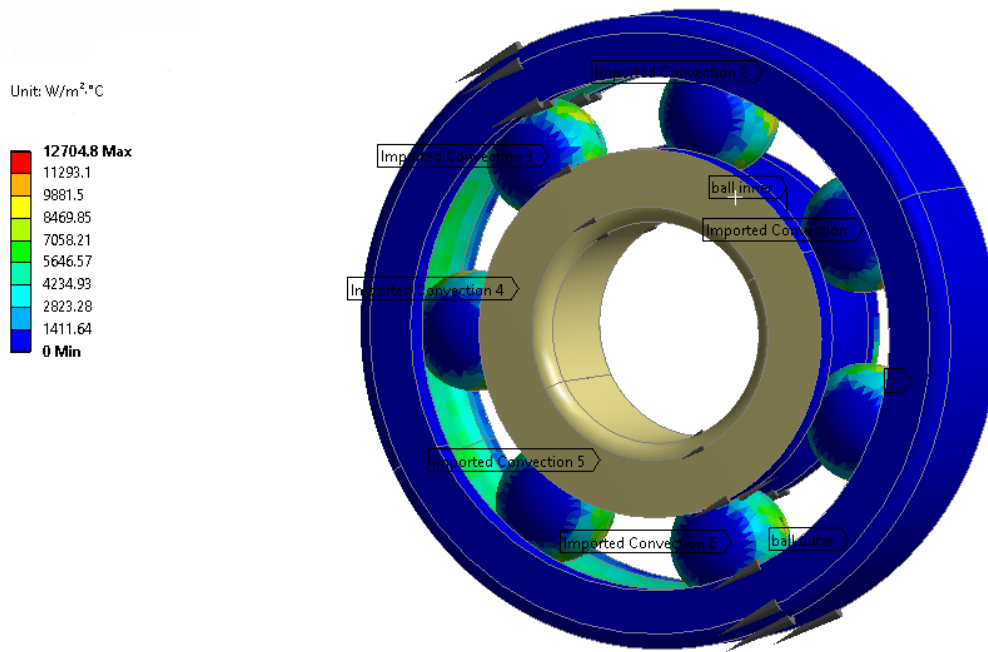


Fig. 5. 3b. Heat transfer coefficient on ball bearing.

Moreover, the heat transfer coefficient on shaft and gear is shown in following figures:

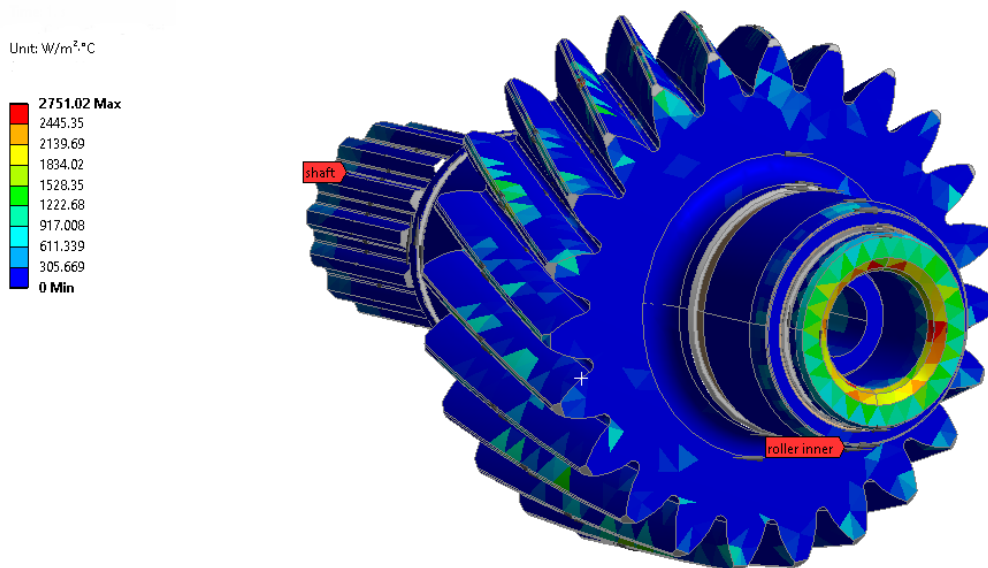


Fig. 5. 3c. Heat transfer coefficient on shaft.

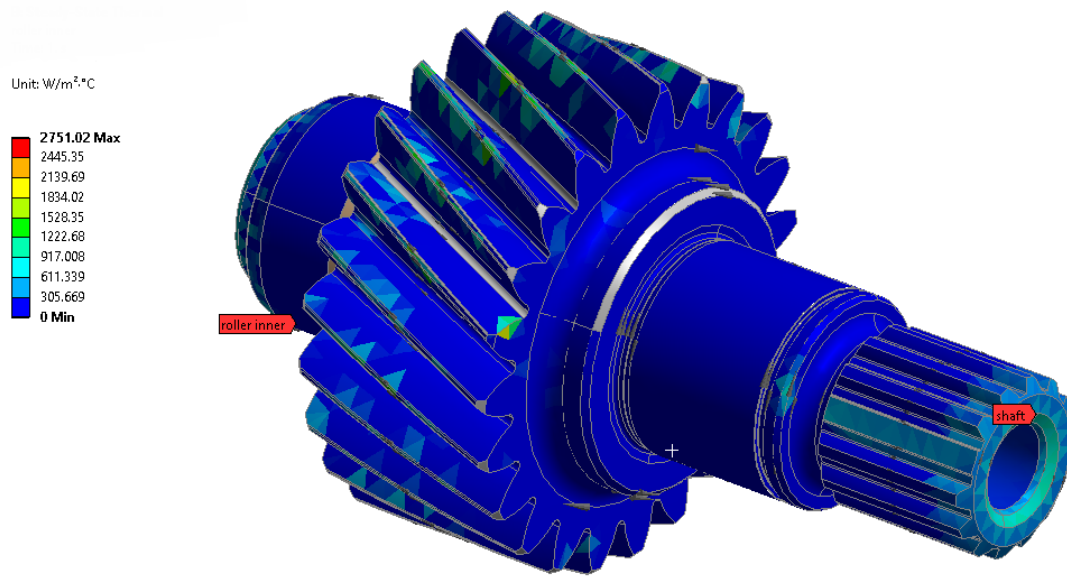


Fig. 5. 3d. Heat transfer coefficient on shaft.

The figures shown describing oil distribution and consequent heat transfer coefficient between ball bearing and oil that can hint at act of cooling. It should be noticed that this oil distribution is only jet lubrication and the lubricant related to railways. Because, both bearings in input shaft get wet by this method. The lubricant temperature considered in this case is 70°C and the component temperature varies between 110°C and 120°C. The roller bearing properties are listed as follow:

Parameter	Value
Roller inner ring diameter d	30 mm
Roller outer ring diameter D	62 mm
Ring thickness B	20 mm
Basic static load rating C_0	49 kN
Basic dynamic load rating C	55 kN

Table 5. 1. Roller bearing properties

Likewise, the ball bearing properties can be written as follow:

Parameter	Value
Ball bearing inner ring diameter d	35 mm
Ball bearing outer ring diameter D	100 mm
Ring thickness B	25 mm
Basic static load rating C_0	31 kN
Basic dynamic load rating C	55 kN

Table 5. 2. Ball bearing properties

Using MPS, the heat transfer coefficient for complicated flow is obtained and is imposed to finite element model related to this shaft.

5.1. Internal heat generation of bearing

Complex correlations exist between component temperature and power loss, and these interactions in turn depend on a wide range of other parameters, including bearing sizes, loads, and lubrication conditions. Depending on the operational state, such as at startup or normal operation, when steady-state conditions is achieved, they have a significant impact on a variety of performance parameters of an application and its constituent parts. A crucial component of the examination of an application is determining the operating temperature and confirming speed restrictions. Many of an application's performance qualities are significantly influenced by temperature. The temperature of an application's components is determined by the heat input, output, and internal heat. The steady-state temperature that a bearing reaches while working and in thermal equilibrium with its surrounding components is known as its operational temperature. The final temperature is related to internal heat generation via bearing and seal frictional power loss, heat transmitted to bearing by shaft and gear, heat transferred from bearing to other components. The application design and friction created by the bearing both have an impact on the bearing operating temperature. Consequently, a thermal analysis of the bearing, its companion components, and the application is required.

In general, the bearing size depends upon velocity, oil condition as well as load imposed to bearing. The temperature of bearing is according to bearing size, velocity, load and oil condition. Similarly, oil condition is based on lubricant viscosity and velocity. To achieve the best design for a bearing

arrangement and choose the most suitable components for it, these interdependencies are addressed by using an iterative approach to the study.

The generated heat in bearings is derived from bearing frictional power loss and the heat conduction by adjacent component. As mentioned before, the friction of bearing includes chiefly oil drag loss, seal friction, sliding friction and rolling friction. In this analysis, in addition to internal heat generation, the heat conduction between bearing and adjacent parts are considered. The friction in bearings isn't fixed and depends on specific tribological events that take place in the lubricant film between the rolling components, raceways, and cages for bearing friction to vary. Speed-dependent friction occurs in a bearing with a certain lubricant.

The bearings in input shaft tolerate axial and radial loads due to weight and high rotational speeds and these loads have been calculated as follow:

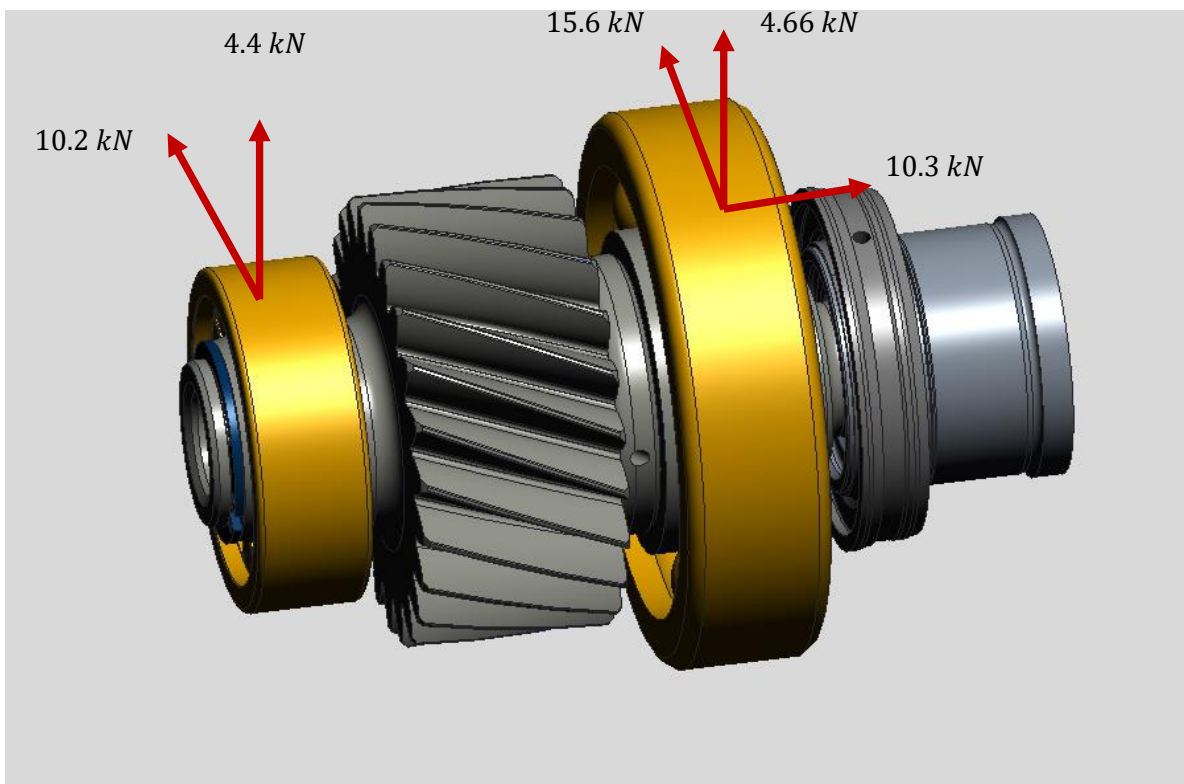


Fig. 5. 4. Axial and radial loads applied on bearings

Rolling frictional moment play key part in bearing heat generation and according to [23] is based on axial and radial loads, rotational speed. In case of roller bearing and considering $\varphi_{ish} = 0.73$ and $\varphi_{rs} = 0.95$ according Eq. 3. 1, we have:

$$M_{rr} = \varphi_{ish}\varphi_{rs}G_{rr}(nv)^{0.6} = 236 (Nmm)$$

Sliding frictional moment is related to bearing size, radial and axial loads applied on the bearing. In addition, there is sliding friction coefficient depending on film lubrication. According to Eq. 3. 4, sliding frictional moment can yields:

$$M_{sl} = G_{sl}\mu_{sl} = 15.3 (Nmm)$$

It should be noted that the frictional moments related to drag loss and seals are negligible compared to abovementioned moments. Therefore, for roller bearing, the total frictional moment can be written according to Eq. 3. 8 as follow:

$$M = M_{rr} + M_{sl} = 252 (Nmm)$$

Bearing heat generation is a serious problem since it can cause early failure and reduced performance. Bearings provide support for rotating shafts, and as they move through friction during rotation, heat is produced. The heat generated from bearings are the main heat source in transmission system. According to Harris [24] the heat generated can be calculated as:

$$H_f = 1.047 \times 10^{-4}nM = 251 (W)$$

In which n refers to rotational speed of bearing which is 9500 (rpm) and M is total frictional moment that has been computed in previous stage.

The heat generated for ball bearing is followed similarly and frictional moments related to drag loss and seals are negligible compared other frictional moments. Hence, rolling frictional moment and sliding frictional moment are written as follow:

$$M_{rr} = \varphi_{ish}\varphi_{rs}G_{rr}(nv)^{0.6} = 504 (Nmm)$$

$$M_{sl} = G_{sl}\mu_{sl} = 1080 (Nmm)$$

Total frictional moment can be calculated by summing up rolling frictional moment and sliding frictional moment:

$$M = M_{rr} + M_{sl} = 1590(Nmm)$$

Finally, the heat generated can be calculated as:

$$H_f = 1.047 \times 10^{-4}nM = 1585 (W)$$

It should be noted that the rotational speed of bearing is 9500 (rpm) as well.

Oil is utilized for lubrication and cooling in industrial or automobile gearboxes. However, the heat and friction produced by the moving parts have a tendency to heat up the oil and in particular, it is intense in EVs. The oil heat exchanger is useful in this situation. By transferring heat to a coolant or

air flow, the heat exchanger aids in keeping the oil at its ideal temperature. As a result, the gearbox is shielded from heat-related damage, the wear and tear on the gears and bearings is decreased, and the gearbox's overall effectiveness and performance are enhanced. The oil heat exchanger is a crucial component of the gearbox system since it aids in preserving the oil's quality and longevity, assuring the gearbox's dependable and smooth operation throughout the duration of its useful life. Therefore, the oil temperature in this analysis is considered 70°C and its properties are listed as follow:

Density (kg/m^3)	860
Thermal conductivity (W/mK)	0.139
Specific heat (J/kgK)	2008
Kinematic viscosity (m^2/s)	6×10^{-5}
Surface tension coefficient (N/m)	0.072

Table 5.3. Properties of lubricant

The material considered for both bearings and gear, in this case study, is stainless steel and its material properties are listed as follow”

Density (kg/m^3)	8000
Elastic modulus (GPa)	193
Tensile strength (MPa)	485
Yield strength (MPa)	170
Thermal conductivity (W/mK)	16.3
Specific heat (J/kgK)	500

Table 5.4. Stainless steel material properties

Furthermore, the main oil flowrate in this case is $1 \frac{l}{min}$ that can be distributed by nozzle in roller bearing and ball bearing.

5.2. Temperature and stress analyses

Hypothesizing contacts play a crucial role in simulations. It is necessary to model the contact or interface between them because the simulation calls for the interaction of numerous diverse pieces or items. Inaccurate results from such interactions' modeling might have a negative impact on the final

product's design and functionality. To adequately simulate the mechanical, thermal, and fluid dynamics of the system, the contacts must be defined correctly and their behavior must be understood. The following figures illustrate the contacts between balls and rollers and bearing rings which is “no separation”. The remained contacts between shaft and inner rings are considered “bonded”.

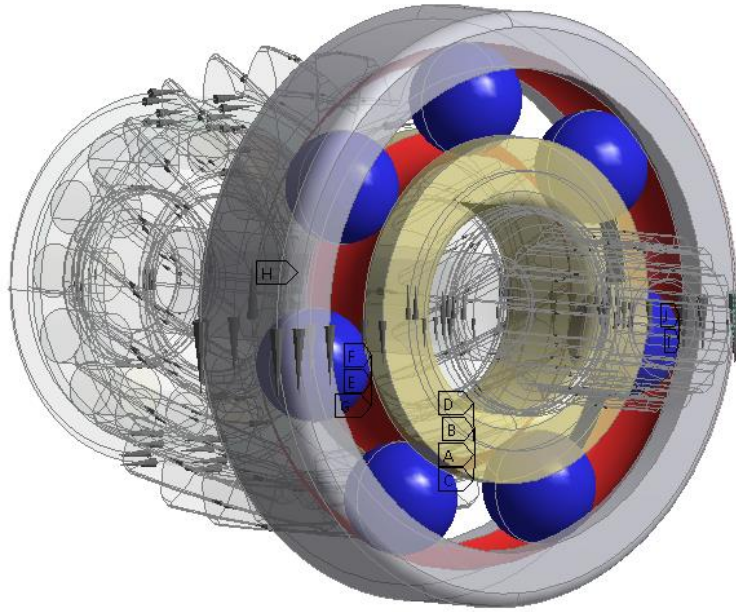


Fig. 5. 5.a. Contacts in ball bearing

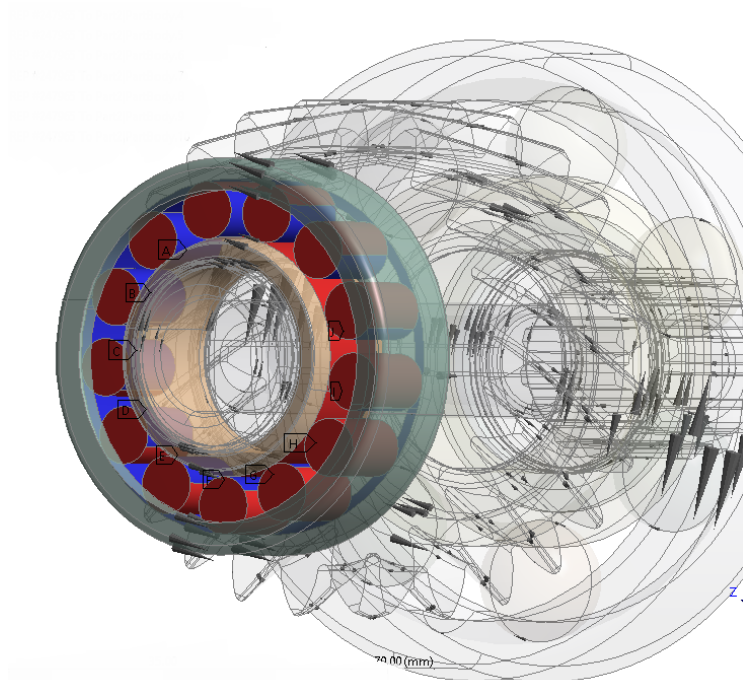


Fig. 5. 5.b. Contacts in roller bearing

The following figure illustrates the temperature distribution on roller bearing according to overall $1 \frac{l}{min}$ of oil entering nozzle, 9500 (*rpm*) of rotation and the applied load (Fig. 5. 4). It should be noted that average heat transfer coefficients are obtained and the temperature is achieved by steady-state boundary conditions. As seen in the heat transfer coefficient figures, lubricants are directed almost outward roller bearing and ball bearing due to high centrifugal force. Hence, the lubricant distributions are uneven in this case. The oil received by inner ring is lower compared to outer ring so that the maximum oil volume is on outer ring. The ring's temperatures decrease with oil splashing and according to Fig. 5. 6, the inner ring goes through higher temperature (about 97 °C) because of lower oil distribution and higher contact zone with other parts of shaft.

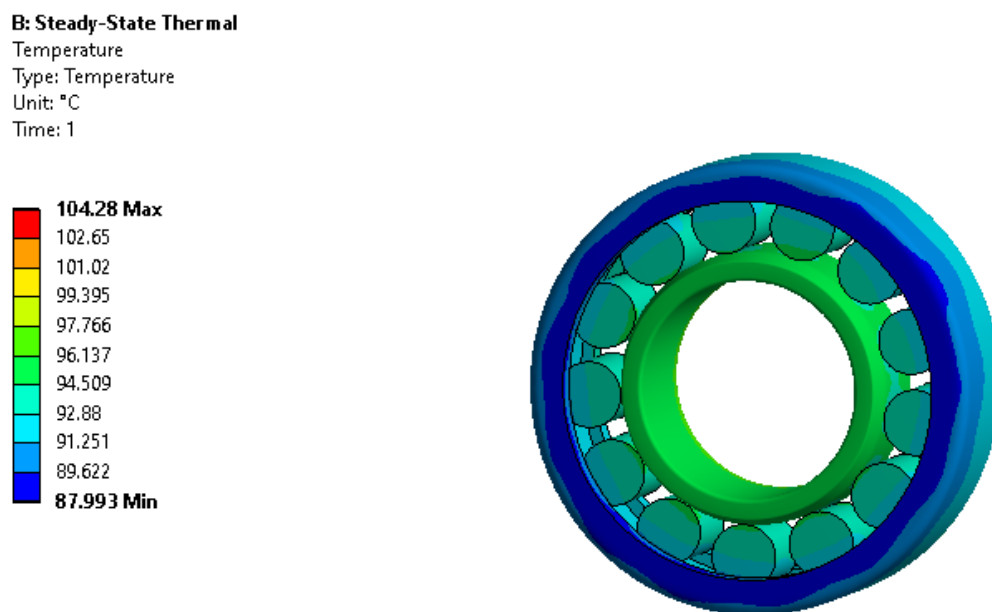


Fig. 5. 6. Temperature distribution in roller bearing

Total heat flux is the quantity of heat energy released or transmitted from a surface or item per unit of time. Convective, radiative, and conductive heat transfer are all included in it. But, in this study, the radiative heat transfer is omitted. Total heat flux is a key idea in thermal engineering because it facilitates the design of heat transfer systems for a variety of uses. The effectiveness of thermal insulation technologies and a system's energy efficiency can both be assessed using total heat flux. Hence, the total heat flux in roller bearing is depicted in Fig. 5. 7. As mentioned, the heat flux depends on convective heat transfer as well and due to oil splashing outward, thus the rate of energy heat on rollers and outer ring is higher. The convective heat transfer coefficients differed at different positions on the rollers and rollers with a higher convective heat transfer coefficient had a lower temperature.

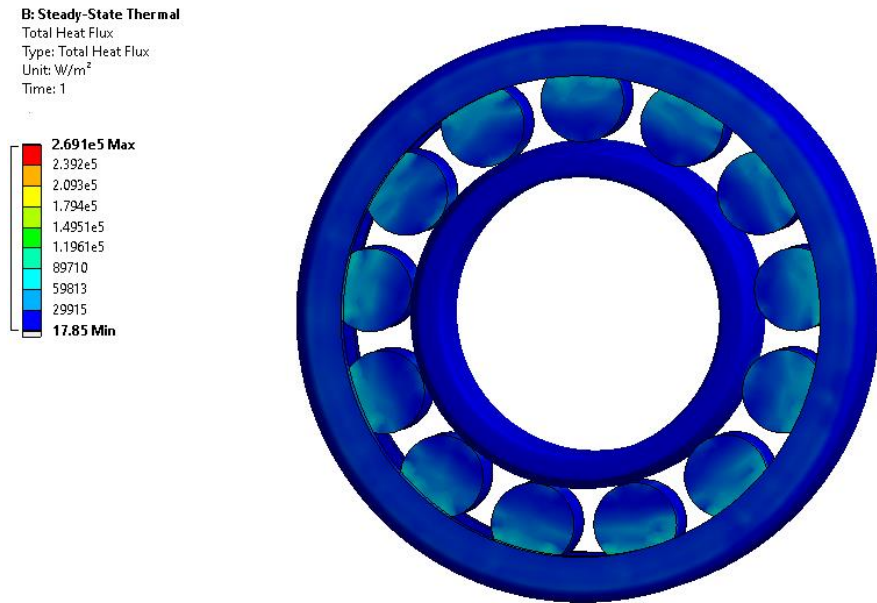


Fig. 5. 7. Total heat flux in roller bearing

In the figure below, temperature distribution on the ball bearing with overall $1 \frac{l}{min}$ of oil entering nozzle and 9500 (*rpm*) of rotation is depicted. Average heat transfer coefficients are obtained and the temperature is derived by steady-state boundary conditions. As mentioned before, the lubricant distributions are uneven owing to high centrifugal forces. The oil received by inner ring is lower compared to outer ring so that the oil volume is more gathered inside outer ring. The ring's temperatures decrease with oil splashing and according to Fig. 5. 8, the inner ring goes through higher temperature. The temperature on the balls is about 104 °C which has difference of 8°C with outer ring.

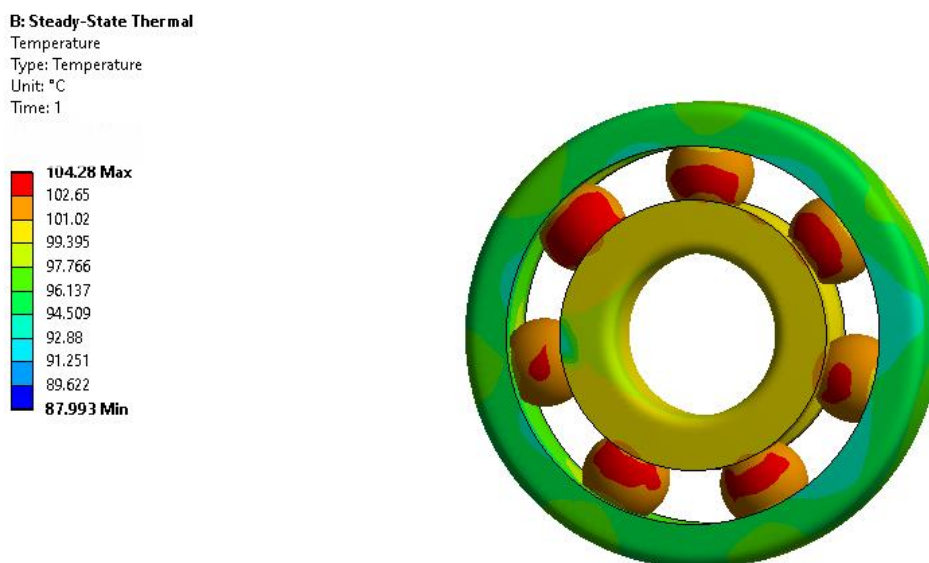


Fig. 5. 8. Temperature distribution in ball bearing

Total heat flux in ball bearing is shown in Fig. 5. 9. The heat flux depends on convective heat transfer as well and due to oil splashing outward, thus the heat flux on balls is higher.

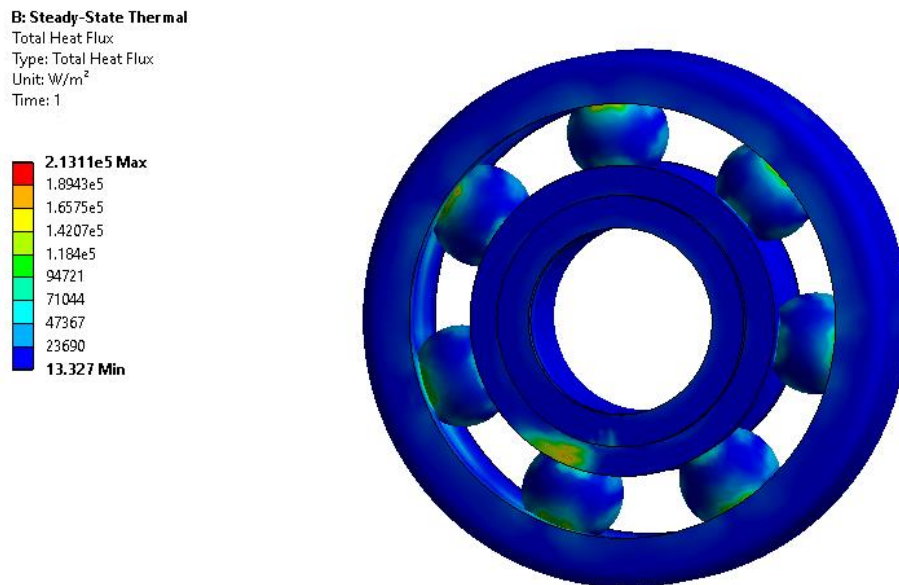


Fig. 5. 9. Total heat flux in ball bearing

As explained before, the ball and roller bearings withstand notable temperature alterations and these changes can lead to creation of thermal strains and stresses. Hence, thermal stress analysis is essential to measure warpage generated with thermal strain and to predict failure because of additional strains. For this purpose, we require to do implement temperature distribution analysis over assembly and in the next step, perform stress analysis. Neglecting thermal stress in design and operation stages results in deformation, premature degradation and cracks in components causing failure and heavy losses. Therefore, thermal stress analysis gives engineers the opportunity to improve and optimize design, materials and manufacturing processes to assure long-term performance, durability and safety of components.

Taking advantage of amount of internal heat generations in bearings and heat flux, thermal stress analysis can be applied. Figs. 5.10a and 5.10b show thermal stress of roller bearing in a static analysis according to equivalent stress (Von-Mises stress). Considering appropriate boundary conditions, the results yield and as can be seen due to thermal expansion of inner ring and rollers, stress on the outer ring (close to rollers) would be higher and is about 20 MPa.

C: Static Structural
Equivalent Stress
Type: Equivalent (von-Mises) Stress
Unit: MPa
Time: 1

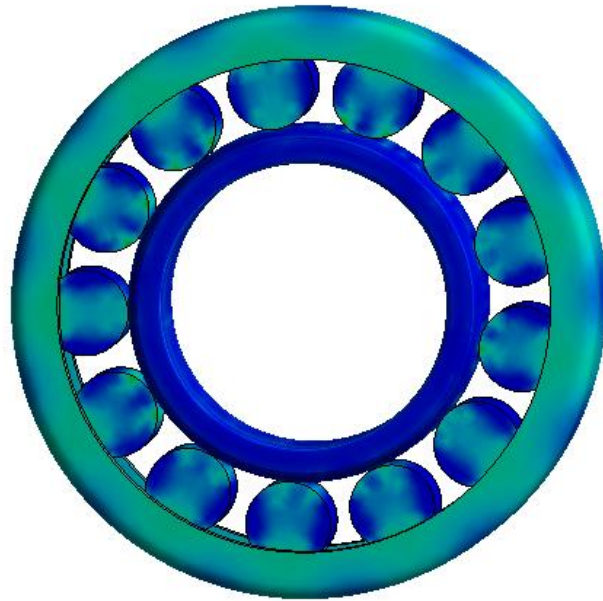
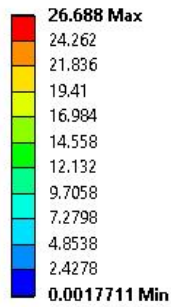


Fig. 5. 10a. Thermal stress analysis on roller bearing

C: Static Structural
Equivalent Stress
Type: Equivalent (von-Mises) Stress
Unit: MPa
Time: 1

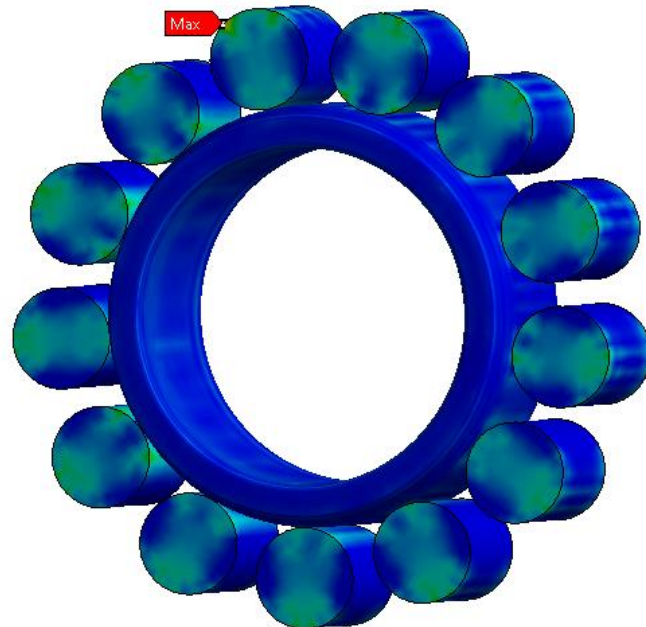
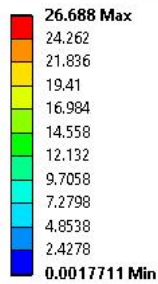


Fig. 5. 10b. Stress distribution over rollers

Similarly, static stress analysis for ball bearing is implemented as shown in Figs. 5.11a and 5.11b. In previous step, it was revealed that temperature is highest in ball bearing. Hence, thermal stress in

balls is at maximum value and is about 26.6 MPa . Moreover, expansion of balls results in stress generation inside outer ring.

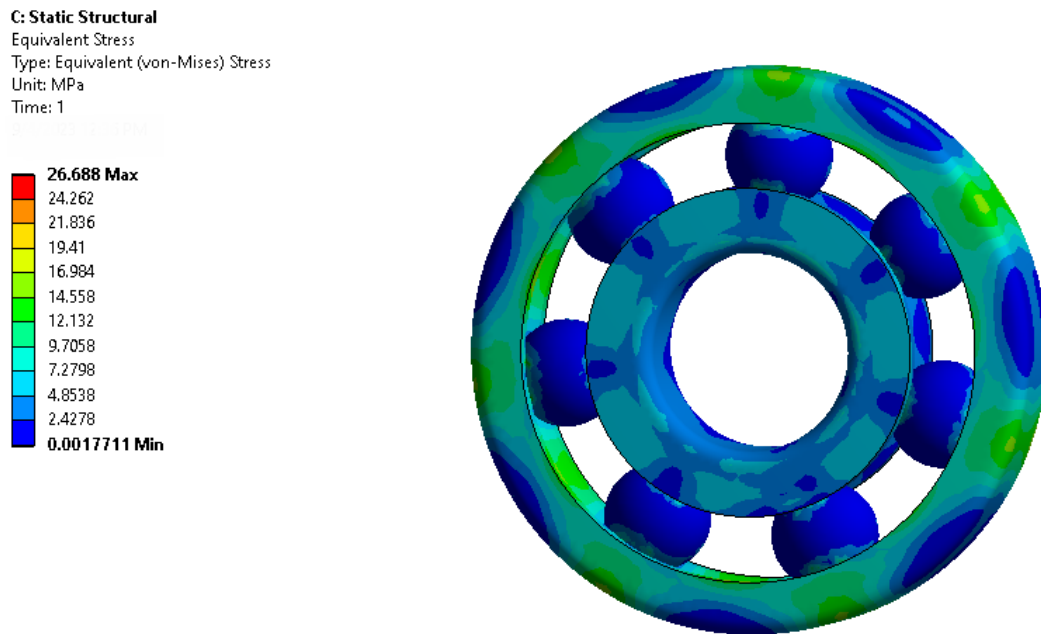


Fig. 5.11a. Thermal stress analysis on ball bearing

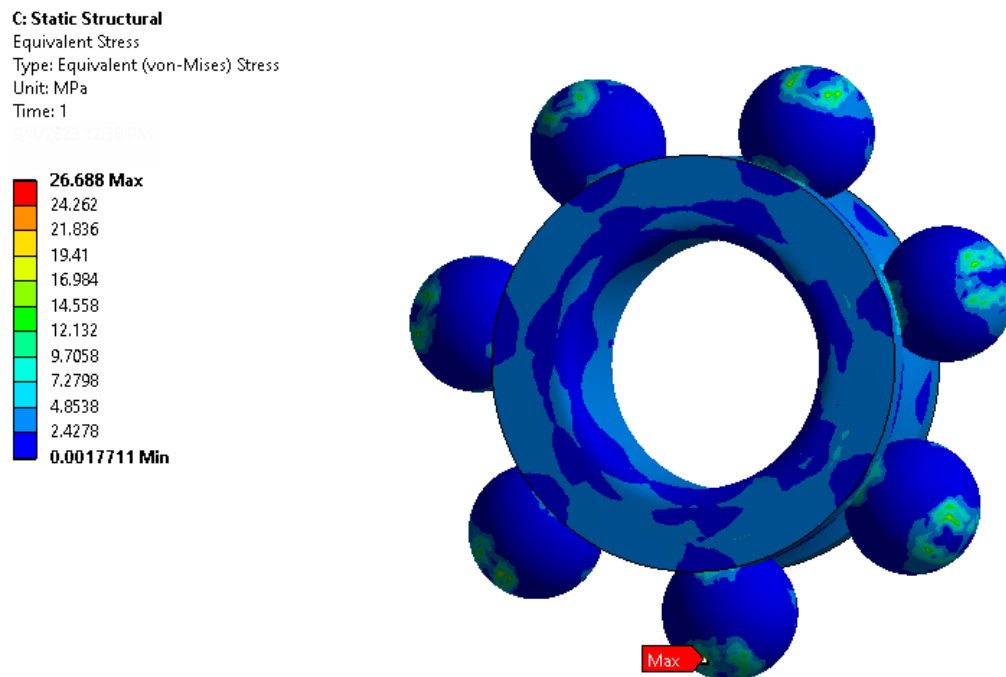


Fig. 5. 11b. Stress distribution over balls

When it comes to gearboxes, optimized lubrication is crucial. Gearboxes depend on the efficient and smooth rotation of gears to transmit power and allow various pieces of machinery to operate as

intended. Without the right lubrication, the gears can soon wear out, causing more heat, friction, and possible gearbox damage. By keeping the gears adequately lubricated, optimized lubrication lowers friction and wear while also dissipating heat produced during operation. This increases the gearbox's overall performance and efficiency while also extending its lifespan. Furthermore, improved lubrication can reduce energy loss in the gearbox, resulting in lower power usage and greater operational reliability. As explained before, in this project, the toothless spline has been selected in order to guarantee more efficiency and wet areas. According to temperature and stress analysis, the picked lubrication method can reduce temperatures and therefore thermal stresses which can cast light on long lifespan and reliability of bearings and gears. Because, in electric vehicles the final temperature in gearbox is high owing to higher rotation speeds and efficient lubrication system is needed. By appropriate lubrication, additional expansion can be prevented.

6. Conclusion

In this study, the lubrication system in truck gearbox was optimized in order to improve efficiency and reliability in case of final temperature and stress. Taking advantage of MPS method, a meshless CFD procedure, the simulation would be more accurate and require lesser time. Additional railways carrying lubricants into the shafts were provided to compensate insufficient lubricant making wet bearings and meshing areas and the analysis was done considering two different speeds and temperatures. In case of shaft number 1, considering radial channel couldn't fulfill sufficient amount of lubricant and hence, spline modification was considered to convey essential amount of oil over ball bearing in both high and low temperatures. Moreover, adjusting shield can be helpful to gather oil and gear impingement with oil happens. Calculating churning losses indicated that these designs are efficient in case of power loss even considering higher speeds. Furthermore, using internal heat generations in bearings, final temperature of bearings after lubrication was calculated showing reliability of new lubrication designs that led to decrease in their temperature. In addition, reduction of temperature causes decrease in thermal stress due to expansion of inner rings, balls and rollers. The bearings are of the most vulnerable parts of transmission systems and their failure accounts for a major part of danger, therefore this optimization can lead to longevity avoiding failures.

References

- [1] Jiang Y, Hu X, Hong S, Li P, Wu M. Influences of an oil guide device on splash lubrication performance in a spiral bevel gearbox. *Tribology International*. (2019), 136, 155-164.
- [2] Liu H, Jurkschat T, Lohner T, Stahl K. Detailed investigation on the oil flow in Dip-lubricated gearboxes by finite volume CFD method. *Lubricants*. (2018), 47. doi:10.3390/lubricants6020047.
- [3] Malakova S, Sivak S. Particle example of modification of a gearbox lubrication system. *Lubricants*. (2022), 110. doi.org/10.3390/lubricants10060110.
- [4] Singh D, Kurien J, Villayamore A. Study and analysis of wind turbine gearbox lubrication failure and its mitigation process. *Materials Today: Proceedings*. (2021), 44, 3976-3983.
- [5] Mastrone M, Concli F. CFD simulation of grease lubrication: analysis of the power losses and lubricant flows inside a back-to-back test rig gearbox. *Journal of Non-Newtonian Fluid Mechanics*. (2021), 297.
- [6] Lu F, Wang M, Bao H, Huang W, Zhu R. Churning power loss of the intermediate gearbox in a helicopter under splash lubrication. *Proceeding Journal of Mechanical Engineering Part J*. (2021) 236, 49-58.
- [7] Marques P, Fernandes C, Martins R, Seabra J. Power losses at low speed in a gearbox lubricated with wind turbine gear oils with special focus on churning losses. *Tribology International*. (2013), 62, 186-197.
- [8] Dai Y et al. Numerical simulation and optimization of oil jet lubrication for rotorcraft meshing gears. *International Simulation Modeling*. (2018), 17, 318-326.
- [9] Deng X et al. Lubrication mechanism in gearbox of high-speed railway trains. *Journal of Advanced Mechanical Design, Systems and Manufacturing*. (2020), 14 (4).
- [10] Guo D, Chen F, Liu J, Wang Y, Wang X. Numerical modeling of churning power loss of gear system based on moving particle method. *Tribology Transactions*. (2019), DOI: 10.1080/10402004.2019.1682212.
- [11] Yang J, Feng Z, Wang X. Oil injection lubrication analysis of a silent chain drive system. *Advances in Engineering Software*. (2022), 172, <https://doi.org/10.1016/j.advengsoft.2022.103210>.
- [12] Kondo M, Koshizuka S. Improvement of stability in moving particle semi-implicit method. *International Journal For Numerical Methods In Fluids*. (2011), 65, 638-654.
- [13] Khayyer A, Gotoh H. Enhancement of stability and accuracy of moving particle semi-implicit method. *Journal of Computational Physics*. (2011), 230, 3093-3118.
- [14] Wu W, Wei C, Yuan S. Numerical simulation of ball bearing flow field using the moving particle semi-implicit method. *Engineering Applications of Computational Fluid Mechanics*. (2022), 16, 215-228.

- [15] Deng Q et al. A combined experimental and computational study of lubrication mechanism of high precision reducer adopting a worm gear drive with complicated space surface contact. *Tribology International*. (2020), 146, <https://doi.org/10.1016/j.triboint.2020.106261>.
- [16] Patil P, Kumar A. Dynamic structural and thermal characteristics analysis of oil-lubricated multi-speed transmission gearbox:variation of load, rotational speed and convection heat transfer. *Iranian Journal of Science and Technology, Transactions of Mechanical Engineering*. (2017), 41, 281-291.
- [17] Liu J, Xu Z. A simulation investigation of lubricating characteristics for a cylindrical roller bearing of a high-power gearbox. *Tribology International*. (2022), 167, <https://doi.org/10.1016/j.triboint.2021.107373>.
- [18] Lu F, Wang M, Pan W, Bao H, Ge W. CFD-based investigation of lubrication and temperature characteristics of an intermediate gearbox with splash lubrication. *Applied Science*. (2021), 11, <https://doi.org/10.3390/app11010352>.
- [19] Douglas C, Thite Anand. Effect of lubricant temperature and type on spur gear efficiency in racing engine gearbox across full engine load and speed range. *Proceeding Journal of Mechanical Engineering Part J*. (2015), 1-19.
- [20] Li W, Zhai P, Tian J, Luo B. Thermal analysis of helical gear transmission system considering machining and installation error. *International Journal of Mechanical Science*. (2018), 149, 1-17.
- [21] Magerramova L et al. Design, simulation and optimization of an additive Laser-Based manufacturing process for gearbox housing with reduced weight made from AlSi10Mg alloy. *Metals*. (2022), 12, <https://doi.org/10.3390/met12010067>.
- [22] Nasser M. A, Gomaa F. R, Asy M. A, Deabs A. Structural modifications of 1K62 engine lathe gearbox casing. *International Journal of Advanced Engineering and Global Technology*. (2015), 3(2).
- [23] Patel M, Patil A. Stress and design analysis of triple reduction gearbox casing. *International Journal for Innovative Research in Science & Technology*. (2015), 2(2).
- [24] Koshizuka S, Shibata K, Matsunaga T. Moving particle semi-implicit method. (2018), <https://doi.org/10.1016/B978-0-12-812779-7.00008-4>.
- [25] Gotoh H, Shibahara T, Sakai T. Sub-particle-scale turbulence model for the mps method. *Advanced Methods for Computational Fluid Dynamics*. (2001), 339-347.
- [26] Harris T. A. Rolling bearing analysis. 4th edition. John Wiley & Sons New York.

